THE NEUROETHOLOGY OF INSECTICIDE TOXICITY: EFFECTS ON LOCUST VISUAL MOTION DETECTION AND COLLISION AVOIDANCE BEHAVIOUR

A Thesis Submitted to the College of
Graduate and Postdoctoral Studies
in Partial Fulfilment of the Requirements
for the Degree of Doctor of Philosophy
in the Department of Biology
University of Saskatchewan
Saskatoon

By

RACHEL H. PARKINSON

© Copyright Rachel H. Parkinson, September 2019. All rights reserved

Permission to Use

In presenting this thesis in partial fulfillment of the requirements for a postgraduate degree from the University of Saskatchewan, I agree that the Libraries of this University may make it freely available for inspection. I further agree that permission for copying of this thesis in any manner, in whole or in part, for scholarly purposes may be granted by the professor who supervised my thesis work or, in their absence, by the Head of the Department or the Dean of the College in which my thesis work was done. It is understood that any copying or publication or use of this thesis or parts thereof for financial gain shall not be allowed without my written permission. It is also understood that due recognition shall be given to me and to the University of Saskatchewan in any scholarly use which may be made of any material in my thesis.

Requests for permission to copy or to make other uses of materials in this thesis in whole or part should be addressed to:

Head of the Department of Biology
University of Saskatchewan
112 Science Place
Saskatoon, Saskatchewan S7N 5E2
Canada

OR

Dean
College of Graduate and Postdoctoral Studies
University of Saskatchewan
116 Thorvaldson Building, 110 Science Place
Saskatoon, Saskatchewan S7N 5C9
Canada

Abstract

Agrochemicals are paramount to supporting current agricultural practices, despite the costs to ecosystems. However, sublethal effects of agrochemicals on non-target organisms are poorly understood. Additionally, novel insecticides are being developed continuously, and often can be found in complex pesticide mixtures applied as seed treatments. One of the most controversial of these are the class of insecticides categorized as neonicotinoids, which are nicotinic acetylcholine receptor agonists. These insecticides, lauded for their specificity for the insect receptor, are known to affect many aspects of insect behaviour and physiology. Wild and domestic bees are especially sensitive to these insecticides, which are thought to affect their flight and navigation ability and contribute to colony collapse disorder. Here, I explore whether a common neonicotinoid, imidacloprid, affects visual motion detection and collision avoidance behaviours in the locust, *Locusta migratoria*. These behaviours and neural circuits are well conserved among species, but are especially well described in the locust, making this a highly tractable system for exploring these effects *in vivo*. Through a series of three projects I uncovered how imidacloprid affects the responses of important descending visual interneurons to an ecologically-important visual stimulus: the image of an object on a direct collision course (looming). This stimulus elicits robust escape behaviours in the locust, either while in flight or while standing. I show that low, sublethal exposure to imidacloprid resulted in reduced visual motion processing in multiple descending neurons, and that these effects were present between 1 and 24 hours after treatment. I correlated these effects with reduced escape behaviours - animals treated with a single dose do not steer or jump to avoid an impending collision. I show that these effects also resulted from treatment with metabolites of imidacloprid. This is significant as these metabolites exist both in the environment and within insects for a longer time and sometimes at a higher concentration than the parent compound, suggesting an additional source of exposure. Finally, using a comparative analysis I show that another agonist of the nicotinic acetylcholine receptor, the novel insecticide sulfoxaflor, did not produce the same effects as an equal dose to that used with imidacloprid. I argue for the utility of using neuroethological assays to answer questions in toxicology, as these assays link neural and behavioural effects thus offering a more complete picture than single endpoint assays often employed by toxicologists. My results show effects of imidacloprid on visual motion detection and escape behaviours, suggesting that similar effects may occur in non-target insects, including bees, when exposed to these insecticides.

Acknowledgements

I dedicate this thesis to my son, Silvio, who came to be at the same time I began the research that grew into this thesis. I hope you find joy on the path less travelled and experience the humbling satisfaction that arises from climbing mountains, academic or otherwise. This path, however, would have been infinitely more treacherous without the love and support from my family, especially Gilbert Vega, Mary Vandergoot, David Parkinson, Robin Hawrysh, Heather Giles, and my extended family in Peru, who have never wavered in their confidence in me or questioned the sacrifices made to bring this project to fruition.

It goes without saying that a supervisor's role is to support and guide the student, but my supervisor, Prof. Jack Gray, truly exceled. Jack gave me the freedom to make mistakes and to follow my intuition, freedom which taught me to trust myself as a scientist. Beyond ensuring I had the training required to complete my project, Jack honed my skills in writing, critical thinking, and problem-solving, skills that will be invaluable to me as I move forwards in science. Thank you, Jack, for empowering me and offering your unending support.

I never could have imagined how pivotal my coworkers in the lab would be to this experience. Not only through helping me troubleshoot electrophysiology and analyses, but by giving me a sense of home on campus. You all made coming to work an absolute pleasure, and I will cherish the memories we made. Thank you, Cody Manchester, Sinan Zhang and Erik Olson for the endless hours of entertaining conversations. I have learned so much from you all, including more than I ever thought possible about MMORPGs. Jasmine Yakubowski, Glyn McMillan, Jacelyn Little, Tarquin Stott, Maha Mansoor, and Gayatri Sivalenka, you each added to my experience in different ways. I am grateful for the chance to meet and work with you all.

I am indebted to my advisory committee for their wisdom and guidance: Tracy Marchant, for encouraging me to pursue graduate studies and keeping an open door for questions and conversation; Som Niyogi for inspiring me to stick with toxicology, a decision I will never regret; and Veronica Campanucci for reminding me of the importance of relating the molecular with the macro. Thank you to my external examiner, Mel Robertson, who has been a mentor throughout my graduate studies. I am grateful to the Margaret MacKay Scholarship fund for funding my first two years of research, NSERC for funding the final year, and the University of Saskatchewan and Department of Biology for funding in my third year, and for providing me with awards and teaching opportunities that funded travel to conferences.

Table of Contents

Permission to Use i
Abstract ii
Acknowledgements iii
Table of Contents iv
List of Tables viii
List of Figures ix
List of Abbreviations xii
Chapter 1: Literature Review & Objectives 1
1.1. Introduction 1
1.1.1. Toxicology through the lens of Neuroethology 1
1.1.2. Agrochemicals 2
1.1.3. *Locusta migratoria*: in neuroethology and agriculture 3
1.2. Adaptive behaviours 4
1.2.1. Avoidance behaviour 4
1.2.2. Escape behaviours 4
1.3. Visual motion detection 5
1.4. *Locusta migratoria* 6
1.4.1. Biology and ecology 6
1.4.2. Visually-evoked escape behaviours 6
1.4.3. Neural anatomy and biophysical properties 7
1.4.4. Vision and visual processing 8
1.4.5. Visual motion-sensitive interneurons 10
1.4.6. Lateral and feedforward inhibition 12
1.4.7. Other visual motion-sensitive descending interneurons 14
1.4.8. Neurotransmitters 14
1.4.9. Comparative biology of locust nicotinic acetylcholine receptors 15
1.5. Cholinergic insecticides 17
1.5.1. The neonicotinoids 17
1.5.2. Environmental presence and persistence 17
1.5.3. Toxicokinetics 18

1.5.4. The molecular initiating event: neonic binding the nAChR 20
1.5.5. Cellular effects 22
1.5.6. Effects on brain and behaviour 25
1.5.7. Novel cholinergic insecticides 28
1.6. Research questions 29
1.7. Projected significance 30
Chapter 2: A sublethal dose of a neonicotinoid insecticide disrupts visual processing and collision avoidance behaviour in *Locusta migratoria* 31
2.1. Abstract 31
2.2. Introduction 32
2.3. Methods 34
2.3.1. Animals 34
2.3.2. Solutions 34
2.3.3. LD50 35
2.3.4. Wind tunnel 35
2.3.5. Behaviour assays 35
2.3.6. Flight simulator 36
2.3.7. Electrophysiology 36
2.3.8. DCMD (2h) 37
2.3.9. DCMD (24h) 37
2.3.10. Data analysis 37
2.3.11. Statistical analysis 38
2.4. Results 38
2.4.2. LD50 38
2.4.3. Behavioural responses 39
2.4.4. DCMD responses (2h) 40
2.4.5. DCMD responses (24h) 45
2.5. Discussion 48
Chapter 3: Neural conduction, visual motion detection, and insect flight behaviour are disrupted by low doses of imidacloprid and its metabolites 54
3.1. Abstract 54

3.2. Introduction 55
3.3. Methods 56
3.3.1. Animals 56
3.3.2. Treatments 56
3.3.3. Behaviour 56
3.3.4. Electrophysiology 57
3.3.5. Data analysis 58
3.3.6. Statistical analysis 59
3.4. Results 59
3.4.1. Behaviour 59
3.4.2. DCMD responses to looming stimuli 60
3.4.3. Conduction velocity 62
3.5. Discussion 65
Chapter 4: Attenuation of excitation in optic lobes by imidacloprid, not sulfoxaflor, results in ineffective visual motion detection in a neural population 70
4.1. Abstract 70
4.2. Introduction 71
4.3. Methods 73
4.3.2. Treatments 73
4.3.3. Visual stimuli 73
4.3.4. Collision avoidance behaviour assay 74
4.3.5. Electrophysiology 74
4.3.6. Spike sorting 75
4.3.7. Spike train analysis 75
4.3.8. Statistical analysis 76
4.4. Results 76
4.4.1. Collision avoidance behaviour 76
4.4.2. Electrophysiology 78
4.4.3. Dynamic factor analysis 81
4.4.4. Habituation 82
4.5. Discussion 84

Chapter 5: General discussion 88
5.1. Effects of imidacloprid on object motion detection 88
5.2. Effects on escape behaviours 89
5.3. Implications for visually-guided flight 90
5.4. Adverse Outcome Pathway of imidacloprid toxicity 90
5.5. Comparative effects of sulfoxaflor 91
5.6. Toxicology through the lens of Neuroethology 92
5.7. Future directions 93
Literature cited 94

List of Tables

Table 2.1 Experimental procedure for 2 hour electrophysiology experiments performed in a flight simulator with looming stimuli presented over simple (S) and flow field (FF) backgrounds…… 37

Table 2.2: Results of statistical analyses for figures 2.6, 2.8, 2.9, and 2.10 ……. 45

Table 4.1 Summary statistics for sorted spikes for each animal by treatment group…….… 78

Table 4.2. Results from the dynamic factor analysis…….……. 81

List of Figures

Figure 1.1: The locust central nervous system is arranged into ganglia linked by paired ventral connectives…… 8

Figure 1.2: Drawings of a sectioned compound eye and optic lobe and a single ommatidium. Visual information regarding light intensity and wavelength are passed from the photoreceptor of the ommatidium down through several layers of interneurons in the optic lobe, where complex features and quality of visual stimuli are encoded……. 9

Figure 1.3: Raw continuous data and peristimulus time histograms (PSTHs) constructed from an extracellularly recorded DCMD response to a looming stimulus……. 11

Figure 1.4: Schematic representation of layers of neurons from photoreceptor to LGMD that are activated as a looming stimulus expands over the ommatidia of the eye. These pathways include excitation and lateral and feedforward inhibition……. 13

Figure 1.5: Schematics of the insect nAChR …….. 16

Figure 1.6 Proposed metabolic pathway of imidacloprid in the honeybee…….. 20

Figure 1.7: The molecular initiating event (MIE) and two Key Events (KEs) proposed in Adverse Outcome Pathways (AOPs) by Lalone et al (2017)…… 22

Figure 2.1: Percent mortality at 48 hours after injection with imidacloprid (IMD) solutions ranging in concentrations from 10 to 10,000 ng/g (on log scale), fitted with iterative non-linear regressions (solid lines)……... 39

Figure 2.2: Effect of IMD on escape behaviours……. 40

Figure 2.3: Joint inter-spike interval (ISI) distribution heatmaps comparing one ISI (y-axis, ms) with the following ISI (x-axis, ms)…… 41

Figure 2.4: Rasters and peristimulus time histograms (PSTHs) constructed from DCMD responses to looming stimuli…… 42

Figure 2.5: Median temporal properties of DCMD response parameters over 100 minutes after treatment with 0.1 (n=5), 1 (n=5), 10 (n=5) and 100 (n=20) ng/g IMD during stimulus presentations against a simple background……43

Figure 2.6: Response parameters (mean ± SEM) of the four DCMD rates (full DCMD, burst spikes, isolated spikes, and bursts) at 110 (S background) and 120 minutes (FF background) after treatment with an IMD dose (ng/g) or the vehicle (V)…… 44

Figure 2.7: Mean PSTH overlays of DCMD responses to a looming stimulus against simple (top row) or flow field (bottom row) backgrounds, at 2 (n = 20) and 24 (n = 10) hours after injection with 100 ng/g IMD……. 46

Figure 2.8: Response parameters (mean ± SEM) of the four DCMD rates (full DCMD, burst spikes, isolated spikes, and bursts) 24 hours after treatment with an IMD dose (ng/g) or the vehicle……. 47

Figure 2.9: Time of maximum firing rate relative to collision (peak time; mean ± SEM) across doses and background types at 2 and 24 hours after treatment……. 47

Figure 2.10: Effect of IMD on burst spike peak firing rate (f_p) and correlation with observed behavioural deficits……48

Figure 3.1: Electrophysiology, experimental procedures and data analysis. A) Suction electrodes recorded the activity of the DCMD axon at three points along the ventral nerve cord: posterior to the prothoracic ganglion, and anterior and posterior to the mesothoracic ganglion……. 58

Figure 3.2: Flight and escape behaviours before (PRE) and after treatment with IMD, OLE or 5OH……60

Figure 3.3: Mean peristimulus time histograms (PSTHs). Data are from all animals in each treatment group normalized as a percent of the pre-treatment peak firing rate before treatment (pre-treatment), 30 minutes, and 60 minutes after treatment with 10 ng/g of locust of IMD (n=9), OLE (n=6) or 5OH (n=8), or the vehicle control (n=7)…….. 61

Figure 3.4: Comparison of DCMD response parameters……. 62

Figure 3.5: Effects of treatment on conduction velocity. Relative DCMD conduction velocity versus time to collision for all DCMD spikes recorded along the ventral connective (CVC) and across the mesothoracic ganglion (CVM) for all animals in each treatment group during the approach of a looming stimulus at 60 minutes after treatment, and the corresponding mean PSTHs…….. 63

Figure 3.6: Relative conduction velocity as a function of instantaneous firing rate along the ventral connective (CVC) and across the mesothoracic ganglion (CVM)…… 64

Figure 4.1: Collision avoidance behaviour and classification of spikes belonging to units that respond to a looming stimulus based on treatment with vehicle, sulfoxaflor and imidacloprid……... 77

Figure 4.2: Spatiotemporal properties of descending interneurons are affected by IMD, not SFX..…….. 80

Figure 4.3: Dimensionality reduction of population response shows reduced variation in common trends when treated with imidacloprid……82

Figure 4.4: Habituation of populations of visual interneurons shows that some units habituate, while others do not…… 83

Figure 5.1: Diagram showing the relative degree of attenuation by imidacloprid of the excitatory and inhibitory pathways in the optic lobes that are activated during the approach of a looming stimulus (left) and the effects on the DCMD PSTH compared to the vehicle control (right)……88

Figure 5.2: Adverse Outcome Pathway linking the molecular initiating event (green) of imidacloprid binding to the nAChR to the adverse outcome (red) of decreased survival…….. 91

List of Abbreviations

$[Ca^{2+}]_i$	intracellular calcium concentration
5OH	5-hydroxy-imidacloprid
ACh	acetylcholine
AChE	acetylcholinesterase
ADME	absorption digestion metabolism excretion
AOP	adverse outcome pathway
Ca^{2+}	calcium ion
CaM	calmodulin
CNS	central nervous system
CV	conduction velocity
CYP450	cytochrome P450 monooxygenase
DCMD	descending contralateral movement detector
DDT	Dichlorodiphenyltrichloroethane
DFA	dynamic factor analysis
DIMD	descending ipsilateral movement detector
EPSP	excitatory post-synaptic potential
FETi	Fast extensor tibiae
FF	flow-field background
GABA	gama-aminobutyric acid
IMD	imidacloprid
IPSP	inhibitory post synaptic potential
ISI	inter-spike interval
KE	key event
KER	key event relationship
LDCMD	late descending contralateral movement detector
LGMD	lobula giant movement detector
mAChR	muscarinic acetylcholine receptor
MIE	molecular initiating event
nAChR	nicotinic acetylcholine receptor
neonic	neonicotinoid insecticide

OLE	imidacloprid-olefin
PER	proboscis extension reflex
PSTH	peristimulus time histogram
ROS	reactive oxygen species
S	simple background
SFX	sulfoxaflor
TOC	time of collision
VGCC	voltage gated calcium channel

Chapter 1: Literature Review & Objectives

1.1. Introduction

1.1.1. Toxicology through the lens of Neuroethology

The sublethal effects of environmental toxicants tend to be subtle and are influenced by the presence of other toxicants and underlying physiological conditions. Linking sublethal effects across levels of biological organization poses a significant obstacle when employing single-outcome testing methods, or when extrapolating sublethal effects from high dose assays. An ideological shift is occurring in toxicology towards valuing the complexity of sublethal effects and their downstream consequences (Krewski et al. 2010). A conceptual framework was developed to aid in linking toxicological responses across levels of biological organization, with the goal of prioritizing risk-based assessment (Bradbury et al. 2004). This framework, termed the Adverse Outcome Pathway (AOP), portrays the cascade of toxicological effects from the molecular initiating event to some final adverse effect of interest to policy makers, such as the population decline of a species (Ankley et al. 2010). The AOP requires that effects measured at various levels of biological organization, including cellular, physiological, and behavioural, be linked by key event relationships that may be causal, mechanistic, inferential, or correlation based (Ankley et al. 2010). Defining these relationships poses the greatest challenge, as the links between physiology, behaviour, and population dynamics are often unclear or incomplete. Neuroethology is the study of brain and behaviour. It employs interdisciplinary approaches to understand how the nervous system encodes and processes relevant environmental stimuli to produce natural behaviours (Zupanc 2010). Traditionally, neuroethologists have focussed on invertebrates that possess tractable nervous systems and react to salient environmental stimuli with predictable and robust reflex-like behaviours, such as the crayfish tail flip escape response (Wine and Krasne 1972). Exploration of these “simple circuits” has led to many discoveries regarding the function and capabilities of the nervous system, and ultimately has revealed the

immense diversity of strategies employed by animals to contend with a stimulus-rich environment. A major goal of this thesis is to explore the use of neuroethological methods to answer questions in ecotoxicology. I argue that this interdisciplinary approach has dual benefit: experiments can be designed to link toxic effects spanning from cells to behaviour, and the pharmacological manipulation of these circuits fosters the understanding of normal function.

1.1.2. Agrochemicals

While agriculture has shaped global ecosystems for thousands of years, the advent of chemical pesticides supported a shift in agriculture characterized by large-scale monoculture croplands. The ecological impacts of agrochemicals were not widely considered until the publication of Rachel Carson's *Silent Spring* (Carson 1962). This book, which focused on the environmental persistence of the insecticide dichlorodiphenyltrichloroethane (DDT), led to an awakening in science that resulted in restrictions of DDT use and inspired the formation of the field of ecotoxicology (Banks and Stark 1998). The message of *Silent Spring* remains pertinent: insecticide use continues to increase to support agricultural practices that favour landscape simplification (Meehan et al. 2011). Insecticide developers are evolving insecticides in an arms race against insecticide resistance and environmental degradation. This has favoured insecticides that pose reduced risks to mammals due to increased insect-specific targets, including the class of neonicotinoid insecticides.

Neonicotinoid insecticides (neonics) are among the top five pesticides used globally, and since their introduction in 1990 their use has grown to dominate a quarter of the global pesticide market (Jeschke et al. 2011). Neonics are neurotoxicants: they are nicotine mimics, binding selectively to insect nicotinic acetylcholine receptors (nAChRs) (Tomizawa and Casida 2005). They are moderately water soluble, which allows for assimilation in plant tissues (Bonmatin et al. 2015). Seeds and soil can be pre-treated and the pesticide becomes incorporated in all parts of the plant, eliminating need for spraying or re-treating crops (Jeschke et al. 2011). Unfortunately, toxicity is greater than previously expected for non-target insects, birds, and other organisms (Fischer et al. 2014; Main et al. 2014; Rundlöf et al. 2015), and the prophylactic use of these insecticides results in massive quantities of neonicotinoids introduced into the ecosystem. Neonics can be found in soil (Schaafsma et al. 2016), wetlands (Main et al. 2016), groundwater (Id et al. 2018), and untreated wildflower fields (Botías et al. 2015). Modern seed treatments

contain mixtures of insecticides and fungicides, and the effects of these pesticide mixtures, and their metabolites on non-target organisms are not fully understood (Botías et al. 2017; Maloney et al. 2018).

1.1.3. *Locusta migratoria*: in neuroethology and agriculture

The locust, *Locusta migratoria*, is one of the most devastating agricultural pests due to its ability to form high-density, mobile swarms (Burrows 1996). Research on the locust nervous system was originally inspired by organizations such as the Anti-Locust Research Centre in London, UK, to develop novel pesticides (Burrows 1996). Locust flight became a major focus of neurophysiological studies, including investigations of proprioceptive feedback of the wing stretch receptor and tegula, as well as bursting properties of interneurons associated with flight motor neurons (Robertson et al. 1982; Wolf and Pearson 1988; Ramirez and Pearson 1993). Stemming from these early investigations, *Locusta migratoria* has become an important model in neuroethology. Locusts are ideally suited for neuroethological assays because they are easily bred, and they exhibit robust neural and behavioural responses to specific stimuli. Many features of locust neuroethology, including vision, flight, and escape behaviours, have been quantified (Rind 1984; Gabbiani et al. 2001; Gray 2005; Gray et al. 2010). Neural circuits that produce rhythmic behaviour and process visual information are evolutionarily conserved, thus information about the locust nervous system can inform our understanding of neurological phenomena across diverse taxa.

Many pesticides have been used to control locust plagues, including organochlorines (dieldrin), pyrethroids, phenyl pyrazoles (fipronil) and organophosphates, but these display high toxicity to mammals and other non-target organisms. Although neonics display reduced mammalian toxicity, they have been shown to elicit a wide range of behavioural and physiological effects in non-target insects, especially in wild and domestic bees (Rundlöf et al. 2015; Woodcock et al. 2016). Of these, foraging and navigational ability, and predator avoidance are known to be compromised with sublethal exposures of various neonics (Henry et al. 2012; Tan et al. 2014; Fischer et al. 2014). Despite these behavioural effects, the effects of neonics on visual processing has not previously been examined. Collision avoidance pathways similar to that of the locust display convergence across taxa (Medan et al. 2007; Yamawaki and Toh 2009a), and can be studied to gain insight into other systems. Using this tractable pathway, my

goal is to understand the effects of neurotoxic insecticides on visual motion detection and connect these effects with downstream behavioural output.

1.2. Adaptive behaviours

1.2.1. Avoidance behaviour

The threat of predation provides a strong selective pressure for animals to develop adaptive behavioural strategies to promote survival. Avoidance behaviour requires that the threat be detected, either visually or through another temporally-relevant modality, and the prey avoid being detected in the process. This may be achieved behaviourally by avoiding habitat, reducing activity during times predators are active, or by using some form of camouflage to hide from predators. If the animal fails to avoid detection, then another strategy must be employed, that is to intimidate, fight, or escape.

1.2.2. Escape behaviours

Escape behaviours are of broad interest to neuroethologists. These behaviours are generally easy to elicit, predictable in nature, and are often described as "reflex-like" as they are governed by simple circuits of, often large, neurons and tend to be elicited quickly. These behaviours, however, are not true reflexes, in that they involve central processing and may be modified through learning or environmental stimuli. There are many examples of escape behaviours that have been studied extensively, and entire neural pathways have been described in various species. Invertebrates tend to display robust escape behaviours, and their nervous systems are accessible and tractable. The caridoid escape reaction, commonly named the tail-flip, is an example of an escape behaviour for which the neural mechanisms are completely understood. This behaviour is elicited in freshwater crustaceans, including crayfish, via tactile stimulation of the body or direct stimulation of the lateral giant interneuron or medial giant interneuron (Wiersma 1947; Wine and Krasne 1972).

A source of difficulty for neuroethologists striving to understand how the nervous system controls animal behaviour is the challenge bridging laboratory studies with the animal's behaviour in its natural environment, in which context has a strong influence on neural processing and behaviour (Palmer and Kristan 2011). Although escape behaviours may be

"reflex-like" they are still highly adaptive behaviours. Escape behaviour has been studied in crabs both in the laboratory and in the field in an attempt to merge these methods and understand how context modifies these behaviours (Hemmi and Tomsic 2012). Other important escape behaviours have been studied extensively in the cockroach (Domenici et al. 2008), fruit fly (Card and Dickinson 2008), and locust (Santer et al. 2005b).

1.3. Visual motion detection

Visual motion detection is required for many aspects of visual processing, including depth perception and the perception of self- and object motion. While visual motion detection requires retinal input, its processing involves integrating visual information with time information, and is accomplished by comparing the movement between two images sampled after a delay (Borst and Egelhaaf 1989). The detectors can adapt to image velocity by shortening or lengthening this delay, in accordance with the visual requirements of a given animal, such as for observing predators or perceiving self-motion during low velocity activities like hovering (O'Carroll et al. 1996). The ability to detect motion is essential for insect orientation and navigation, this ability being heavily dependent on the optomotor response. The optomotor response describes the tendency of insects to follow the direction of movement of the visual scene in order to stabilize the image on the retina, and serves to maintain heading and orientation when the insect may be inadvertently diverted from the intended course (Borst and Egelhaaf 1989; Taylor and Krapp 2007). The response requires detecting wide field visual motion, or optic flow, and calculating the velocity of the optic flow to perceive self-motion (Srinivasan and Zhang 2004). In addition to functioning in course stabilization, the optomotor response has been shown to be critically important for other aspects of flight and navigation, including landing (Baird et al. 2013), and to estimate height (Portelli et al. 2010), speed (Portelli et al. 2011), and distance (Si 2003; Dacke and Srinivasan 2007). The optomotor response involves detecting wide field visual motion to stabilize and direct flight, while the ability to detect object motion is important for perceiving threats and avoiding collisions. For animals that are in flight, the task of detecting object motion is complex, as the image motion from objects that are moving must be balanced against self motion. The strategies posed by the insect nervous system to encode object motion have been studied extensively in the migratory locust.

1.4. *Locusta migratoria*

1.4.1. Biology and ecology

Locusta migratoria are native to Africa, Japan, the Philippines, and Australia (Chapman 1998). They belong to the family *Acrididae* in the order Orthoptera. Locusts express phase polymorphism, with gregarious and solitary phases characterized by distinct morphologies and behaviour (Simpson et al. 1999). In the solitary phase, they may live in small groups or alone, and fly infrequently and for short distances only (Matheson et al. 2004). Locusts pose little threat to agriculture while solitarious, but when they change to gregarious forms the results can be disastrous (Simpson et al. 1999). Phase change occurs when population densities increase sufficiently so that locusts are in direct contact with one another, and stimulation of the back legs elicits the change most effectively (Simpson et al. 2001). Gregarious locusts are more active and are attracted to conspecifics, contrasting with solitarious locusts that tend to avoid other locusts except during mating (Simpson et al. 1999). Behavioural changes may occur within hours of the appropriate stimulation, while changes in morphology occur over 1-2 generations (Simpson et al. 1999). There are thousands of identified phase-related genes and metabolites, but the shift between the gregarious and solitarious phases is governed primarily though several key pathways (Wang and Kang 2014). One of these pathways that modulates the behavioural shift from repulsion to attraction between conspecifics involves chemosensory genes (Guo et al. 2011). Additionally, there is a profound change in the relative amounts of various neurotransmitters and neuromodulators with phase change (Rogers et al. 2004).

1.4.2. Visually-evoked escape behaviours

Flying within a dense swarm requires an accurate and precise collision detection system to avoid collisions with conspecifics (Baker et al. 1981). In addition, the locust must remain sensitive to avian predators. The locust displays escape behaviours that can be elicited reliably from a looming stimulus. These behaviours include jumping while standing, or steering manoeuvres that are elicited in flight. The structure, context, timing, and motor control of these behaviours have been studied extensively.

While standing, locusts can escape only by jumping. Locusts can control the direction, timing, elevation, and distance of the jump (Santer et al. 2005b; Sutton and Burrows 2008), but

the trajectory is unpredictable to the predator, allowing this behaviour to be an effective escape strategy. Jumping behaviour requires some preparation: the metathoracic (hind) legs function like a catapult, with energy stored pre-jump by contracting the hind leg flexor muscles and stretching the extensor muscles. There are three stages for a jump: the contraction of the flexor muscle, which positions the tibia against the femur (100-300 ms); isometric co-contraction of the extensor and flexor muscles to build up elastic energy (300-600 ms); and finally a relaxation of the flexor muscles which extends the tibia powerfully (Heitler and Burrows 1977). The duration of the extension of the hind legs during a jump at the tibio-femoral joint is 20 msec, with the maximum force is reached by 3-8 msec (Brown 1967), however the motor programme requires a minimum of 400 ms of preparation (Heitler and Burrows 1977).

During flight, locusts display several steering behaviours to escape an impending collision that can be grouped into three categories: turning, either towards or away from the stimulus; gliding, which would decrease the locust's altitude gradually; or a full stop, which allows the locust to achieve a rapid drop in elevation (Santer et al. 2005a; Simmons et al. 2010; Chan and Gabbiani 2013; McMillan et al. 2013). Gliding and stopping behaviours are commonly thought to be 'last ditch' behaviours to avoid collisions without sufficient time for more directed course change, such as a turn (Santer et al. 2005a). However, all steering behaviour types can be elicited from looming stimuli of the same size and speed (Chan and Gabbiani 2013; McMillan et al. 2013), and this variability is advantageous for survival of the locust to predator attack. The adaptability of these collision avoidance behaviours is additionally important to allow locusts to avoid predators while flying in close range with conspecifics (Benaragama and Gray 2014).

1.4.3. Neural anatomy and biophysical properties

The basic unit of the nervous system is the neuron. In locusts, most neurons are monopolar with a single projection from the soma that branches to form the dendrites and axon (Chapman 1998). Neurons are bundled into paired nerve cords, which run ventrally down the length of the animal connecting the brain and ganglia (Figure 1.1). Nerves are surrounded by the perineurium, or nerve sheath, which is formed from specialized glial cells to maintain homeostasis in the environment immediately surrounding neurons (Chapman 1998). The perineurium is comparable to the blood-brain barrier in vertebrates. No vessels penetrate the

sheath, and substances in hemolymph must cross the barrier and diffuse toward neurons before they can have any effect (Burrows 1996).

In the insect nervous system, acetylcholine (ACh) is the most common excitatory neurotransmitter (Burrows 1996). ACh binds to nicotinic acetylcholine receptors (nAChRs) on the dendrites of many neurons in the central nervous system (CNS) and motorneurons. When bound, ACh causes a conformational change in the nAChR that opens the ion channel and allows positively charged ions to enter the cell. If enough nAChRs have been activated, the threshold voltage may be reached, and the result will be an action potential. Action potential waveform shape differs between neurons, a direct result of various biophysical properties of the axon, including its diameter and the density of voltage-gated channels (Hodgekin and Huxley 1952; Hodgkin and Huxley 1952a).

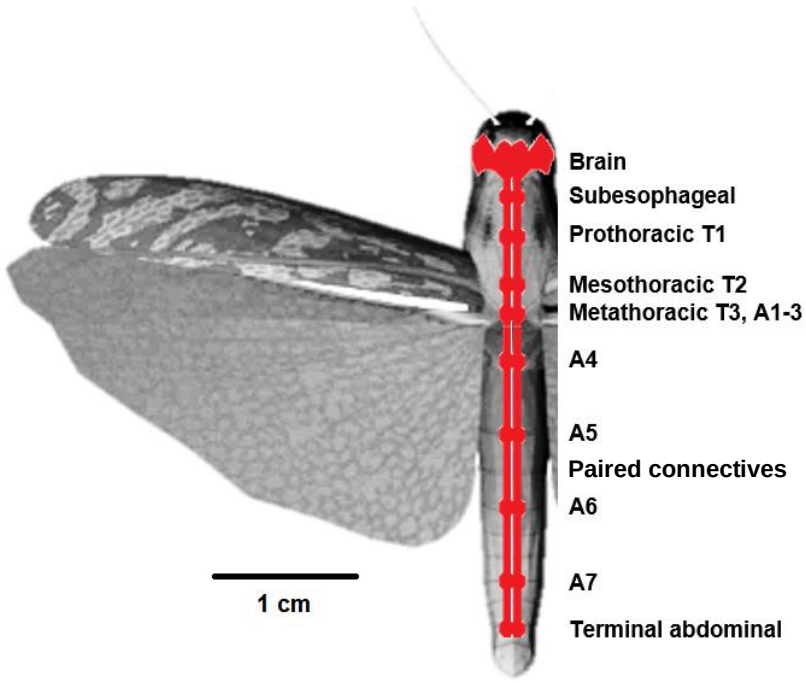

Figure 1.1: The locust central nervous system is arranged into ganglia linked by paired ventral connectives.

1.4.4. Vision and visual processing

Locusts have a pair of compound eyes and three simple eyes (ocelli). Ocelli were traditionally viewed as functioning only to maintain directionality during flight and measure changes in photoperiod, but have been found to have some level of spatial resolution as well (Berry et al. 2007). Interneurons project from each ocellus, and these large, second order neurons

(L-neurons) are well adapted for monitoring the horizon due to having wide but low resolution receptive fields (Wilson 1978). L-neurons interact with wind-sensing neurons in the locust brain, this further elucidating the role of the ocelli in course correction and flight stabilization (Simmons 1982). Contrasting this, each compound eye is formed from approximately 3000 ommatidia, with the ~1º acceptance for each ommatidium set at a slightly different angle to allow for a wide visual field (Burrows, 1996) (Figure 1.2). When the photoreceptor of an ommatidium is activated by a change in light intensity and wavelength, an action potential is conducted along the receptor axon and passed through several layers of interneurons in the optic lobe, where the signal is processed (Burrows 1996).

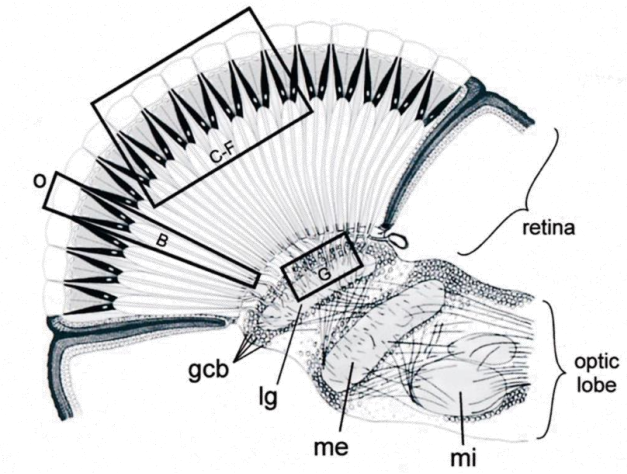

Figure 1.2: Drawings of a sectioned compound eye and optic lobe. Visual information regarding light intensity and wavelength are passed from the photoreceptor of the ommatidium down through several layers of interneurons in the optic lobe, where complex features and quality of visual stimuli are encoded. Labels are: gcb, ganglionic cell bodies; lg, lamina ganglionaris; me, medulla externa; mi, medulla interna, or lobula; o, ommatidium; B, photoreceptor cell; C-F, lens' and crystalline cones of several ommatidia; and G, photo receptor axons (from Burrows, 1996).

Photoreceptors detect changes in light intensity and wavelength, but processing of these signals occurs in the optic lobes and protocerebrum. The optic lobes consist of three layers (the lamina, medulla, and lobula) and each layer is connected by an area of crossing axons (Figure 1.2; Burtt and Catton, 1956). Neurons have been identified in the optic lobes that respond preferentially to various stimuli, including dimming, brightening (Osorio 1987), or forwards or backwards directional movement (Kien 1974a). Signal processing is enhanced through the optic lobes, and descending neurons contain highly processed signals for specific visual stimuli. For

example, neurons that encode information about the directionality of a flow field have been identified (Baader et al. 1992), and other neurons can detect stimuli moving either clockwise or counter clockwise around the visual field, termed "binocular directional" neurons (Kien 1974b).

1.4.5. Visual motion-sensitive interneurons

Locust visual motion detection has been studied intensively, and arguably more is known about motion detection in locusts than in any other invertebrate. Individual neurons have been identified that encode specific aspects of a moving stimulus. Two pairs of identified interneurons have been found to respond preferentially to stimuli approaching at a constant velocity on a direct collision course (looming): the Lobula Giant Movement Detector (LGMD) and the Descending Contralateral Movement Detector (DCMD) (Judge and Rind 1997; Gabbiani et al. 1999; Gray et al. 2001). The dendritic trees of each LGMD expand into the optic lobes of the locust brain and the axons synapse chemically and electrically with the DCMD (Rind 1984). Each LGMD receives converging visual information from sensory receptors of the ommatidia, and synapses directly with a DCMD in a 1:1 spiking ratio (Rind 1984). The axon of each DCMD crosses the midline and descends contralaterally via the ventral connectives (Rind 1984). The DCMD synapses onto motor centres involved in flying and jumping, suggesting that the LGMD/DCMD are responsible for eliciting collision-avoidance behaviours (Gabbiani et al. 1999). The response of the DCMD to looming stimuli has been studied extensively, due largely to its accessibility and tractability. An extracellular recording of either of the ventral nerve cords will result in the detection of many interneurons, but action potentials of the DCMD are discernible as these spikes have the largest amplitude and show a stereotypical response to a looming object.

Many firing properties of the DCMD have been characterized and show that the interneuron is both finely tuned to looming stimuli, and capable of encoding complex visual stimuli (Gabbiani et al. 1999; Dick and Gray 2014). The DCMD responds preferentially to objects on a direct collision course with the eye, and responds least to objects receding from the eye (Rind and Simmons 1992). The DCMD encodes information about the size and velocity of the stimulus, as well as trajectory changes (Judge and Rind 1997; McMillan and Gray 2012; Dick and Gray 2014). The response of the DCMD to a looming stimulus is dependent on the speed and size of the stimulus, as well as the angle from which it is approaching. Various

parameters of the full DCMD response profile are typically measured, including the maximum firing rate, time at maximum firing rate (relative to collision), total number of spikes, rising phase, and decay phase (Figure 1.3). These measurements are based on the LGMD/DCMD conveying information in a rate code: the firing rate increases as the looming object approaches (Rind and Simmons 1992).

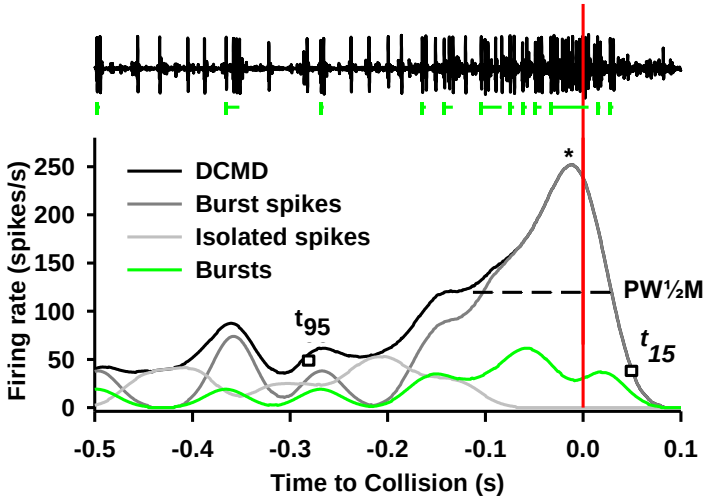

Figure 1.3: Raw continuous data and peristimulus time histograms (PSTHs) constructed from an extracellularly recorded DCMD response to a looming stimulus. The time the object would have collided with the locust (TOC) is marked with a vertical red line. Bursts, which comprise a minimum of two spikes occurring within 8 ms of each other, are highlighted with a vertical green line to signal the start, and horizontal lines to show the duration. PSTHs show the firing rates of the full DCMD response, spikes within bursts only, isolated spikes only, and bursts, smoothed with a 50 ms Gaussian filter. PSTHs response profile parameters included: peak firing rate (f_p), time of the peak relative to TOC, denoted by an asterisk; peak width at half maximum (PW½M), rise phase, from the last time the histogram crosses the 95% confidence interval with a positive slope (*t99*) to the peak, and decay phase from the peak until it had decreased to 15% (*t15*). From Parkinson et al (2017).

Recent data show that DCMD bursting properties may contain behaviourally relevant information (McMillan and Gray 2015). DCMD bursting is defined as trains of two or more action potentials with inter-spike intervals (ISI) of 8 ms or less, and isolated spikes are defined as those with ISIs >8 ms (McMillan and Gray 2015). An algorithm developed by McMillan and Gray (2015) extracts spike times of isolated spikes, burst spikes, and bursts (the first spike in a burst train) and these can be compared with the overall DCMD rate (Figure 1.3). The DCMD synapses onto motor neurons that innervate wing and leg muscles, and various studies suggest the DCMD is involved with generating collision avoidance behaviours (Simmons and Rind

1992; Judge and Rind 1997; Gabbiani et al. 1999; Gray et al. 2001; Santer et al. 2006). It is likely that a threshold frequency of DCMD spikes is required to elicit an action potential in a motor neuron (Santer et al. 2006; Rogers et al. 2007), but that high frequency DCMD firing must occur in phase with the activity of the motor neuron, as some degree of membrane excitation must already be present in order for the DCMD to elicit a motor neuron action potential (Santer et al. 2006). This process is known as flight gating (Santer et al. 2006). Further evidence supporting the importance of DCMD bursting in flight gating is that the frequency of DCMD bursts correlates with the locust's forewing beat frequency at ~25 Hz (McMillan et al. 2013).

Responses of the LGMD/DCMD are tuned to encode specific features of moving objects in the visual field, including its edge acceleration, size, and speed. When an object is approaching on a collision course, the firing rate of the DCMD increases to a maximum, which occurs before collision (Judge and Rind 1997). Timing of the maximum firing rate is dependent on the speed at which the stimulus approaches, with slower stimuli eliciting earlier maximum firing rates (Judge and Rind 1997). LGMD/DCMD firing is modulated by a combination of excitatory and inhibitory inputs from upstream interneurons of the optic lobes. A model of this modulation involves two distinct types of inhibition: lateral and feedforward.

1.4.6. Lateral and feedforward inhibition

Retinotopic units of the ommatidia connect via excitatory and inhibitory synapses in the optic lobes (Rind and Simmons 1998). The retinotopic unit of the locust ommatidium includes the photoreceptor cell and downstream neurons, which ultimately synapse onto the LGMD (Figure 1.4). Excitatory synapses link the neurons in each retinotopic unit, and additionally there are inhibitory synapses projecting from each photoreceptor, constituting two inhibitory paths: lateral and feedforward (Rind and Bramwell 1996).

Lateral inhibition occurs between retinotopic units (Figure 1.4). Inhibitory synapses connect retinotopic units one and two units apart (Rind and Bramwell 1996). When a retinotopic unit is activated, an excitatory postsynaptic potential (EPSP) is transmitted along the unit toward the LGMD, while simultaneously inhibitory postsynaptic potentials (IPSPs) are sent to nearby units (Rind and Simmons 1998). IPSPs are slower, longer lasting signals compared to EPSPs, which are transmitted quickly and have a short duration (Rind and Bramwell 1996). The result is a "critical race" when the image of a looming stimulus is projected on the eye (Rind and

Simmons 1998). As additional retinotopic units are excited by the expanding stimulus, adjacent units that have already been excited are inhibited. This results in the LGMD/DCMD being preferentially stimulated by looming stimuli (Rind and Simmons 1992).

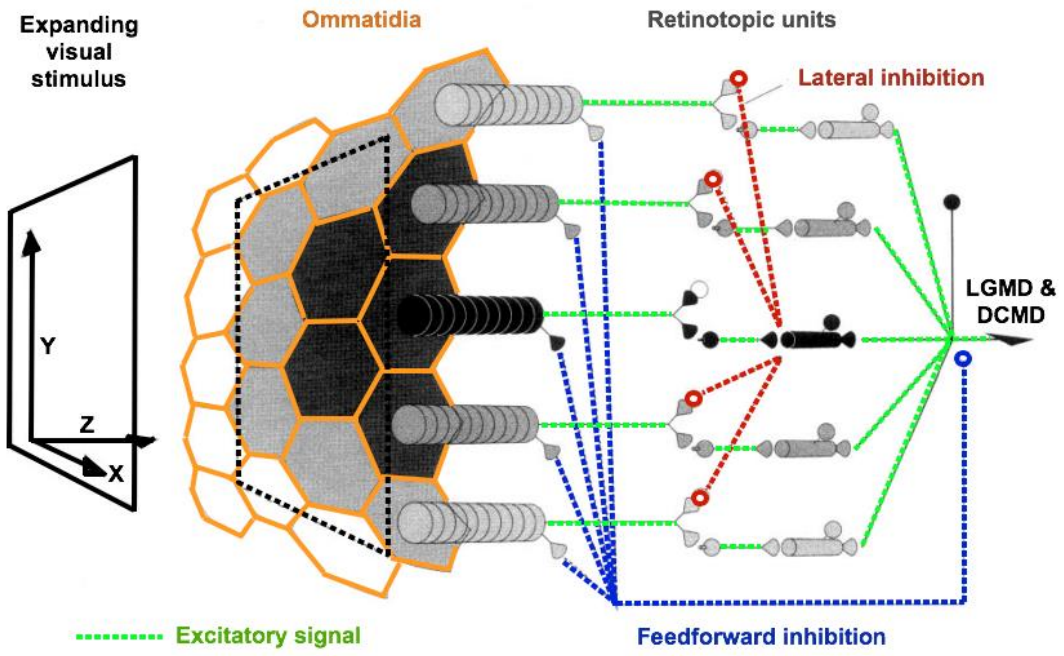

Figure 1.4: Schematic representation of layers of neurons from photoreceptor to LGMD that are activated as a looming stimulus expands over the ommatidia of the eye. These pathways include excitation and lateral and feedforward inhibition. Adapted from Rind and Bramwell (1996).

The second form of inhibition, feedforward inhibition, is activated when many photoreceptors are excited (Rind 1996). These inhibitory connections originate from the photoreceptor cells, and bypass other neurons of the retinotopic unit to synapse directly with the LGMD (Figure 1.4). Feedforward inhibition results in hyperpolarizing currents in the LGMD that directly modulate the response of the LGMD when many photoreceptors are activated (Rind 1996). The basic role of feedforward inhibition is to terminate the LGMD/DCMD response to a looming stimulus (Rind and Bramwell 1996). When feedforward inhibitory signals are pharmacologically blocked at the dendrites of the LGMD, the response profile of the LGMD to a looming stimulus is altered, resulting in an elevated number of action potentials with a longer decay phase (longer period of spiking after time of collision) compared to the control (Gabbiani et al. 2005). Gabbiani et al. (2005) also found that the feedforward loop is only activated when

an image subtends an angle greater than 20º on the locust eye. Feedforward inhibition has more recently been shown to encode the angular size of expansion of a looming stimulus, which interacts with excitatory pathways that encodes the angular velocity of expansion to form a precise and detailed code that represents both the size and speed of the looming object in descending neurons (Wang et al. 2018a).

1.4.7. Other visual motion-sensitive descending interneurons

In addition to the LGMD/DCMD neurons, other descending interneurons have been identified in the locust. Two of these neurons are the descending ipsilateral movement detector (DIMD) and the late-DCMD (LDCMD). Similarly to the DCMD, the DIMD synapses with metathoracic motorneurons, with a spike resulting in an EPSP in these motorneurons, but its axon runs along the ipsilateral axis of the body (Burrows and Rowell 1973). While the DIMD is thought to be implicated in jumping behaviours, its contributions to flight behaviour has not been examined. The response profile of the LDCMD to looming stimuli is similar to that of the DCMD, but its response is seen later during the approach of a looming stimulus, with a lower peak firing rate, and its action potential is a lower amplitude, characterized by an afterhyperpolarization period (Gray et al. 2010). Recently, many additional interneurons have been shown to respond to visual motion, with a variety of response types that differ with stimulus trajectory (Dick et al. 2017). This demonstrates that the locust visual motion detection system is more complicated than previously described.

1.4.8. Neurotransmitters

The primary neurotransmitter employed by neurons in the optic lobes is acetylcholine. Rind and Simmons (1998) found that both inhibitory and excitatory neurons in the optic lobe are cholinergic based on the presence of acetylcholinesterase in the synaptic clefts and absence of GABA in the terminals. While G-protein-linked muscarinic acetylcholine receptors (mAChRs) are the likely mode of transmission for inhibitory signals, excitatory synapses along the retinotopic unit and the dendrites of the LGMD must contain nAChRs that result in fast, excitatory signals (Trimmer 1995; Rind and Simmons 1998). Inhibitory muscarinic receptors act slower, with longer lasting results than the nAChRs, explaining why lateral inhibition does not initially overcome excitation during the processing of images of approaching objects (Rind and

Simmons 1998). Using picrotoxin, a GABA-receptor antagonist, Gabbiani et al. (2005) determined that the only GABA-mediated synapses are feedforward inhibitory synapses on the dendritic fields of the LGMD. Photoreceptor cells use the neurotransmitter histamine, as demonstrated by Elias and Evans (1983) who found high levels of histamine in the locust retina and lamina neuropil of the optic lobe, where it was also found to be synthesized and metabolized. While they also found low levels of histamine in the metathoracic ganglion and optic lobe, acetylcholine is accepted as the major neurotransmitter of the optic lobe. Although the inhibitory synapses in the optic lobe are mediated with GABA and acetylcholine via the mAChR, it is likely that inhibitory neurons are activated via nAChRs due to a lack of alternate excitatory synapses in the optic lobes. The nAChR is thus highly important in the optic lobes for controlling both excitatory and inhibitory pathways.

1.4.9. Comparative biology of locust nicotinic acetylcholine receptors

The nicotinic acetylcholine receptor (nAChR) mediates fast synaptic transmission in the insect CNS (Weeks and Jacobs 1987; Sattelle and Breert 1990). The nAChR is a ligand-gated cation channel, assembled from five subunits (Tomizawa and Casida 2003) (Figure 1.5). When a ligand binds to the receptor, a conformational change occurs, which opens the associated ion channel (Tomizawa and Casida 2001). The nAChR is so named because it binds nicotine, while the endogenous ligand for the nAChR is acetylcholine (ACh). ACh binds at the interface between two adjacent nAChR subunits, which causes the cation-permeable channel to open (Dupuis et al. 2012). Subunit type is defined primarily by the N-terminal extracellular domain: α nAChR subunits have two adjacent cysteine residues that form disulphide bonds (Figure 1.5b) while non-α subunits do not have this feature (Dupuis et al. 2012). nAChRs can exist in three configurations: open, closed, or desensitized. A desensitized nAChR resembles an open configuration but with the pore blocked by one loop of an alpha subunit (Kouvatsos et al. 2016). Receptor function may be modified intracellularly, as the receptor contains several phosphorylation sites on a large cytoplasmic loop between the first and fourth transmembrane domain of each subunit (Dupuis et al. 2012).

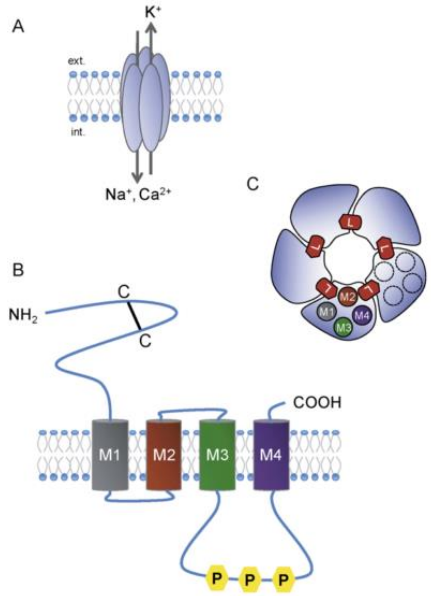

Figure 1.5: Schematics of the insect nAChR. (A) Homomeric receptor formed by five identical subunits with a central cation-permeable channel. (B) Representation of a single subunit, with four transmembrane domains, a large intracellular loop with phosphorylation sites, and large extracellular N-terminal domain with a disulphide bond between two cysteine residues. (C) Top view of the pentameric receptor. The M2 segments of each subunit define the channel. ACh binding sites are at the interface between subunits. Adapted from Dupuis et al (2012).

Mammalian and insect nAChR subunits differ in amino acid composition, and this influences the pharmacological properties of the receptors (Tomizawa and Casida 2003). Vertebrate nAChRs are assembled with five of sixteen possible subunits, including 9 ligand-binding α units, four structural β units, δ, γ, and ε units; and a single organism may express various nAChR types in different tissues, although only α and β units are found on neuronal receptors (Tomizawa and Casida 2001). Insect nAChRs are composed of α and β units only and the gene families tend to be more compact, with just 10 identified genes in drosophila (Sattelle et al. 2005), and 11 in the honeybee (Dupuis et al. 2012). However, the size of the gene family may not be directly indicative of the diversity of insect nAChRs, as several genes show diversification through post-transcriptional modifications (Sattelle et al. 2005; Jones and Sattelle 2010; Dupuis et al. 2012). The locust genome dwarfs other insect genomes in size by an order of magnitude, with 6,500 Mb in the locust versus 180 Mb in drosophila or 467 Mb in the aphid (Wang et al. 2014), and as many as 39 nAChR subunit-encoding sequences have been identified (Wang et al. 2015a). Alternative splicing of locust nAChR subunit genes has been demonstrated to alter

agonist potency of acetylcholine on the receptors (Zhang et al. 2017), proving that post-transcriptional modifications further amplify nAChR diversity in the locust.

1.5. Cholinergic insecticides

1.5.1. The neonicotinoids

Many insecticides target cholinergic signaling, as the nAChR is the primary excitatory receptor in the insect CNS, and the differences between insect and mammalian nAChRs allows for reduced mammalian toxicity when insecticides are specific for the insect nAChR (Millar and Denholm 2007). To disrupt cholinergic signalling, insecticides have been created that target the breakdown enzyme for ACh, acetylcholinesterase (AChE). This group of organophosphate insecticides is highly effective, but also poses danger for humans and other non-target animals that may be exposed (Kazemi et al. 2012). To mitigate these risks, increasingly more insecticides have been developed that are specific for the insect nAChR, including the large class of neonicotinoid insecticides (neonics) with structural similarities with nicotine. Neonics are classed into three major groups based on structure, including the nitroimines (imidacloprid, clothianidin, thiamethoxam, dinotefuran), nitromethylenes (nithiazine, nitromethylene-IMI, cycloxaprid, nitenpram), and cyanoimines (thiacloprid, acetamiprid) (Casida 2018).

Neonics were developed in the late 1980s from nitromethylene heterocycles, which were known nAChR agonists (Jeschke and Nauen 2008), and since have become extremely popular due to having a high affinity for insect nAChRs, being moderately water soluble, non-ionizable, and functioning as systemic pesticides (Tomizawa and Casida 2001). Neonics can cross the nerve sheath (perineurium) by and enter the insect CNS. They bind to nAChRs, and are not metabolized by AChE (Tomizawa and Casida 2003). The most defining feature of neonics, however, is their use as seed treatments: effective pest control can be applied prophylactically during planting, which has led to a greater dependence and overall use of insecticides in agriculture (Jeschke et al. 2011).

1.5.2. Environmental presence and persistence

Neonics are known to have serious adverse effects on non-target organisms, including important pollinators like the honeybee (*Apis mellifera*), and wetland species including

waterfowl, insectivorous birds, and amphibians (Main et al. 2014). Neonics are currently the most widely used pesticides on the Canadian Prairies: 44% of prairie cropland is treated annually, with canola, wheat, barley, field pea and oat seeds coated with the pesticide. Huge quantities of these pesticides are entering aquatic systems annually: high concentrations are accumulating in wetlands (Main et al. 2014), and can be detected in groundwater, which can have implications for drinking water (Id et al. 2018). Although industry-funded studies claim that neonics do not accumulate in soils (Hilton et al. 2016), neonics have been detected in production fields prior to planting at concentrations above 10 ng/g (Stewart et al. 2014). Neonics pose a threat to aquatic ecosystems, and high concentrations of neonics have been detected in wetlands across the Canadian Prairie, with peaks in detection levels after the winter snowmelt (Main et al. 2016).

1.5.3. Toxicokinetics

To describe the toxicokinetics of an exogenous compound, toxicologists consider the absorption, distribution, metabolism, and excretion (ADME) of the compound. These analyses are often achieved with the use of isotopic labeling, such as carbon-14, which can be tracked as it is processed in an organism. Insects and other organisms are most often exposed to neonics via contact or oral routes. As neonics are commonly applied as seed treatments, contact exposure is most likely to occur via contact with contaminated soil, or with the dust from agricultural planters (Krupke et al. 2012), and thus the risk of contact exposure is highest during planting. Oral exposure can occur through consumption of any part of the treated plant, including its foliage, nectar and pollen (Byrne et al. 2013; Bonmatin et al. 2015). For the purposes of this review, focus will be directed to the pharmacokinetics of neonics in insects only.

Contact exposure requires that the neonic absorbs through the cuticle, which is comprised of a lipophilic epicuticle and a hydrophilic chitin-protein procuticle (Giraud-Guille 1984). A comparison of the absorption of three neonics (imidacloprid, thiacloprid, acetamiprid) through the cuticle of honeybees shows that not all neonics are absorbed at the same rate: thiacloprid absorbs the least, while imidacloprid absorbs the fastest and accumulates quickly in the bee (Zaworra et al. 2019). These differences in absorption are related to the polarity of the molecules: imidacloprid is more polar (log P_{ow}=0.57) than thiacloprid (log P_{ow}=1.26). After oral exposure to neonics, the compounds first must pass through the gut before being distributed

throughout the insect's body in the hemolymph. The distribution of ^{14}C-imidacloprid in the honeybee after oral exposure is fast: radiation peaks in the thorax and abdomen just 20 minutes after oral exposure, while that in the hemolymph, head, midgut and rectum peak only 2, 6, 10 and 24 hours after exposure, respectively (Suchail et al. 2004). Similarly, the distribution of ^{14}C-acetamiprid in the honeybee has a peak in radioactivity in the abdomen 30 minutes after exposure, while in the midgut, thorax, hemolymph and head levels were low until 2 hours after exposure and then remained stable until 72 hours (Brunet et al. 2005).

Contrasting the natural nAChR ligand, acetylcholine, neonics are not broken down by AChE and must either be displaced by high concentrations of acetylcholine, or metabolized by detoxification enzymes (Tomizawa and Casida 2005). The largest group of detoxification enzymes are the cytochrome P450 monooxygenases (CYP450) isozymes. These enzymes are involved in oxidative metabolism of a wide variety of pesticides in locusts (Guo et al. 2012; Wang et al. 2015b), with CYP6G1 being primary in phase I metabolism of IMD (Saha 2016). Imidacloprid is metabolized via hydroxylation, oxidative cleavage of the methylene bridge, or reduction of the nitro group (Suchail et al. 2004; Casida 2011) (Figure 1.6).

In honeybees, IMD has a 5 hour elimination half-life and is completely metabolized within 24 hours, while its metabolites persist for over 30h (Suchail et al. 2004). IMD-olefin and the hydroxy-imidacloprid metabolites may be more neurotoxic than the parent compound (Suchail et al. 2000), so, despite clearance of the parent compound, toxic effects may be sustained or secondary effects may occur. The IMD-olefin metabolite is more lipophilic than IMD (low Pow = 1.22 versus 0.57), suggesting its toxicokinetics would differ from the parent compound. In addition, the epoxide formed spontaneously from the olefin metabolite could cause oxidative damage. Neonic metabolites can be detected in beehives and honey at much higher concentrations than the original forms (Codling et al. 2016). As the metabolites display insecticidal properties, increased focus should be on all neonicotinoid derivatives when determining environmental concentrations and describing toxicological endpoints.

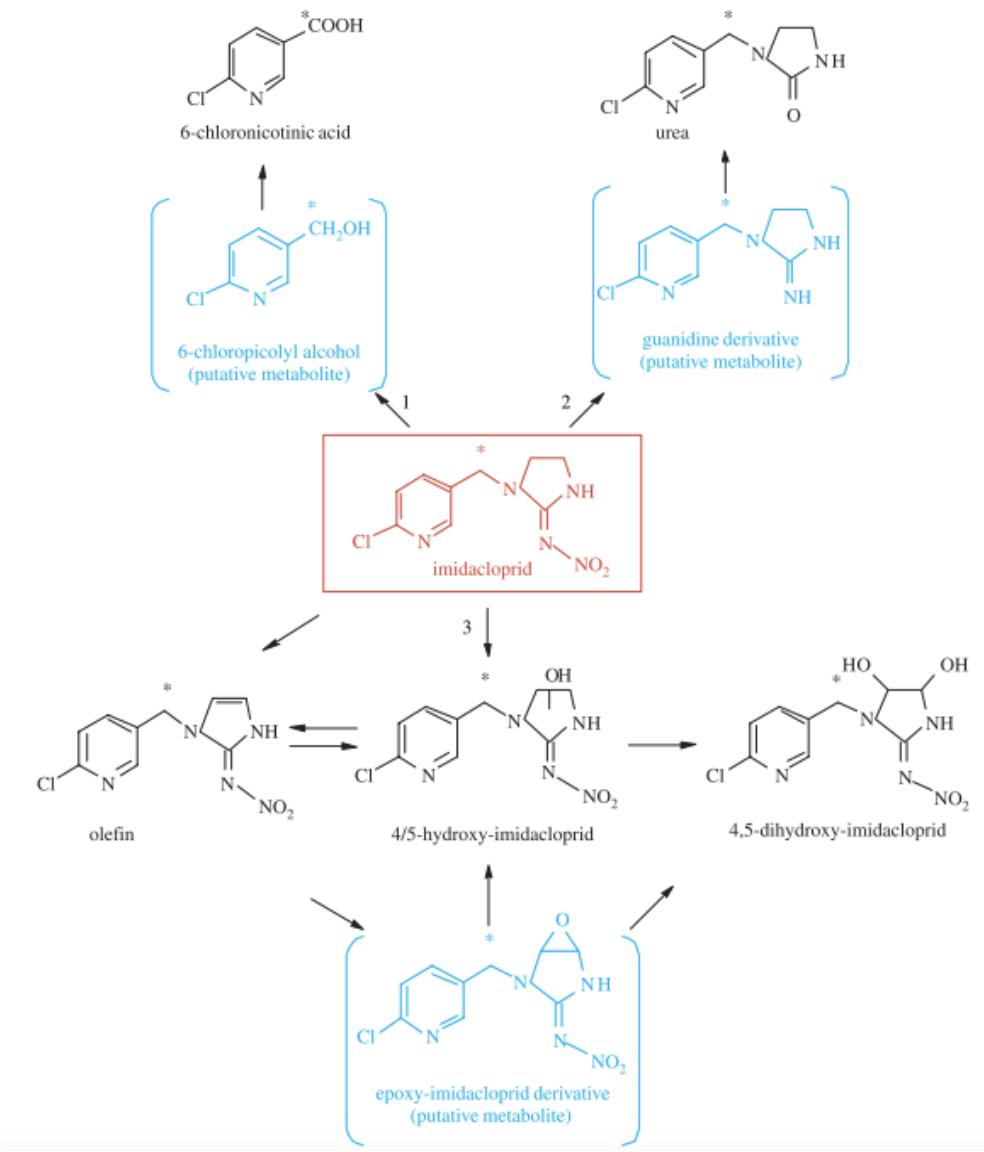

Figure 1.6: Proposed metabolic pathway of imidacloprid in the honeybee. The 6-chloronicotinic acid metabolite is formed by oxidative cleavage of the methylene bridge (1). The urea derivative is formed by reduction of the nitro group (2). CYP6G1 catalyzes the hydroxylation of IMD to 4/5-hydroxyimidacloprid and 4,5-dihydroxyimidacloprid (3), while the olefin metabolite may be produced non-enzymatically or via 4/5 hydroxyimidacloprid. Hydroxy-imidacloprid metabolites can also be formed via the epoxide derivative from the olefin metabolite. From Suchail et al (2004).

1.5.4. The molecular initiating event: neonic binding the nAChR

The nAChR has proven to be an effective insecticide target, due to the differences in subunit composition between mammals and insects, and the localization of these receptors throughout the insect CNS. In addition to enhancement of detoxification pathways, neonic

resistance may arise from alterations to the target site (Saha 2016). Neonics affect the expression of nAChR subunits by regulating the transcription of these genes, which results in an alteration in sensitivity to the neonic (Markussen and Kristensen 2010; Wang et al. 2015b). Both ACh and neonics bind the orthosteric site of the insect nAChR (Taly et al. 2009; Ihara et al. 2015). Despite ACh being the endogenous ligand of all nAChRs, specificity of neonics to invertebrate nAChRs is dependent on differences in charge within the binding site. Although neonics are nicotine mimics, nicotine binds to the anionic subunit of mammalian nAChRs, while neonics bind a cationic subunit of insect nAChRs (Tomizawa and Casida 2003). The result is that despite structural similarities to nicotine, neonics are specific to insect nAChR subunits. Neonics are generally considered agonists, and binding to the nAChR opens cation channels (Casida and Durkin 2013), resulting in the influx of sodium (Na^+) and calcium ions (Ca^{2+}), and the efflux of potassium ions (Jones and Sattelle 2010). There is also interaction with voltage-gated calcium channels (Jepson et al. 2006), which further disrupts Ca^{2+} signalling within affected neurons. Although neonics show specificity to insect versus mammalian nAChRs, there exists a vast diversity of nAChR subunits within and between insect species, and this results in differential binding and activity at these receptors. In locusts, there are three identified β subunits, and two of these, Locβ1 and Locβ3 form two distinct low (K_d = 10.31 nM) and high (K_d = 0.16 nM) affinity imidacloprid binding sites, respectively (Bao et al. 2017).

In the cockroach, two identified nAChR subtypes, one that is sensitive to imidacloprid (nAChR1) and one insensitive (nAChR2), are shown to be affected by chronic treatment with imidacloprid (Benzidane et al. 2017). The nAChR1 displays reduced sensitivity with chronic treatment, shown through reduced current density flowing through the receptor, and the conductance of both subtypes was altered, related to altered steady-state intracellular calcium $[Ca^{2+}]_i$ (Benzidane et al. 2017). The desensitization of nAChR1 in the cockroach with chronic exposure to imidacloprid may be an adaptive mechanism to optimize the functional properties of the insensitive nAChR2. Receptor desensitization by imidacloprid has also been shown to be subtype-specific in neurons of other insects, including the stick insect (Oliveira et al. 2011). Desensitization can be caused by prolonged stimulation by any exogenous or endogenous nAChR ligand resulting in the pore being blocked and inactivated (Quick and Lester 2002). The desensitized receptor has a high affinity for the agonist, which results in an inactivated state that remains until the agonist is removed (Ochoa et al. 1989). Receptor desensitization has been

shown to be elicited by various nAChR agonists in thoracic ganglion neurons of the locust, effectively blocking ACh-induced inward currents with prolonged exposure (Zwart et al. 1994). The rate of recovery from receptor desensitization is dependent on receptor phosphorylation, and phosphorylation sites exist on the nAChR for calcium-calmodulin-dependent protein kinase (Thany et al. 2007). Adverse Outcome Pathways (Figure 1.7) have been proposed for honeybees exposed to neonics, that attempt to link the activation of nAChRs with ultimate effects on whole colony survival (LaLone et al. 2017). These pathways propose differing mechanisms of neural dysregulation that are discussed in detail in the following section.

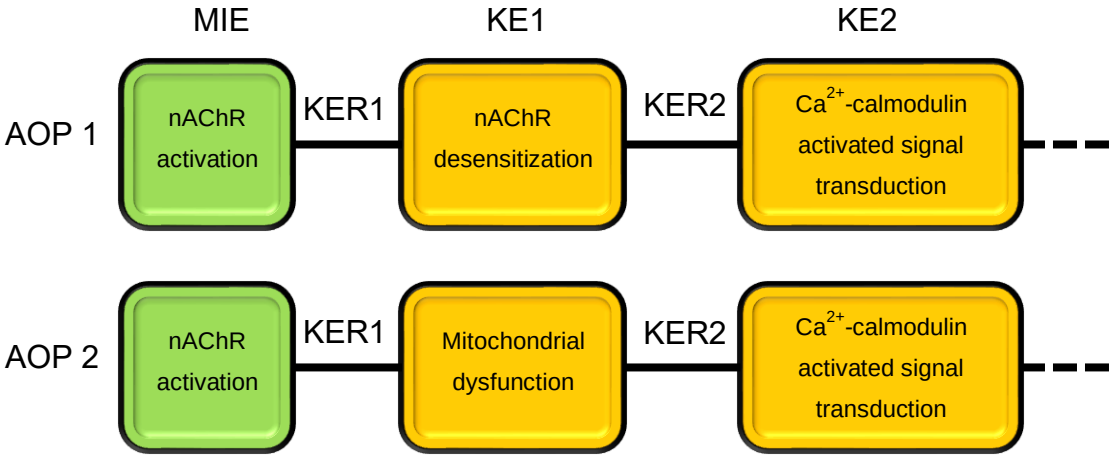

Figure 1.7: The molecular initiating event (MIE) and two Key Events (KEs) proposed in Adverse Outcome Pathways (AOPs) by Lalone et al (2017). These pathways differ in the first KE following nAChR activation, but both lead to the eventual disruption of calcium-calmodulin activated signal transduction.

1.5.5. Cellular effects

Disrupted neural function is the primary proximal effect of neonicotinoid exposure, resulting in major downstream effects on many aspects of animal physiology and behaviour. However, the agonistic effect of neonicotinoids has additional cellular effects compared to ACh, which result in a cascade of downstream consequences that can jeopardize the function and survival of cells.

Mitochondrial dysfunction

Mitochondrial dysfunction related to neonic toxicity can be explained by the localization of nAChRs on the outer membrane of the mitochondria (Gergalova et al. 2012), in addition to high levels of $[Ca^{2+}]_i$ that result from prolonged excitation (Peng and Jou 2010). Although

nAChRs have not been directly identified on insect mitochondria, their presence has been demonstrated by mitochondrial depolarization of isolated bumblebee mitochondria following exposure to nAChR agonists, including the neonics clothianidin and imidacloprid (Moffat et al. 2015). Imidacloprid, additionally, has been shown to inhibit ATP production in isolated honeybee mitochondria (Nicodemo et al. 2014). Mitochondria have important roles in mediating apoptosis, in addition to their importance for ATP production. This is achieved via the sequestration of Ca^{2+} and release of cytochrome *c*, processes which are mediated by the voltage dependent anion-selective channel that is likely coupled with the mitochondrial nAChR (Gergalova et al. 2012). A second mechanism by which neonics affect mitochondria is via the increase in $[Ca^{2+}]_i$ that follows prolonged stimulation of the nAChRs on the cell membrane (Tomizawa 2002; Jepson et al. 2006). When $[Ca^{2+}]_i$ reaches a critical level of concentration, Ca^{2+} channels are opened on the mitochondrial membrane, where high concentrations of Ca^{2+} will disrupt normal metabolic function and may lead to cell death (Ermak and Davies 2002). Thus, the involvement of mitochondria may be important both in the initial phase prior to receptor desensitization as well as offering an additional target for the insecticides.

Calcium and calcium signalling

Calcium acts as a messenger within the neuron, where it binds to calmodulin (CaM) and initiates a signalling cascade that leads to the production of proteins that direct synaptic plasticity, and an imbalance of $[Ca^{2+}]_i$ can lead to cell death (Uteshev 2012). Under normal conditions, such as those elicited by presynaptic release of the endogenous ligand ACh, Ca^{2+} is then sequestered primarily by the endoplasmic reticulum, and the intracellular environment is returned rapidly to resting conditions. Imidacloprid, however, induces transient and repeatable increases in $[Ca^{2+}]_i$ in cultured cholinergic drosophila central neurons, that is blocked by 60-70% with the addition of Cd^{2+}, a voltage-gated calcium channel (VGCC) antagonist (Jepson et al. 2006). The neonic-induced increase in $[Ca^{2+}]_i$ is thus mediated primarily by the VGCC, which may be due to close localization of these channels on the membrane. This influx of Ca^{2+} resulting from nAChR and VGCC activation is further amplified by the recruitment of intracellular Ca^{2+} stores (Tsuneki et al. 2000). Thus, the interaction of neonicotinoids and $[Ca^{2+}]_i$ are intimately linked, both in a transient manner, as seen during the agonistic activity of the ligand, and as a

downstream effect of either mitochondrial dysfunction, or reduced Ca^{2+} permeability, resulting from nAChR desensitization.

Calcium-calmodulin (Ca^{2+}-CaM) activated signal transduction may be disrupted with neonicotinoid toxicity due to effects on mitochondrial function, as a critical step in the pathway is the input of ATP produced by the mitochondria (Nicholls and Budd 2000). The mechanism by which receptor desensitization could result in altered Ca^{2+}-CaM signalling involves a sustained decrease in $[Ca^{2+}]_i$ resulting from blocked nAChR pores (LaLone et al. 2017). This effect would be self-perpetuating, due to the phosphorylation sites on the nAChR that regulate the rate of receptor recovery after desensitization by altering the activity of Ca^{2+}-CaM -dependent protein kinase (Thany et al. 2007). This mechanism of Ca^{2+} dysregulation contrasts the mitochondrial dysfunction mechanism, but ultimately would result in similar downstream effects on the pathway. An investigation of protein kinase A transcripts in honeybee brain following neonic exposure (imidacloprid) found a significant decrease in expression, confirming neonic-induced effects on Ca^{2+}-CaM signalling (Christen et al. 2016).

Oxidative stress

The generation of reactive oxygen species (ROS) can result as a downstream effect of Ca^{2+} excitotoxicity (Hermann et al. 2015). This process occurs as a result of mitochondrial Ca^{2+} overload, with potential mechanisms of ROS production including a Ca^{2+}-induced increase in metabolic rate, nitric oxide production, cytochrome *c* dissociation, and Ca^{2+}-CaM dependent protein kinase activation (Peng and Jou 2010). Oxidative stress is associated with many downstream effects on vertebrate and invertebrate cells including increased lipid peroxidation, DNA damage, and protein damage, and this has been identified as a key mechanism of neonicotinoid toxicity (Wang et al. 2018c). In cotton bollworm larvae, dose and time-dependent increases in oxidative stress result from exposure to imidacloprid (Nareshkumar et al. 2018). This increase is measured as an increase in lipid peroxidation, lactate dehydrogenase activity, and accumulation of H_2O_2, with a reduction in catalase and superoxide dismutase (Nareshkumar et al. 2018). Importantly, ROS can cause calcium to be released from $[Ca^{2+}]_i$ stores, including the endoplasmic reticulum (Roveri et al. 1992), resulting in a feedforward loop.

Apoptosis

Ca^{2+} plays a major role in cell death, both in necrosis, which results from severe Ca^{2+} dysregulation, and in apoptosis. Ca^{2+} release from the endoplasmic reticulum and Ca^{2+} influx through Ca^{2+} channels are implicated in the initiation of apoptotic pathways, which generally follow a more controlled increase in $[Ca^{2+}]_i$ (Pinton and Rizzuto 2006). The primary effector of the apoptotic pathway is cytochrome *c*, which is released from the mitochondria when Ca^{2+} concentrations are too high. This molecule drives the assembly of the 'apoptosome' consisting of a caspases activating complex together with apoptosis-protease activating factor 1 and caspase 9 (Hill et al. 2003; Pinton et al. 2008).

There are several examples of neonicotinoid-induced apoptosis in the literature, both in vertebrate and invertebrate systems. Imidacloprid induces apoptosis in hippocampal neurons in the Formosan leaf-nosed bat, resulting in impaired spatial memory (Hsiao et al. 2016). In the honeybee, imidacloprid induces apoptosis in the central nervous system resulting in increased apoptotic markers, including neuronal activated caspase-3 and mRNA levels of caspase-1 (Wu et al. 2015). Condensed cells, that result from apoptotic cell death, are concentrated specifically in the optic lobes following treatment with imidacloprid in the Africanized bee (De Almeida Rossi et al. 2013), suggesting that this brain area may be affected to the greatest degree in this species.

1.5.6. Effects on brain and behaviour

There are many documented effects of neonicotinoids on myriad behavioural traits and outcomes. Between studies these effects may contrast completely, these differences depending primarily on dose and time. Toxic effects often initially involve increased motor activity and increased nervous system excitability, while over time these effects shift towards decreased function and activity, which may be associated with the agonistic versus desensitizing effects of the compounds. In general, purely behavioural experiments show results that may be explained in different ways, and often the meaning of the results is disputed between scientific groups. To properly explain whether a behavioural deficit is due to issues on learning and memory, motor control, or sensory processing, it is necessary to look to the nervous system. The studies below that employed neuroethological methods, or those that strived to explain effects of neonicotinoids on behaviour by also determining what aspect of neural processing was affected, are far stronger and have more conclusive results.

Learning and memory

Many experiments have been performed testing the effects of IMD on the proboscis extension reflex (PER) in honeybees. When honeybees are chronically exposed to field realistic concentrations of imidacloprid, olfactory learning and memory formation is impaired resulting in an impaired conditioning of the PER towards an odor associated with reward (Williamson et al. 2013). Contrasting this, however, is that a slight improvement in olfactory learning is produced with an acute, sublethal dose of imidacloprid (Williamson et al. 2013). This is likely due to the low dose causing a slight increase in cholinergic signalling within the mushroom bodies and antennal lobes (Thany and Gauthier 2005). Neonics act as partial agonists of nAChRs on dissociated Kenyon cells (Déglise et al. 2002), which are the primary neural cell types of the mushroom bodies. A mechanism by which neonicotinoids are affecting learning and memory involves Kenyon cell inactivation in the mushroom bodies following prolonged activation of Kenyon cells by neonics (Palmer et al. 2013). Neonics affect odour coding in antennal lobes upstream of the mushroom bodies (Andrione et al. 2016), which signifies that the perception of odour is altered. Traditional odour-association tests are used as measures of learning and memory ability, and do not control for ineffective odour perception. Whether there are similar effects of neonics on primary gustatory processing areas has yet to be shown, but this may offer an alternate explanation to the effects observed on learning and memory.

While the disruption of olfactory learning by neonics and pesticide mixtures has been well established, effects on visual learning are contested. A recent study on bumblebee foraging behaviour found that while motivation and return to rewarding food sources was decreased after imidacloprid exposure, the ability to associate a floral colour with reward was not affected (Muth and Leonard 2019). The authors suggest that imidacloprid does not affect learning and memory, but rather affects food motivation and motor control. A previous study, however, found that exposure to low levels of imidacloprid (2.6 and 10 ppb) affected the ability of bumblebees to associate flower colour with reward value, and while this may be associated with reduced flower sampling, it could also result from impaired visual learning (Phelps et al. 2018).
Other forms of memory retention, including association of an aversive stimulus such as a biting predator with a floral odour, are affected by chronic imidacloprid exposure (Zhang and Nieh 2015).

Foraging & Navigation

Significant evidence exists showing the detriment of neonic pesticides to many important pollinators, especially bees. It is argued, however, that pollinators may not be at a high risk due to its low field concentrations and the presence of untreated food sources, such as wildflower fields. Unfortunately, very low chronic doses can have significant effects on both individuals and the hive. Even when protective measures are in place to reduce bee toxicity, such as planting floral plants in the margins between fields in the hopes that pollinators will choose these flowers instead of the treated plants, toxicity remains high among pollinators. Neonics in dust produced during sowing can drift to these nearby plants (Botías et al. 2015), and perhaps even more importantly, honeybees and bumblebees have been found to prefer foods that contain neonics despite not being able to detect these compounds in nectar (Kessler et al. 2015). Another study found that bumblebees will preferentially visit feeders that are laced with neonics, even when these feeders are moved (Arce et al. 2018). Although this may present evidence that the bees can detect the compounds, it could also indicate that the preference for treated food is acquired rapidly at novel locations. Other honeybee species, including *Apis cerana* which are native to Asia, also show a strong preference for neonic-laced foods, and show decreased predator avoidance at these feeders (Tan et al. 2014).

A common effect of neonicotinoids that occurs shortly after intoxication with a sublethal concentration is agitation and excitation, which can be expressed by increased flight duration and distance in honeybees (Tosi et al. 2017). This effect, however, tends to be reversed with chronic exposure, where a decrease in flight duration, distance and even velocity is observed (Tosi et al. 2017). Low doses of neonics have been shown to affect bee navigation. Reduced navigational ability for both vector and homing flight has been observed with doses as low as 2.5 ng/bee, while treatment at this dose did not affect flight ability nor demonstrated desire to return to the hive (Fischer et al. 2014). This shows the pesticide preferentially affects long-term memory, as the homing phase of flight, which requires activating remote memories from the bee's exploratory flights earlier in life, are most significantly inhibited. Solitary bees are also important pollinators, and their retrieval of navigational memory is significantly impaired with low, ecologically relevant doses of neonics (Jin et al. 2015). Chronic exposure of bumblebees with neonic (2.4 ppb thiamethoxam) results in longer foraging trips and improved homing ability, despite returning with less pollen, indicating reduced foraging performance (Stanley et al. 2016).

Contrasting this, honeybees exposed to low doses of thiamethoxam display reduced homing flight ability, with many exposed bees displaying mortality due to postexposure homing failure, and a significantly reduced proportion of treated bees returning to the hive (Henry et al. 2012). Although many studies looking at the effects of neonics on foraging and navigation associate affected behaviours with deficits in learning and memory, it is equally possible that these effects derive from deficits with visual motion detection. Bees use visual motion detection to calculate speed and distance (Dacke and Srinivasan 2007), thus disruption of this processing could result in bees that ineffectively estimate the distance of food sources from the hive resulting in decreased return trips to favorable food sources and to the hive. Despite this plausible explanation, no studies have looked into whether neonics affect visual motion detection in bees.

1.5.7. Novel cholinergic insecticides

Novel cholinergic insecticides are being developed to provide alternatives to widely used insecticides that become less effective following target organism resistance, or to replace insecticides that are known to cause severe damage to the ecosystem. A major class of these insecticides are the sulfoximines, with its primary compound sulfoxaflor already being used in pesticide mixtures like Visivio (Syngenta Seed Care, Switzerland). Sulfoxaflor targets the nAChR and is highly effective as a broad-spectrum insecticide against many sap-feeding pests (Zhu et al. 2011). These insecticides are detoxified through a different pathway than the neonicotinoids (Zhu et al. 2011), which results in low cross-resistance with neonics in species that display reduced sensitivity to neonics (Longhurst et al. 2013). Sulfoximines possess different structure activity relationships compared to other insecticides, which are thought to provide increased insecticidal activity and set this class of insecticides apart from the neonics (Sparks et al. 2013). There is concern from the scientific community over the mitigation measures implemented in light of the development of new insecticides, with major concerns arising over the potential of novel insecticides to harm the ecosystem (Centner et al. 2018). Indeed, one study has already reported a reduction in bumblebee reproductive success following chronic exposure to sulfoxaflor (Siviter et al. 2018). The implementation of toxicity testing that can define sublethal effects of these novel compounds on non-target organisms is vital to ensure a reduction of the detriment caused by agrochemicals in the environment.

1.6. Research questions

Neonics are known to affect various aspects of flight and navigation, although the cause of these effects is not always clear using purely behavioural experiments. It is generally thought that navigational deficits result from impairments to memory, although another option exists: insects, like bees, use neural calculations of optic flow, or the movement of the visual scene during flight, to calculate distance and velocity. If there are deficits with the processing of visual information, we would expect these insects to have trouble calculating distance during flight, which would result in insects that could not perform accurate homing flights or return to a rewarding food source. We can use the well-described collision avoidance pathway in the locust to answer questions related to whether cholinergic insecticides affect visual motion detection. My main objective was to assess how these nAChR agonists may be disrupting this important and highly conserved pathway. The following questions guided the experiments:

How does the neonic imidacloprid affect visual motion detection by a looming-sensitive interneuron, and what effects does it have on collision avoidance behaviour? In Chapter 2, I perform electrophysiological assays to record DCMD responses to looming stimuli, 2 and 24 hours after treatment with a sublethal dose of imidacloprid. I additionally test two escape behaviours, jumping and flight steering, at these doses and time points. Chapter 2 strives to reveal whether imidacloprid, a neonic, affects the activity of the DCMD neuron in response to looming stimuli, and if there are downstream effects on collision avoidance behaviour. I hypothesized that imidacloprid would alter the firing properties of this neuron, resulting in impaired flight and avoidance behaviour. The results from Chapter 2 led to the design of experiments for Chapters 3 and 4, which answer the following questions.

Do metabolites of imidacloprid display neurotoxicity and effects on behaviour, and how does this compare to the parent compound? The main purpose of Chapter 3 was to characterize whether two metabolites of imidacloprid, imidacloprid-olefin (OLE) and 5-hydroxy-imidacloprid (5OH) affect DCMD firing and collision avoidance behaviour. Additionally, using a different electrophysiological method, I examined putative effects on conduction velocity along the DCMD axon. I hypothesized that neonicotinoid metabolites would cause an effect similar to the

parent compound measured at 2 hours after treatment, due to the parent compound requiring time to metabolize into these compounds. Additionally, I hypothesized that I would see an effect on conduction velocity, due to the effect of these compounds on $[Ca^{2+}]_i$ that would affect VGCCs.

How does the toxicity of imidacloprid compare to the novel cholinergic insecticide sulfoxaflor on population responses of descending visual interneurons? In Chapter 4, I propose the utility of these neuroethological assays in comparative toxicology. For these experiments I compared the effects of imidacloprid with sulfoxaflor on visual motion detection and collision avoidance behaviour. Additionally, I used a more sophisticated electrophysiological technique to record the population responses of multiple descending neurons responding to object motion.

1.7. Projected significance

These studies are among the first to examine whether neonicotinoid and sulfoxaflor insecticides affect visual motion processing in an insect. If visual motion processing is disrupted by exposure to low doses of these insecticides, this could result in effects on a variety of downstream behaviours, including navigation and escape behaviours. Neonics are already known to affect navigation, but whether there are effects on escape behaviour has not previously been tested. The results from Chapter 3 show whether neonic metabolites display toxicological properties similar to the parent compound. As these metabolites are found both in the environment and are metabolized within affected organisms, results from these experiments highlight the risks posed to insects. The results from Chapter 4 are important in that they show effects of imidacloprid and the novel insecticide sulfoxaflor on multiple descending neurons and facilitate the construction of a more complete picture of what is occurring with neonic toxicity the optic lobes to result in these observed effects. The results from this chapter additionally inform basic science: few studies have looked at the population responses of descending visual interneurons in insects, and no previous studies have examined how the population of neurons habituates in the locust.

Chapter 2: A sublethal dose of a neonicotinoid insecticide disrupts visual processing and collision avoidance behaviour in *Locusta migratoria*[1]

2.1. Abstract

Neonicotinoids are known to affect insect navigation and vision, however the mechanisms of these effects are not fully understood. A visual motion sensitive neuron in the locust, the Descending Contralateral Movement Detector (DCMD), integrates visual information and is involved in eliciting escape behaviours. The DCMD receives encoded input from the compound eyes and monosynaptically excites motorneurons involved in flight and jumping. I show that imidacloprid (IMD) impairs neural responses to visual stimuli at sublethal concentrations, and these effects are sustained two and twenty-four hours after treatment. Most significantly, IMD disrupted bursting, a coding property important for motion detection. Specifically, IMD reduced the DCMD peak firing rate within bursts at ecologically relevant doses of 10 ng/g (ng IMD per g locust body weight). Effects on DCMD firing translate to deficits in collision avoidance behaviours: exposure to 10 ng/g IMD attenuates escape manoeuvers while 100 ng/g IMD prevents the ability to fly and walk. I show that, at ecologically-relevant doses, IMD causes significant and lasting impairment of an important pathway involved with visual sensory coding

[1] The content of this chapter comes from the following published manuscript. Formatting and layout changes have been made to provide consistency between chapters.

Parkinson RH, Little JM, Gray JR (2017). A sublethal dose of a neonicotinoid insecticide disrupts visual processing and collision avoidance behaviour in Locusta migratoria. Scientific Reports 7:1-13.

Author contributions & justification for use in this thesis: R.H.P. designed and carried out experimentation, analyzed the data, interpreted the results, prepared the figures, and wrote and revised the manuscript. J.M.L. carried out experimentation and analyzed video data. J.R.G. conceived and designed experiments, interpreted the results, revised the manuscript, and approved the final version of the manuscript.

and escape behaviours. These results show, for the first time, that a neonicotinoid pesticide directly impairs an important, taxonomically conserved, motion-sensitive visual network.

2.2. Introduction

Neonicotinoid insecticides dominate a quarter of the global pesticide market (Jeschke et al. 2011). Widespread neonic crop treatment has increased overall pesticide use across North America (Douglas and Tooker 2015), despite growing evidence of toxic effects on wild and domestic bee populations (Rundlöf et al. 2015; Woodcock et al. 2016), aquatic invertebrates (van der Sluijs et al. 2015; Vehovszky et al. 2015; Cavallaro et al. 2016), and insectivorous birds (Hallmann et al. 2014). Neonics contaminate wetlands, via runoff and snowmelt from treated fields (Main et al. 2016), and wildflower and soil samples near treated fields at concentrations exceeding 10 ng/g (Stewart et al. 2014).

Neonics are nicotine mimics, binding to invertebrate nicotinic acetylcholine receptor (nAChR) subunits (Tomizawa and Casida 2005). Although commonly considered nAChR agonists, neonics also display antagonistic activity in some invertebrate species (Nguyen et al. 2012; Vehovszky et al. 2015) and at certain doses (Benson 1992), suggesting that there are multiple nAChR binding sites (Matsuda et al. 2009). Different neonic compounds target different neurons and nAChR subtypes (Moffat et al. 2016) and neonic metabolites may cause toxicity (Suchail et al. 2001; Nauen et al. 2001), accumulating at higher concentrations than the parent compounds (Codling et al. 2016). For example, imidacloprid (IMD) has a 5 hour elimination half-life in honey bees and is completely metabolized within 24h, while its metabolites persist for over 30h (Suchail et al. 2004). In addition, IMD metabolites, including IMD-olefin, are more toxic than IMD (Suchail et al. 2004).

Neonics display sublethal, neurotoxic effects in honeybees that range from altering food preferences (Kessler et al. 2015) to impairing navigation and foraging success (Henry et al. 2012; Tan et al. 2014; Fischer et al. 2014). Bee mushroom bodies have been a major focus of neonicotinoid research, given observed behavioural effects and speculation of a connection between neonic use and colony collapse disorder. Chronic neonic toxicity results in apoptosis and neuronal inactivation in the central nervous systems of bees and bats (Palmer et al. 2013; Wu et al. 2015; Hsiao et al. 2016) and markers of apoptosis have been shown to concentrate in the

optic lobes of the honey bee within 24 hours of an acute dose (De Almeida Rossi et al. 2013). Although generalized neuronal effects on the central nervous system have been demonstrated (Palmer et al. 2013; Wu et al. 2015), the effects on an important visual networks has not been examined. The locust offers a highly tractable, ubiquitous system to directly address putative effects of neonic toxicity on a well characterized motion sensitive network.

The locust nervous system has been studied extensively, initially in search of novel insecticide targets, and then increasingly as a system to investigate fundamental neural processes that control behaviour. Locusts display varied collision avoidance behaviours and possess tractable motion-sensitive visual neurons. Two of these neurons are the lobula giant movement detector (LGMD), which receives encoded visual information from retinotopic units (photoreceptors and corresponding optic lobe interneurons), and its postsynaptic partner, the descending contralateral movement detector (DCMD) (Rind 1984). The LGMD/DCMD pathway responds robustly to objects approaching on a direct collision course (looming) (Judge and Rind 1997), with peak firing rates occurring when the object surpasses an angular threshold on the retina (Gabbiani et al. 2001). These neurons also encode trajectory changes (Dick and Gray 2014) and maintain robust responses with the addition of complex backgrounds (Silva et al. 2015; Yakubowski et al. 2016). The response profile of the LGMD/DCMD results from an interplay of excitatory and inhibitory inputs. Optic lobe interneurons effect excitatory post synaptic potentials in the dendritic field of the LGMD (Burrows 1996). These synapses are nicotinic cholinergic, based on the presence of the enzymes for acetylcholine synthesis in the LGMD and retinotopic units (Rind and Leitinger 2000), and cholinesterase in the synapses (Rind and Simmons 1998). Inhibitory synapses between neighboring retinotopic units (lateral inhibition) and between retinotopic units and the LGMD (feed forward inhibition) act to modulate and shape responses to object motion (Rind and Simmons 1998).

The axon of each DCMD synapses monosynaptically with motorneurons in the thorax, including the fast extensor tibiae (FETi) and flight motorneurons in the meso- and metathoracic ganglia (Simmons 1980; Burrows 1996). DCMD action potentials evoke subthreshold EPSPs in these motorneurons (Simmons 1980; Santer et al. 2006; Rogers et al. 2007), and high-frequency DCMD spikes may summate temporally, resulting in spiking in motorneurons during flight as the membrane potential fluctuates due to activity (Santer et al. 2006; Rogers et al. 2007). Bursting (brief intervals of high frequency spiking) of DCMD spikes occur in response to object

approach and may play an important role in collision detection and generating escape behaviours (McMillan and Gray 2015).

This tractable locust collision detection system provides a unique opportunity to examine the effects of a commonly used pesticide on visual sensory coding and visually-guided behaviours. Here, I show that an ecologically-relevant sublethal dose of IMD disrupts normal firing properties of the DCMD when the locust is presented with a looming stimulus, and that these disruptions are reflected by deficits in their ability to avoid collisions by flight steering or jumping. I show that behavioural effects are sustained 2 and 24 hours after an acute dose of IMD, and these correspond to significant decreases in peak DCMD firing rates within bursts. These findings support the hypothesis that collision avoidance behaviours depend critically on high DCMD firing rates within bursts. As DCMD-like neurons have been found in other invertebrate species, including the praying mantis (Yamawaki and Toh 2009b), crab (Medan et al. 2007), and fruit fly (Fotowat et al. 2009), these results have broader implications for invertebrates that rely on vision for navigation. For the first time, I show IMD directly impairs a visual motion detection pathway and collision avoidance behaviours at sublethal doses.

2.3. Methods

2.3.1. Animals

Adult locusts (*Locusta migratoria*) were selected at least 2 weeks past the last imaginal moult and reared on a diet of wheat grass and bran in a crowded colony in the Department of Biology, University of Saskatchewan, Canada, at 25-30°C, with a 12h light:12h dark cycle. Males were used for behavioural assays (n = 35) and electrophysiology (n = 65), while both males and females were used for the LD50 tests (n = 226). All locusts were weighed prior to experimentation to adjust injected dose by weight. Median locust weight was 1.4 g (range = 1.1 to 1.9 g) for males, and 2.5 g (range = 1.6 to 3.6 g) for females.

2.3.2. Solutions

Imidacloprid (IMD; Pestanal, Sigma-Aldrich, Oakville, Ontario, Canada) was dissolved in acetone (100% v/v) and diluted with locust saline (147 mmol NaCl, 10 mmol KCl, 4 mmol CaCl2, 3 mmol NaOH, 10 mmol Hepes, pH 7.2) to produce final concentrations ranging from

0.1 µg/ml to 10 mg/ml. Final solutions were adjusted to each contain 0.2% (v/v) acetone. A solution containing locust saline and 0.2% acetone was used as the vehicle control in all experiments.

2.3.3. LD50

Prior to tests, animals were given ad libitum access to food. A total of 160 male and 66 female animals were used in LD50 assays over 22 replicates. 16 IMD doses between 10 and 10,000 ng/g were used. A vehicle control group was included on each trial day. Animals were treated by injecting 1 µl solution per gram of body mass through the lateral cervical cuticle. After 48 hours, the proportion of deceased animals was calculated, and this was normalized to the proportion of deceased animals in the vehicle group. Percent mortality was plotted against the logarithm of the dose to allow estimation of the 48h LD50 with a fitted curve.

2.3.4. Wind tunnel

A 0.9x0.9x3 m Plexiglass wind tunnel was utilized for behavioural assays. A rear projection screen, mounted on the right side of the wind tunnel, displayed the visual stimulus: the image of a 14 cm black disk, approaching the animal at 300 cm/s on a direct collision course. The stimulus was created with Vision Egg visual stimulus generation software (Straw 2008) on a Python programming platform. For jumping assays, locusts were oriented 15 cm from and parallel to the rear-projection screen so that the center of the stimulus was in line with the center of the eye and wind was not used. For flying assays, locusts were loosely tethered with fishing line 35cm from the centre of the stimulus and wind speed was set to 3 m/s, which is comparable to a locust's natural flight speed (3–6 m/s) (Baker et al. 1981). To capture 3D movement of the locusts, two GoPro HERO4 Black (GoPro, Inc., San Mateo, California, United States) cameras were mounted 33° apart, 114 cm behind the animals, set to 1080p, 120 frames per second.

2.3.5. Behaviour assays

35 locusts were tested 2 and 24 hours after injection with 10 (n = 10), or 100 (n = 10) ng/g IMD, or the vehicle (n = 15). A 3D-printed tether (0.2 g) was attached to the dorsal pronotum with VetbondTM Tissue Adhesive 1469SB (3M Animal Care Products, St. Paul, MN, USA) to capture body orientation. Animals were loosely tethered to the roof of the wind tunnel

with fishing line. Stationary animals were presented with three stimulus replicates at 5 minute intervals and scored as responders if they jumped or twitched hind legs in response to at least one stimulus presentation. Suspended animals were scored as responding (R) if they reacted to at least one stimulus presentation by gliding or turning, not responding (NR) if they were flying but not reacting to the stimulus, or not flying (NF) if they were unable to fly.

2.3.6. Flight simulator

Electrophysiological experiments were conducted with animals mounted in a flight simulator with a rear-projection dome, as described in Guest and Gray (Guest and Gray 2006). The stimulus was the image of a 7 cm black disk traveling at 300 cm/s, created with Vision Egg visual stimulus generation software (Straw 2008) on a Python programming platform and represented as a 1,024 x 1,024 pixel portable network graphics (png) file. Vision Egg code contained correction factors to account for the curvature of the dome screen, and the refresh rate was held at 85 frames/s. A 1.2-ms transistor-transistor logic pulse included in each video frame and the vertical refresh synchronization pulse (vsync) from the video card (NVIDIA GeForce4 Ti4200 128 MB) were recorded along with continuous neuronal activity. Neural activity was amplified with a differential AC amplifier (A-M Systems, model no. 1700, gain x 10,000) and sampled at 25 kHz. Data was recorded using an RP2.1 enhanced real-time processor (Tucker-Davis Technologies, Alachua, FL) with Butterworth filter settings of 5 kHz (low pass) and 100 Hz (high pass).

2.3.7. Electrophysiology

Legs were removed and a rigid tether was affixed to the ventral surface of the thorax with beeswax. A square of ventral cervical cuticle was dissected to expose the paired ventral nerve connectives anterior to the prothoracic ganglia. The locust was transferred to the flight simulator where a silver wire electrode was hooked around the left connective. Petroleum jelly was used to insulate and protect the preparation from desiccation. A silver wire was inserted into the abdomen and connected to ground. The locust was then oriented dorsal-side up facing the apex of the dome. In this orientation, the head of the locust was 12 cm from the dome, with 0° being directly in front of the locust, and 90° directly perpendicular to the centre of the eye. Stimuli were presented at intervals of at least 2.5 minutes to prevent neural habituation.

2.3.8. DCMD (2h)

Experiments were conducted using both simple (S) and flow field (FF) backgrounds. Four sublethal doses of IMD (0.1, n = 5; 1, n = 5; 10, n = 5; and 100, n = 20 ng/g) plus the vehicle control (0.2% acetone in saline, n = 5) were injected after pre-treatment recordings. Recordings continued over 120 minutes, first at 2.5 minute intervals, then at 10 minute intervals over a simple background (Table 2.1). At 100 minutes the background was switched to flow field and animals were presented with five stimuli at 2.5 minute intervals.

2.3.9. DCMD (24h)

Animals that participated in behavioural assays were promptly prepared for DCMD recordings approximately 24h after treatment with 10 or 100 ng/g IMD or the vehicle. Animals were presented with the stimulus over S and FF backgrounds.

Table 2.1 Experimental procedure for 2 hour electrophysiology experiments performed in a flight simulator with looming stimuli presented over simple (S) and flow field (FF) backgrounds.

# Stimuli	Interval (minutes)	Background type
2	2.5	S
2	2.5	FF
IMD injection		
12	2.5	S
7	10	S
5	2.5	FF

2.3.10. Data analysis

Post-hoc analysis of continuous neuronal activity was completed in Offline Sorter (Plexon, Dallas, TX), where DCMD spike times were identified by threshold analysis. DCMD spike times, along with corresponding vsync pulse times and transistor-transistor logic pulses for each stimulus presentation were exported to NeuroExplorer analysis software (NEX Technologies, Littleton, MA). Burst analysis was performed on DCMD spike time data, with bursts defined as spike trains of at least two spikes with inter spike intervals (ISIs) of 2 to 8 ms, using an algorithm designed by McMillan and Gray (McMillan and Gray 2015).

The last transistor-transistor logic pulse and corresponding vsync pulse were used to determine the time the last frame was drawn on the screen, and this was extrapolated to

determine the time of collision (TOC) of the black disk had it continued traveling to the locust's eye. The TOC for each stimulus presentation was used to align spike times in peristimulus time histograms (PSTHs) with a 1 ms bin width and smoothed with a 50 ms Gaussian filter. PSTHs were created using the full DCMD rate, spikes within bursts only, isolated spikes only, and initial spike from each burst only. DCMD firing properties were characterized by the maximum firing rate (spikes/s); time of the maximum firing rate relative to TOC (peak time); peak width at half the maximum rate (PW½M); total number of spikes during the stimulus presentation; rise phase, calculated as the time the PSTH last crosses its 95% confidence interval until the time of the peak; and decay phase, calculated as the time from the peak until the firing rate had decayed to 15% of the maximum. Matlab (MATLAB, R2016a, The MathWorks Inc., Natick, MA) was used for calculation of rise and decay phases. Video recordings were analyzed in GoPro Studio (GoPro, Inc., San Mateo, California, United States).

2.3.11. Statistical analysis

Statistical analyses were performed using R (The R Foundation for Statistical Computing) and SigmaStat 3.5, and figures designed with SigmaStat 12.5 (Systat Software Inc., Richmond, CA, USA). DCMD response variables across doses were compared with One Way ANOVAs and Holm-Sidak pairwise multiple comparison procedures for parametric data, and Kruskal-Wallis One Way ANOVAs on Ranks with Dunn's Method pairwise multiple comparison procedures for non-parametric variables. Effects of background type across doses was completed with Mann-Whitney Sum of Ranks tests (non-parametric) or student's t-tests.

2.4. Results

2.4.1. LD50

The 48 hour injected LD50 of IMD was determined with doses between 10 and 10,000 ng/g (ng IMD per gram of locust). At all doses ≥100 ng/g, locusts displayed increasing degrees of twitching, sporadic leg movements, and rapid abdominal movements, followed by periods of paralysis. After 48 hours, animals were scored as alive if they exhibited respiratory movements and moving mouthparts or legs. All male locusts treated with doses >1000 ng/g, and female locusts treated with doses >2000 ng/g were unable to walk in a coordinated manner at 48 hours

and were unresponsive. Percent mortality for males and females at 48 hours after treatment was normalized to the percent mortality in each sex of the vehicle controls. While females were not tested over the entire range of doses, they were more resistant than males to doses tested. Percent mortality was plotted against dose (Figure 2.1), further illustrating the differences in sensitivity of males and females to IMD. I estimated the male 48 h LD50 at 2,500 ng/g, whereas for females it could be as high as 10,000 ng/g, although females were not tested over an adequate range of doses to confirm this. To prevent confounding results due to the large disparity in LD50 between males and females, I used male locusts for subsequent experiments.

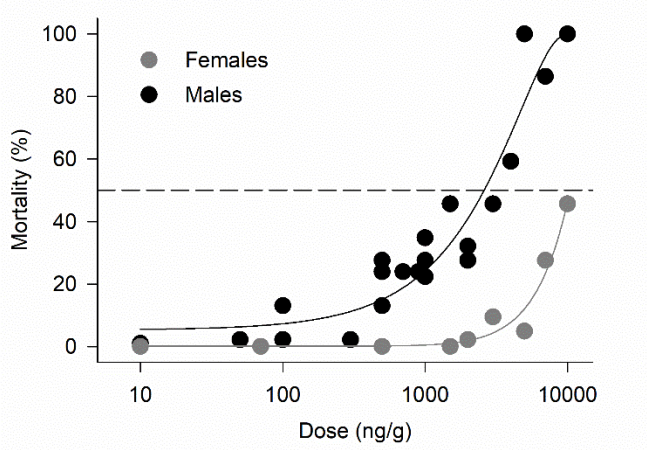

Figure 2.1: Percent mortality at 48 hours for male and female locusts after injection with imidacloprid (IMD) solutions ranging in concentrations from 10 to 10,000 ng/g (plotted on log scale), fitted with iterative non-linear regressions (solid lines). Points represent proportions from groups of 6 to 12 locusts, normalized to the mortality of vehicle control groups used on each testing day. Regression lines revealed an LD50 of approximately 2,500 ng/g for males. The LD50 for females was beyond the highest concentration used.

2.4.2. Behavioural responses

I conducted behavioural assays on three groups of locusts treated with 10 or 100 ng/g IMD (n=10 each), or the vehicle (n=15). Behavioural assays took place in a wind tunnel with animals either standing (no wind) or flying (wind at 300 cm/s). I used a 14cm black disk, approaching at 300 cm/s perpendicular to the orientation of the locust, which reliably evokes escape behaviours (McMillan et al. 2013). The effects of 10 and 100 ng/g IMD on escape behaviours persisted 2 and 24 hours after treatment (Figure 2.2A). During jumping assays, none of the locusts treated with 100 ng/g reacted to the looming stimulus. For this assay, either a full jump or a twitch of the hind legs was scored as a reaction to the stimulus. Only one animal treated with 10 ng/g IMD responded to the looming stimulus at either time (twitch), while an

average of 80% of vehicle controls reacted at both times (jump:twitch ratio = 0.6:0.33 at 2 hours and 0.5:0.2 at 24 hours). IMD also affected locust flight behaviour (Figure 2.2B). Most vehicle controls reacted to the looming stimulus with a collision avoidance behaviour (a glide, turn, or stop (McMillan et al. 2013)) at 2 hours (100%) and 24 hours (60%) after treatment. Although 90% of the animals treated with 10 ng/g IMD flew at both 2 and 24 hours after treatment, only 10% responded to the stimulus and 90% of animals from the 100 ng/g treatment group did not fly. All escape behaviours occurred between 2 and 0.2 s before TOC.

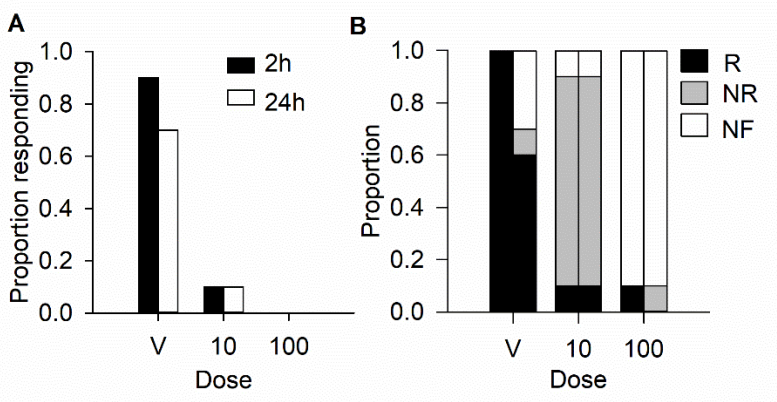

Figure 2.2: Effect of IMD on escape behaviours. a: Proportion of animals responding to a looming stimulus by jumping or twitching hind legs at 2 and 24 hours after treatment with the vehicle, or 10 ng/g or 100 ng/g IMD. b: Proportion of animals responding to looming stimulus while flying (R), flying but not responding to stimulus (NR), or not flying (NF) at 2 (left columns) and 24 (right columns) hours after treatment with vehicle or IMD.

2.4.3. DCMD responses (2h)

To determine whether sublethal, ecologically realistic (Godfray et al. 2014) doses would affect DCMD responses to looming stimuli, I tested four IMD concentrations (0.1, 1.0, 10, and 100 ng/g), plus a vehicle (saline + 0.2% acetone) on male locusts (n=40) over 140 minutes each. The DCMD exhibits properties of bursting, with a minimum of 2 spikes and a maximum inter-spike interval (ISI) of 8ms, and inter-burst intervals of 40-50 ms (McMillan and Gray 2015). When presented with a looming visual stimulus, the frequency of DCMD spikes that are not contained within bursts (isolated spikes) is highest when the stimulus is farther away, while bursting frequency increases in the latter stage of the approach until collision (McMillan and Gray 2015). It is likely that the timing of bursts is important for eliciting collision avoidance behaviours in flying locusts, in a process termed flight gating (Santer et al. 2006; McMillan and Gray 2015). To determine whether the presence of bursting was affected by IMD treatments, I

constructed joint inter-spike interval distribution heatmaps for DCMD responses (Figure 2.3). In the presence of vehicle, ISIs clustered between 1-8 ms regardless of background or time, which is consistent with previously described DCMD bursting (McMillan and Gray 2015). Against a simple background, ISI clusters were broader (5-20 ms) 2 hours after treatment with 100 ng/g IMD whereas against a flow field at either dose and time or against a simple background 24 hours after treatment with 100 ng/g, clustering was less pronounced. Given this apparent disruption of bursting caused by treatment with IMD, full DCMD responses were subdivided by burst frequency, isolated spike frequency, and frequency of spikes contained within bursts (Figure 2.4A). Measurements from the resulting peristimulus time histograms (PSTHs) were used to compare responses.

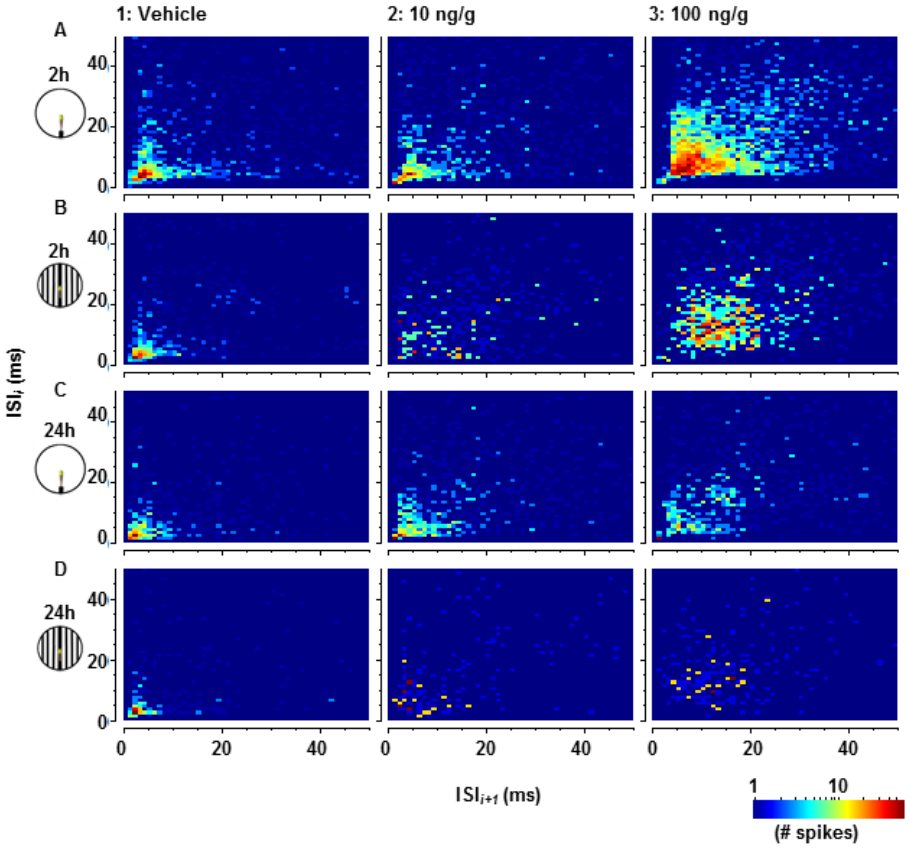

Figure 2.3: Joint inter-spike interval (ISI) distribution heatmaps comparing one ISI (y-axis, ms) with the following ISI (x-axis, ms). Heatmaps in column 1 were compiled from 5 stimulus presentations per animal either before treatment (1A,B, n=25), or 24 hours after treatment with the vehicle (1C,D, n = 10). 2-3A,B were recorded from 80 to 110 minutes after treatment with 10 ng/g (n=5) or 100 ng/g (n=20) IMD. 2-3C,D were recorded 24 hours after treatment with 10 ng/g (2C,D, n=10) and 100 ng/g (3C,D, n=10). White circles represent stimuli presented over a simple background, and striped circles for stimuli presented over a flow field.

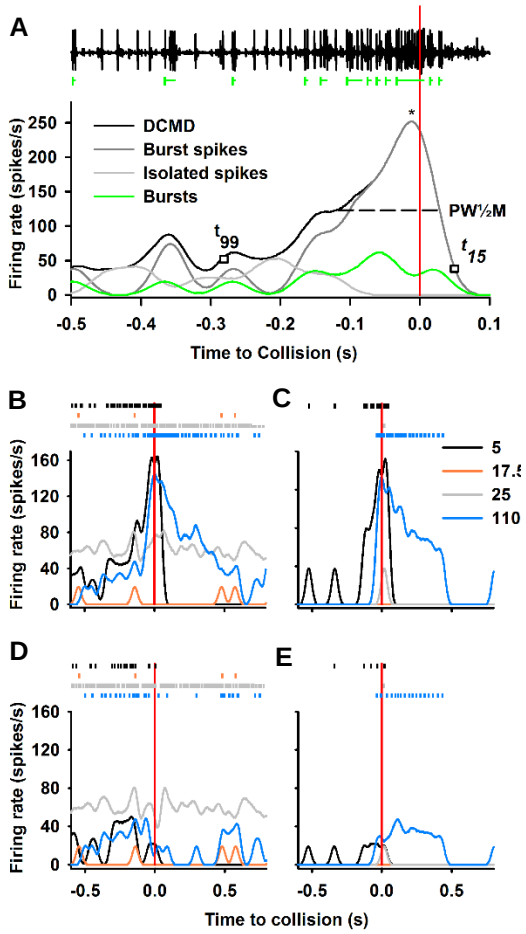

Figure 2.4: Rasters and peristimulus time histograms (PSTHs) constructed from DCMD responses to looming stimuli. A: Raw continuous data from an extracellular recording of the left ventral nerve cord during presentation with the image of a 7 cm looming disk to the right eye (top). DCMD spikes were easily differentiated by their large amplitude. The projected time of collision (TOC) is marked with a vertical red line. Bursts, which comprise a minimum of two spikes occurring within 8 ms of each other, are highlighted with a vertical green line to signal the start, and horizontal lines to show the duration. PSTHs show the firing rates of the full DCMD response, spikes within bursts only, isolated spikes only, and bursts, smoothed with a 50 ms Gaussian filter. PSTHs response profile parameters included: peak firing rate (f_p) and the time of the peak relative to TOC (pt), denoted by an asterisk; peak width at half maximum (PW½M), rise phase, from the last time the histogram crosses the 95% confidence interval with a positive slope (t99) to the peak, and decay phase from the peak until it had decreased to 15% (t15). b-e show rasters (top) and PSTHs (bottom) at four time points after injection with 100 ng/g IMD, 5, 17.5, 25, and 110 minutes. These panels are separated by rate type: full DCMD (B), burst spikes only (C), isolated spikes only (D), and bursts (E).

The effect of IMD was variable over the first hour and stabilized through the second hour (Figure 2.5). I grouped the effect into four general phases (Figure 2.4B-E): 1) pre-effect - within

the first few minutes after injection (which resembled pre-treatment activity); 2) inhibition - a period of sporadic, low frequency firing, or complete neural silence; 3) high frequency, sporadic firing; and 4) post-effect - maintained as a stable response approximately 1 hour after treatment. During phases 1 and 4, most spikes were contained within bursts whereas for phases 2 and 3, most spikes were isolated. All animals tested with 10 or 100 ng/g IMD displayed phases 1 and 4 whereas phases 2 and 3 were less consistent.

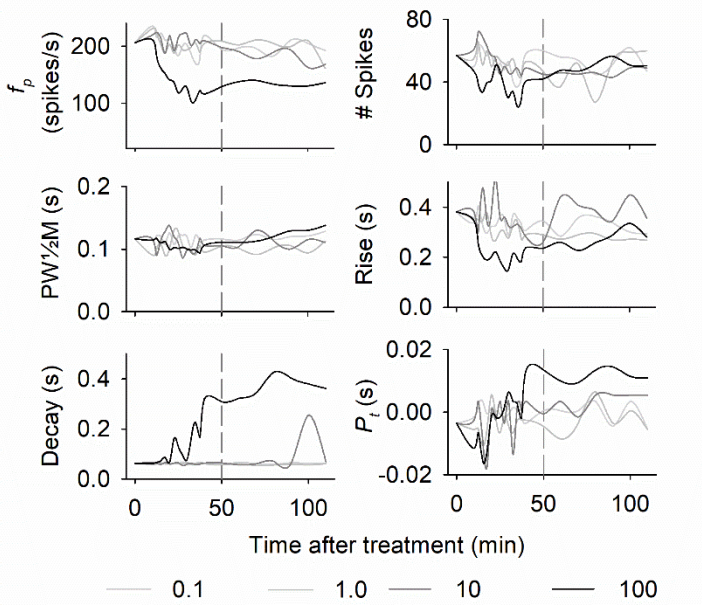

Figure 2.5: Median temporal properties of DCMD response parameters over 100 minutes after treatment with 0.1 (n=5), 1 (n=5), 10 (n=5) and 100 (n=20) ng/g IMD during stimulus presentations against a simple background. Fifty minutes post injection is marked with a vertical dashed line, as the variability of responses at each dose is greatly reduced after this time.

Due to variability of IMD effects within the first hour of treatment, single time points were selected to compare between simple (S) and flow field (FF) backgrounds at 110 and 120 minutes after treatment, respectively. S represents a disc projected against a white background and FF represents a disc against a flow field consisting of vertically oriented, 2 cm wide bars moving outward from the azimuthal plan from the dome apex at 0.138 m/s. The latter elicits DCMD responses with lower peak firing rates, later peak time, shorter rise phase and a longer decay phase (Silva et al. 2015). Doses of 0.1 and 1.0 ng/g did not significantly affect DCMD firing, while doses of 10 and 100 ng/g resulted in significant alterations of several features of DCMD firing (Figure 2.6). Significant effects, for both backgrounds, included: a decreased peak frequency (f_p) for DCMD and burst spikes (1,2a); an increased f_p for isolated spikes (3a); a

decreased number of spikes within bursts (4b); and an increased DCMD decay phase (1e). The total number of spikes within bursts also decreased. Parameters affected for S or FF stimuli may be attributable to the effects of these background types. Summary of statistical results in Table 2.2. Rise phases for the full DCMD response and for spikes within bursts were significantly shorter for S. However, the rising phase did not decrease with FF, though this time period is typically very short for FF due to the effects of lateral inhibition caused by the movement of the background across the visual field (Rind 1996).

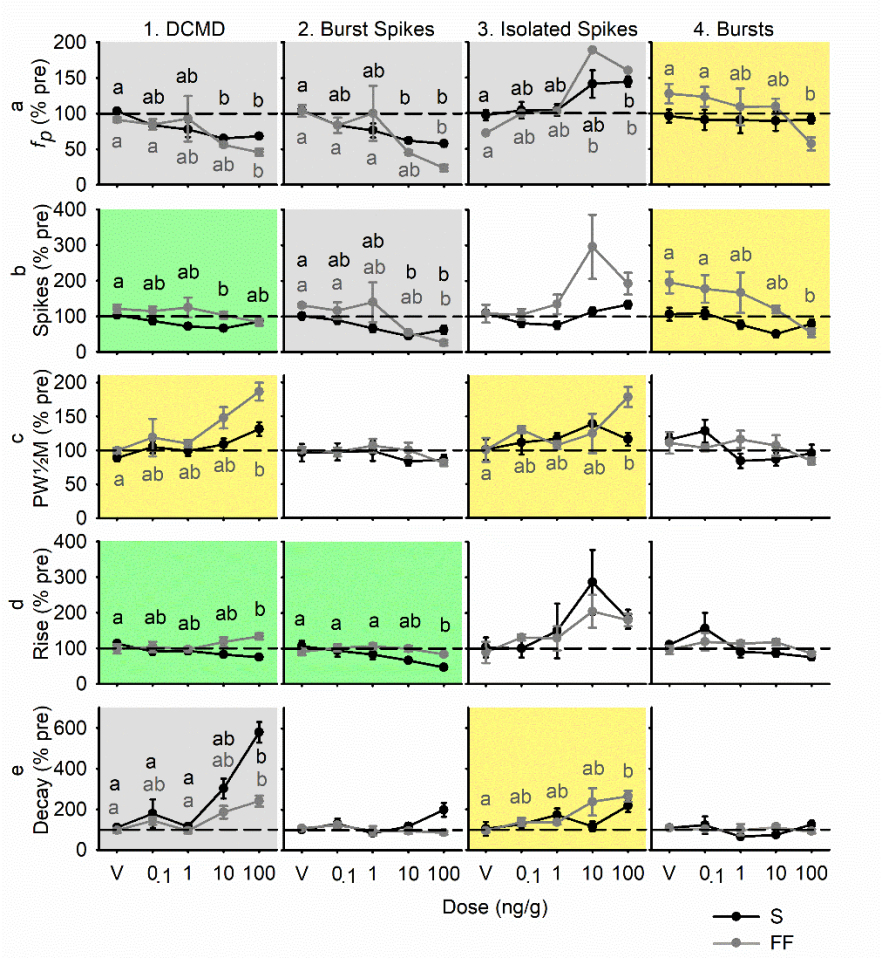

Figure 2.6: Response parameters (mean ± SEM) of the four DCMD rates (full DCMD, burst spikes, isolated spikes, and bursts) at 110 (S background) and 120 minutes (FF background) after treatment with an IMD dose (ng/g) or the vehicle (V). Data plotted as a percent of pre-treatment values within each animal. Grey backgrounds indicate a significant effect of one or more IMD dose for stimuli presented over both S and FF backgrounds, yellow indicates a significant effect within FF background only, and green for S background only.

Table 2.2: Results of statistical analyses for figures 6, 8, 9, and 10.

Resp. var.	DCMD Rate			Burst Spikes Rate			Isolated Spikes Rate			Burst Rate		
		Background			Background			Background			Background	
	Dose	S	FF	Dose	S	FF	Dose	S	FF	Dose	S	FF
Fig. 5												
%Ymax	U=210	19.3_4^D	18.9_4^D	U=204	21.6_4^D	25.0_4^D	U=376	16.5_4^D	4.9_4^{HS}	U=348	0.1_4	6.0_4^H
%Spikes	U=353	12.5_4^D	1.8_4	U=305	14.8_4^D	19.4_4^D	U=307	3.4_4^{HS}	H=9.4_4	U=432	H=8.1_4	17.3_4^D
%PWHH	U=227	H=6.5_4^D	16.5_4^D	U=403	H=1.8_4^D	13.7_4^D	U=287	0.7_4	13.8_4^D	U=410	H=8.3_4	9.7_4^D
%Rp	U=157	3.6_4^{HS}	2.0_4	U=166	8.5_4^{HS}	2.4_4	U=432	H=9.1_4	F=2.4_4	U=351	H=7.4_4	10.8_4^D
%Dp	U=171	28.7_4^D	16.5_4^D	U=226	H=6.2_4	H=8.5_4	U=327	H=7.5	15.8_4^D	U=424	H=6.3	H=4.6_4
Fig. 6												
Ymax	U=101	16.8_2^{HS}	18.8_2^{HS}	U=107	16.3_2^{HS}	25.4_2^{HS}	t=10.7_{47}	H=5.9_2	4.9_2^{HS}	U=89	F=2.0_2	F=1.9_2
Spikes	t=9.1_{47}	6.8_2^{HS}	1.6_2	U=84	16.0_2^D	6.0_2^{HS}	t=9.3_{47}	1.7_2	1.9_2	U=132	10.7_2^D	9.0_2^{HS}
PWHH	U=13	1.7_2	8.0_2^{HS}	U=51	7.4_2^D	H=2.9_2	U=65	H=2.5_2	H=1.6_2	U=69	13.2_2^{HS}	F=0.2_2
Rp	U=0	H=3.0_2	H=0.4_2	U=29	3.9_2^{HS}	H=1.5_2	U=44	3.4_2	H=5.2	U=109	0.8_2	H=1.6_2
Dp	U=227	8.1_2^D	H=2.3	U=136	3.4_2	H=5.7	U=151	2.5_2	H=3.9_2	U=96	11.1_2^D	3.8_2^{HS}
Fig.7												
Pt 2h	U=137	25.5_2^D	27.8_2^D	U=203	28.5_2^D	27.4_2^D	U=490	27.4_2^D	H=12.7_2	U=547	40.8_2^D	13.7_2^D
Pt 24h	U=51	25.5_2^D	32.8_2^D	U=30	28.5_2^D	31.8_2^D	U=134	27.4_2^D	12.7_2^D	U=12	30.8_2^D	13.5_2^D
Fig. 8												
Ymax 2h				t=5.7_{47}	69.9_2^{HS}	42.4_2^D						
Ymax 24h				t=5.1_{28}	14.0_2^{HS}	23.7_2^{HS}						
Behav.					16.3_2^{HS}							
%Inhib.				t=7.1_{81}	77.0_2^{HS}	60.0_2^D						

Columns are divided by rate type and subdivided by dose or background. Rows under "Dose" compare between background types, and below each background (S and FF) compares between doses within each background. Values represent the H statistic from one-way ANOVA on Ranks test. Numerical subscripts indicate degrees of freedom. Post hoc tests denoted as Holm Sidak (HS) or Dunn's (D). Results from Mann-Whitney tests are indicated by the U statistic, and t-tests by the t statistic. Shaded cells indicate a significant effect ($P < 0.05$). Specific differences from post hoc tests indicated on Figures 5-8. Response variables (resp var): Ymax, peak firing rate; Spikes, number of spikes; PWHH, peak width at half height; Rp, rise phase; Dp, decay phase; Pt, peak time. % signifies percent of mean of control.

2.4.4. DCMD responses (24h)

I was interested in whether IMD-induced alterations in DCMD firing persisted 24 hours after treatment, in accordance with behavioural deficits. Animals that participated in behavioural experiments were prepared for electrophysiology 24h after initial treatment. I obtained successful recordings from 25 animals from behavioural assays. Peristimulus time histogram (PSTH) overlays of the 100 ng/g dose at 2 and 24 hours after treatment showed similarities in peak firing rates (Figure 2.7). I measured the same DCMD response parameters at 2 and 24 hours after treatment. Response variables significantly altered by IMD at 24 hours after treatment for both

background types included the maximum firing rate (DCMD and burst spikes), the number of spikes (burst spikes), and the decay phase of bursts (Figure 2.8). For stimuli presented over the S background, the number of spikes (DCMD), peak width at half height (bursts), rising phase (burst spikes), and decay phase (DCMD) were significantly altered by IMD treatment. The time of peak firing was significantly later relative to TOC at the 100 ng/g dose at both time points for S, as well as at 2 hours after treatment for FF (Figure 2.9).

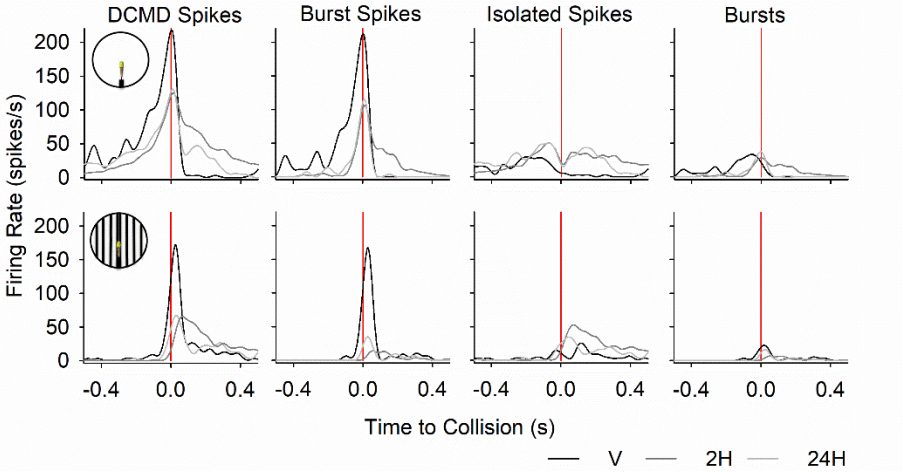

Figure 2.7: Mean PSTH overlays of DCMD responses to a looming stimulus against simple (top row) or flow field (bottom row) backgrounds, at 2 (n = 20) and 24 (n = 10) hours after injection with 100 ng/g IMD. Responses of vehicle controls (n = 10) and untreated animals (n = 20) are displayed in black. Full DCMD response (left column) is subdivided in subsequent columns into burst spikes, isolated spikes, and bursts to show differences in these parameters at the two time points. Vertical red lines indicate TOC.

To determine the overall inhibitory effects of IMD on DCMD firing, I chose to focus on the maximum firing rate of burst spikes (Figure 2.10). This is the only response variable that was significantly altered with 10 and 100 ng/g IMD, at both 2 and 24 hours after treatment, for stimuli presented over both S and FF backgrounds. There was no significant difference in the maximum firing rate of burst spikes 2 and 24 hours after treatment within dose and background type, while the burst spike firing rate significantly decreased with increasing IMD dose. Effects on peak burst spike firing rate are correlated with observed flight behaviours (Figure 2.10). Burst spike firing rate was inhibited to a greater degree with FF: 50% inhibition was achieved with a 10 ng/g dose with FF, while similar inhibition with 100 ng/g dose for S (Figure 2.10).

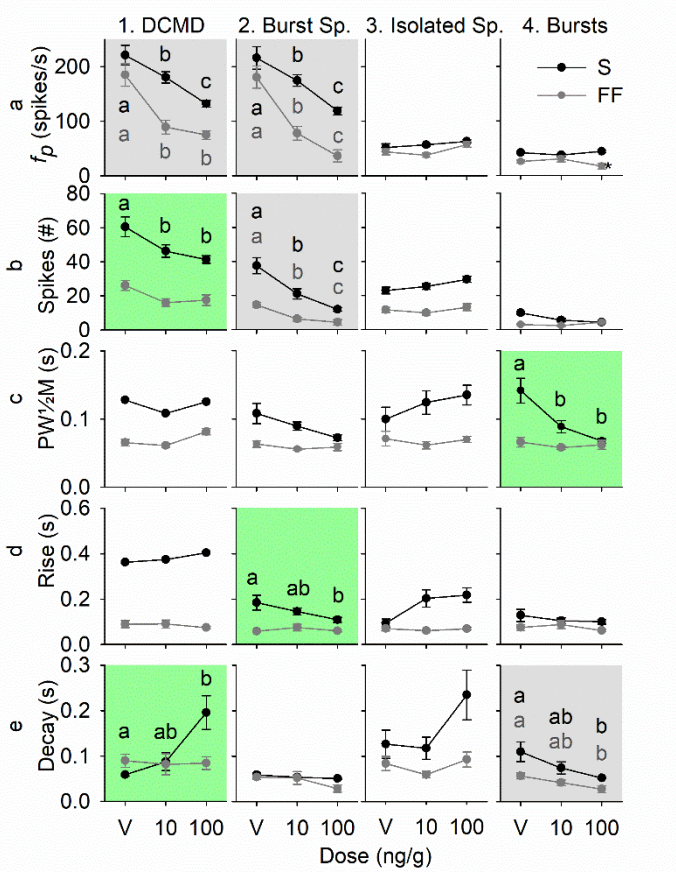

Figure 2.8: Response parameters (mean ± SEM) of the four DCMD rates (full DCMD, burst spikes, isolated spikes, and bursts) 24 hours after treatment with an IMD dose (ng/g) or the vehicle. Gray backgrounds indicate a significant effect of one or more IMD dose for stimuli presented against both S and FF backgrounds, and green indicates a significant effect with S background only. Significant results of post hoc analyses are indicated with letters colour coded to the respective background type.

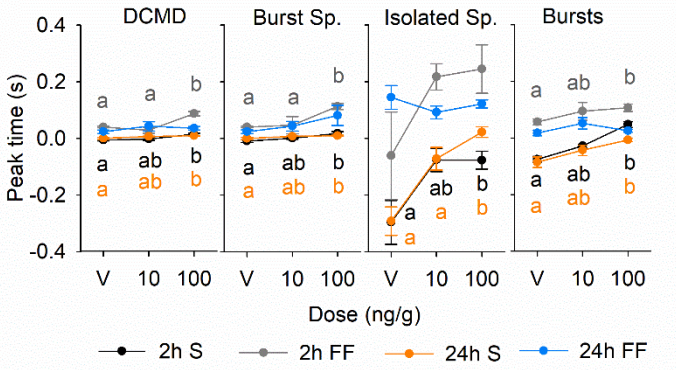

Figure 2.9: Time of maximum firing rate relative to collision (peak time; mean ± SEM) across doses and background types at 2 and 24 hours after treatment. Significant results of post hoc analyses are indicated with letters colour coded to the respective background type.

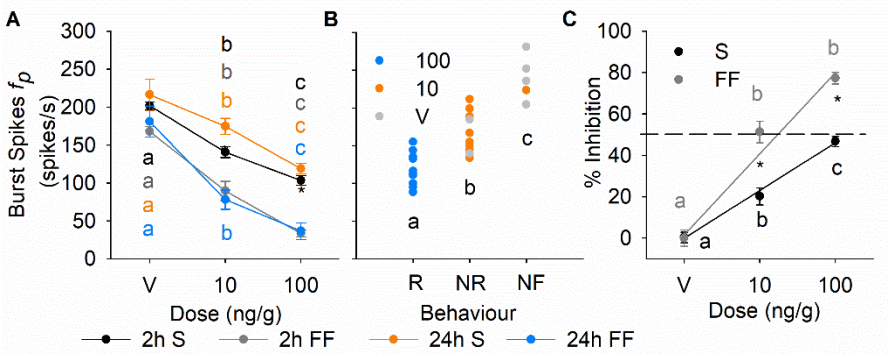

Figure 2.10: Effect of IMD on burst spike peak firing rate (f_p) and correlation with observed behavioural deficits. a) Burst spike peak f_p at 2 and 24 hours after treatment, for stimuli presented against simple (S) and flow field (FF) backgrounds. b) Burst spike f_p correlated with flight behaviour at 24 hours after treatment with IMD or vehicle: NF, not flying; NR, flying but not responding; R, responding with a turn or glide, with a Pearson correlation coefficient of 0.872. Each data point represents measurements from a single animal, and letters denote significant differences between means. c) Percent inhibition with effects at 2 and 24 hours combined for each background type, plotted as percent reduction from the mean of the vehicle treatment group. Colour coded letters denote significant differences between treatments within each background, and asterisks denote significant differences between S and FF within treatment.

2.5. Discussion

I found that the 48 hour injected LD50 of IMD was 2,500 ng/g for male locusts. In the honeybee (*Apis mellifera*) the oral LD50 was estimated at 4.5 ng/bee (approximately 45 ng/g), and contact LD50 at 81 ng/bee (approximately 810 ng/g) (Godfray et al. 2014), although these values can differ greatly between colonies and studies (Suchail et al. 2001). While our reported LD50 is high it may be due to the delivery method, toxicological endpoint, and metabolism. Grasshoppers (*Melanoplus sanguinipes*) sustain a long period of "debilitation" before death, with high oral and contact LD50s of 53.38 and 96 ppm (µg/g), respectively, for IMD at 72 hours after treatment (Tharp et al. 2000). In honeybees, mortality is delayed from high doses of IMD, compared to moderate doses (Suchail et al. 2000), prompting use of a 96h endpoint. Furthermore, suggestions to score insects as dead when moribund result from delayed insecticide toxicity (Stanley et al. 2015). Nevertheless, locusts are known to express a wide range of enzymes involved with xenobiotic detoxification (Wang et al. 2014), and display resistance to many insecticides (Guo et al. 2012). By injecting IMD into the hemolymph, it would bypass detoxification enzymes concentrated in the gut (Guo et al. 2012; Bao et al. 2015), and may not

distribute naturally throughout the body. IMD metabolites are known to be toxic in other species, including honeybees (Suchail et al. 2001; Nauen et al. 2001), and can accumulate in high concentrations (Codling et al. 2016). Metabolism of IMD could be slowed by injection into the hemolymph and limited by diffusion into other tissues. Additionally, locust hemolymph contains the lowest concentration of glutathion s-transferase enzymes, which are involved in pesticide metabolism (Qin et al. 2013). The results of the present toxicity tests are not for direct comparison with values from oral or topical application but provide a basis for scaling the doses I used in behavioural and electrophysiological assays. Interestingly, females displayed a four-fold higher resistance than males to IMD. These results were unexpected as individual females had masses two to three times greater than males, thus receiving a larger volume of IMD solution. Female locusts are more resistant than males to topically applied organophosphate and organochloride pesticides (MacCuaig 1957; Onyeocha and Fuzeau-Braesch 1991), although not at the high factor I report for injected IMD. Further studies are required to determine the cause of this difference between the sexes.

Initial effects of IMD on DCMD responses included periods of spontaneous activity, both high and low frequency firing, and/or periods of neuronal silence (hyperexcited and inhibited phases). These effects were pronounced at the 100 ng/g dose only and commence within 10 minutes of treatment. Approximately 1 hour after treatment, the DCMD again responded to the looming stimulus in a stable manner (post-effect phase) that was maintained until the end of the recording period, two hours and 20 minutes after treatment. Acute behavioural effects of IMD toxicity include periods of trembling and sporadic movements of the abdomen and legs, followed by paralysis in the honeybee (*Apis mellifera)* (Suchail et al. 2001), flea (*Ctenocephalides felis*) (Mehlhorn et al. 1999), beetle (*Tenebrio molitor*) (Zafeiridou and Theophilidis 2004), and grasshopper (*Melanoplus sanguinipes*) (Tharp et al. 2000). Our results are consistent with other studies that found initial neuronal effects to be hyperexcitation followed by neural silence (Nishimura et al. 1994; Zafeiridou and Theophilidis 2004), which may be attributed to receptor desensitization (Buckingham et al. 1997; Nguyen et al. 2012).

The effects observed after the first hour of IMD toxicity could result from lingering upstream receptor desensitization. Debilitation of interneurons that converge onto the LGMD would limit the peak firing rate and number of spikes of the LGMD/DCMD by reducing the cumulative effect of EPSPs evoked by their inputs. The rising phase was shortened under the simple

background only, likely because this period is already extremely short for flow field under normal conditions. The rising phase is associated with the threshold of the LGMD and DCMD (Gabbiani et al. 2002), and could be shortened by effects on excitatory inputs, and down regulation or impairment of nAChRs on the LGMD/DCMD. Decreased DCMD firing rates may also be attributed to reduced excitatory firing of the retinotopic units that synapse with the LGMD (Gabbiani et al. 2002), while increased isolated spikes f_p and lengthened decay phase may result from weakened feed forward and lateral inhibition (Gabbiani 2005).
Differences in the responses of the DCMD after the first hour of toxicity may be attributable to toxicity of IMD metabolites (Suchail et al. 2001; Nauen et al. 2001). Of these, 5-Hydroxy-IMD and IMD-olefin are known to accumulate at higher concentrations than IMD in honeybees (Codling et al. 2016), suggesting their excretion half-life is much longer than for IMD. The olefin metabolite is more toxic than pure IMD (Suchail et al. 2001) and accumulates in nAChR-rich tissues. This metabolite may also bind to nAChRs (Suchail et al. 2004).

At 24 hours after treatment, any effects of IMD on the rising and decay phases of the DCMD response to a looming stimulus have been eliminated. For presentations using the simple background, the number of spikes were reduced, and the time of the maximum burst rate was later relative to TOC. Peak time of the DCMD relates to both the visual acuity of the locust and feed-forward inhibition from the photoreceptors in the optic lobe (Rind and Simmons 1998). Here, I show that peak time was significantly later at the 100 ng/g dose at both 2h with S and FF, and 24h with S. Several parameters, including number of DCMD spikes and spikes within bursts, and peak time of bursts is significantly altered for S only at 24 hours, likely because of IMD effects being masked by flow field stimulation.

A single DCMD response variable, maximum firing rate within bursts, coincided with the effects of IMD on collision avoidance behaviours at 10 ng/g. The elimination half-life of IMD is 5h in the honeybee (Suchail et al. 2004), so the reduced burst spike firing rate at 24h suggests there was impairment of the DCMD and upstream network that was sustained after IMD has been metabolized. This may result from down regulation or damage to nAChRs caused by IMD metabolites, or whole neuron damage or apoptosis in cholinergic interneurons of the optic lobes. Low dose IMD toxicity has been shown to cause apoptosis in the central nervous systems of bats and honeybees (De Almeida Rossi et al. 2013; Wu et al. 2015). In bees, markers of apoptosis are visible within 1 day with doses 1/10th of the LD50, and these are more concentrated in the optic

lobes than other areas of the CNS (De Almeida Rossi et al. 2013). Our results suggest that low doses of IMD cause lasting damage to the visual network of locusts, which may inhibit detection of looming stimuli by affecting visual processing in the optic lobes.

The effect of IMD on the burst spike firing rate was more profound for FF than S. This further suggests that visual processing was reduced as the looming stimulus was somewhat obstructed by the vertical bars of the FF. With reduced visual processing, the expanding edges of the stimulus were more difficult to distinguish. Any damage to the optic lobes or photoreceptors would enhance the masking effect. For these reasons, free flying animals may experience an even greater visual deficit with lower IMD doses than those tested in tethered conditions. When comparing burst spike firing rates in the different treatment groups, I found that a reduction in rate corresponded with deficits in collision avoidance behaviour. It has previously been suggested that a threshold of burst spike firing rate is required to elicit a collision avoidance behaviour (Santer et al. 2006; Rogers et al. 2007; McMillan and Gray 2015), and I provide additional evidence to this effect. However, I did not perform behavioural assays and electrophysiology simultaneously. Nevertheless, burst spike firing rate was the only parameter significantly altered across doses and times.

The bursting algorithm used on the data is based on the results of McMillan and Gray (McMillan and Gray 2015) who found frequent DCMD ISIs occur at 1-8 ms. Our data show that low, sublethal doses of IMD disrupts bursting, with ISIs either clustering at larger intervals or not clustering. ISIs define intra-burst firing rates (burst spike firing rate), and longer ISIs naturally result in lower peak rates. This effect was clear at the 100 ng/g dose with both backgrounds, while at the 10 ng/g dose it was more apparent with a flow field background, which mimics whole-field optic flow produced by self-motion. Given these results, bursting would likely be disrupted in free-flying animals at very low IMD doses.

The larger stimulus was used for behavioural experiments (14cm versus 7cm for electrophysiology) to elicit collision avoidance behaviours more reliably(Chan and Gabbiani 2013). Regardless, stationary animals treated with 100 ng/g IMD do not respond at all to looming stimuli, and only 10% of animals tested with 10 ng/g responded. A jump is initiated in the locust when flexor muscles discharge after a period co-contraction of flexor and extensor tibiae muscles (Santer et al. 2005b). Fast extensor tibiae (FETi) motorneurons receive monosynaptic input from the DCMD (Burrows and Rowell 1973). The DCMD does not directly

initiate a jump, as EPSPs from the DCMD in FETi motorneurons summate, but do not result in an action potential (Rogers et al. 2007). Rather, the DCMD has a role in timing the movement in an animal that is already prepared to jump (Rogers et al. 2007). Lack of summation of EPSPs in the FETi motorneurons resulting from a low DCMD firing rate (Figure 2.6) may explain the absence of jumping responses in locusts treated with IMD. These animals may also be unprepared to jump due to debilitation of the motor control of the flexor and extensor muscles, and input from the DCMD would be ineffective.

At 10 ng/g IMD, flight motor circuitry was minimally affected, as 90% of test subjects could fly. Nevertheless, only one animal from this group responded to the looming stimulus. The DCMD makes excitatory synapses with flight motorneurons in the meso- and metathoracic ganglia (Simmons 1980). Bursts of spikes in the DCMD result in summating EPSPs in flight motorneurons that alone do not result in an action potential (Simmons 1980; Santer et al. 2006). DCMD frequencies >150Hz produce EPSPs in flight motorneurons that result in an action potential during flight, as the electrical potential of the motor neuron membrane oscillates, resulting in flight-gating (Santer et al. 2006). By this mechanism, the DCMD directly initiates collision avoidance behaviours in flight. Thus, the reduction in firing rate caused by 10 ng/g IMD may result in an inability of EPSPs from the DCMD to summate and produce a glide, turn or collision avoidance behaviour. With 100 ng/g, 90% animals were unable to fly suggesting that IMD affects the collision avoidance pathway at lower doses than those required to disrupt flight. Similarly, neonicotinoids are known to disrupt motor function in bees (Williamson et al. 2014), and result in dose-dependent induction of trembling and paralysis in many invertebrates (Mehlhorn et al. 1999; Suchail et al. 2000; Charpentier and Louat 2014). The central pattern generator for locust flight is under muscarinic cholinergic control (Buhl et al. 2008), and the innervation of muscles is glutamatergic (Watson and Schürmann 2002), so disruptions of these pathways by IMD is unlikely. Further studies are required to understand the location of these effects in the central nervous system, or to determine if IMD or one of its metabolites may affect neurons that are not under nicotinic cholinergic control.

I have shown that locusts are highly resistant to IMD, and that this resistance differs between males and females. Further investigation is required to determine why females can sustain such elevated doses, and if this difference is maintained with oral or contact toxicity. Despite the ability to survive high doses of injected IMD, I show that low doses (0.4% and 4% of

the LD50) significantly disrupt the response of a looming-sensitive neuron, and that this disruption has downstream effects on collision avoidance while flying and stationary. Our results strengthen the hypothesis that high frequency DCMD burst spike firing is required to elicit a collision avoidance behaviour (Santer et al. 2006; Rogers et al. 2007), as this is the only firing parameter that is significantly affected under all testing conditions in animals that cannot perform collision avoidance behaviours. Deficits in burst spike firing can be related to damage to the upstream network, and thus, our findings suggest that low, acute doses of IMD results in damage to the optic lobe and motion detection neurons in the locust. More broadly, this research offers insight on sublethal effects of IMD on behaviours observed in non-target insects, as it suggests that IMD can cause significant and lasting impairment of visual circuits in the optic lobes. Mechanisms and extent of this damage will be an important focus of future studies.

Chapter 3: Neural conduction, visual motion detection, and insect flight behaviour are disrupted by low doses of imidacloprid and its metabolites[2]

3.1. Abstract

While neonicotinoid insecticides impair visually guided behaviours, the effects of their metabolites are unknown and measurements of environmental concentrations of neonicotinoids, typically lower than those required to elicit toxic effects, tend to exclude metabolites. Here I examined the contributions of imidacloprid and two of its metabolites, imidacloprid-olefin and 5-hydroxy-imidacloprid, on neural conduction velocity, visual motion detection and flight in the locust (*Locusta migratoria*) using a combination of electrophysiological and behavioural assays. I show reduced visual motion detection and impaired flight behaviour following treatment of metabolite concentrations equal to sublethal doses of the parent compound. Additionally, I show for the first time that imidacloprid and its metabolites result in a decrease in conduction velocity along an unmyelinated axon. I suggest that secondary effects of the insecticide on the biophysical properties of the axon may result in decreased neural conduction. As these metabolites display neurotoxicity similar to the parent compound they should be considered when quantifying environmental concentrations.

[2] The content of this chapter comes from the following published manuscript. Formatting and layout changes have been made to provide consistency between chapters.

Parkinson RH and Gray JR (2019). Neural conduction, visual motion detection, and insect flight behaviour are disrupted by low doses of imidacloprid and its metabolites. NeuroToxicology 72:107-113

Author contributions & justification for use in this thesis: R.H.P. designed and carried out experimentation, analyzed the data, interpreted the results, prepared the figures, and wrote and revised the manuscript. J.R.G. conceived and designed experiments, interpreted the results, revised the manuscript, and approved the final version of the manuscript.

3.2. Introduction

Flight behaviours, including orientation, navigation and collision avoidance are essential to the survival of many animals and are guided primarily by the processing of visual information (Rind and Bramwell 1996; Taylor and Krapp 2007; Ibbotson et al. 2017). Neurotoxic insecticides, including neonicotinoids (neonics) that target cholinergic neurotransmission in the insect central nervous system (Tomizawa and Casida 2003), affect specific behaviours following sublethal exposure (Fischer et al. 2014; Parkinson et al. 2017). Significant concern over the effects of neonics on honey bees and other important pollinators has led to bans that are highly contested (Blacquière and van der Steen 2017). Arguments against these bans point to discrepancies between laboratory and field-realistic doses (Walters 2013). However, measurements in the field often exclude neonic metabolites that may accumulate in pollen and honey and pose the greatest risk to overwintering and nurse-aged worker bees that rely on these stores (Codling et al. 2016; Baines et al. 2017). Some neonic metabolites display similar or increased toxicity to the parent compounds (Nauen et al. 1998; Suchail et al. 2001) suggesting a need for a greater understanding of these toxic effects.

The effects of the neonic imidacloprid (IMD) on visual processing and visually guided avoidance behaviours have previously been examined in the locust (*Locusta migratoria*) (Parkinson et al. 2017). This system is useful in examining neonic toxicity due to the presence of a tractable looming-sensitive visual interneuron, the Descending Contralateral Movement Detector (DCMD). The DCMD receives excitatory input from its presynaptic partner, the Lobula Giant Movement Detector (LGMD) at a 1:1 ratio and the LGMD receives both excitatory and inhibitory signals from the retinotopic units of the compound eye (Rind 1984). The excitatory synapses in the optic lobes and specifically on the LGMD/DCMD are nicotinic cholinergic (Rind and Leitinger 2000), which is a direct target for IMD. Although IMD is an nAChR agonist (Tomizawa 2004), initial agonistic effects may be followed by neural silence, dependent on concentration (Zafeiridou and Theophilidis 2004), an effect that may be due to receptor desensitization (Nauen et al. 2003; Oliveira et al. 2011). Previously I found that a single sublethal dose of IMD resulted in decreased burst firing of the DCMD and attenuated escape behaviours 2 and 24 hours after treatment (Parkinson et al. 2017).

Here I examine the effects of IMD and two metabolites, imidacloprid-olefin (OLE) and 5-hydroxy-imidacloprid (5OH) on action potential propagation, DCMD responses to a looming stimulus, and flight behaviour within 1 hour after treatment to determine the relative effects of the metabolites and parent compound. I hypothesized that the metabolites would display increased toxicity sooner after treatment than the parent compound, as these metabolites could directly cause reduced DCMD firing via receptor desensitization. I show in this paper that IMD, OLE and 5OH affect flight behaviour and visual motion processing within 1 hour of treatment, and additionally that these compounds affect conduction velocity along the axon, suggesting secondary effects of the insecticide on information transfer within a known pathway.

3.3. Methods

3.3.1. Animals

Adult male locusts (*Locusta migratoria*) two weeks past the last imaginal moult were selected for experiments. Locusts were fed a diet of wheat grass and bran flakes and maintained at 25-30°C with a 12h:12h light:dark cycle at the University of Saskatchewan, Canada. All experiments took place during the animals' light cycle. Experiments were performed at 25°C.

3.3.2. Treatments

Imidacloprid (IMD; Sigma-Aldrich, Oakville, Canada), imidacloprid-olefin (OLE; Toronto Research Chemicals, North York, Canada), and 5-hydroxy-imidacloprid (5OH; Toronto Research Chemicals, North York, Canada) were dissolved in DMSO and diluted in locust saline (147 mmol NaCl, 10 mmol CaCl2, 3 mmol NaOH, 10 mmol Hepes, pH 7.2) to produce a final concentration of 10 ng/µl with 0.2% (v/v) DMSO for all experiments. The vehicle control solution contained locust saline and 0.2% (v/v) DMSO.

3.3.3. Behaviour

Locusts were loosely tethered in the centre of a 0.9 x 0.9 x 3 m Plexiglas wind tunnel with a constant wind speed set to 3 m/s, which is the average flight speed of a flying locust (Baker et al. 1981), and presented with the image of a 14 cm disc looming perpendicularly to the axis of the animal (90º to head-on) to elicit collision avoidance behaviours (Parkinson et al.

2017). Flight behaviour was recorded before (PRE) and 1 hour after treatment with 10 ng/g (of locust; mean locust mass = 1.5g) of IMD (n=10), OLE (n=10), or 5OH (n=10). Animals were treated by injecting 1 µl/g of locust of a solution containing 10 ng/µl of IMD, OLE or 5OH in locust saline plus 0.2% (v/v) DMSO into the hemolymph under the cuticle of the pronotum. I showed previously that the vehicle alone had no effect on behaviour and therefore did not use a vehicle control solution here (Parkinson et al. 2017). Flying animals were scored as responding (R) if animals responded to the stimulus with a turn, glide or stop, or not responding (NR) if they did not respond. Animals that were not able to fly were scored as not flying (NF).

3.3.4. Electrophysiology

Locusts were dissected dorsally to expose the ventral connectives and ganglia (Cross and Robertson 2016), filled with 0.2 ml locust saline, and three suction electrodes were attached to the right ventral nerve cord: posterior to the prothoracic ganglion, as well as anterior and posterior to the mesothoracic ganglion (Figure 3.1A). A ground wire was inserted into the abdomen and reference electrode inserted into the flight muscles. The image of a 7cm diameter looming disc was presented to the left eye of the locust at 60 frames/s through a rear-projection screen 20 cm from the eye at an angle of 45 degrees from the front of the animal (Figure 3.1B). The visual stimulus program was written in Python using Pyglet, a program used to write video graphics. An Arduino Uno was coded to output a single 5V pulse at the projected time of collision (TOC), or time the looming stimulus would have collided with the locust. Three repetitions of the looming stimulus with 3-minute inter stimulus intervals were presented for the pre-treatment control, after which saline was removed from the body cavity and replaced by 0.2 ml saline plus 10 ng/g of locust of IMD (n=9), OLE (n=6) or 5OH (n=8), or the vehicle control (n=7). Continuous neural data were amplified with a differential AC amplifier (A-M Systems, model no. 1700, 100 Hz high pass and 5 kHz low pass filters, gain = 100x). Amplified neural data and stimulus pulse were digitized using a Data Translation DT9818 data acquisition board (TechnaTron Instruments, Inc., Laval, QC) and recorded at 30 kHz with DataView version 11 (W.J. Heitler, University of St Andrews, Scotland).

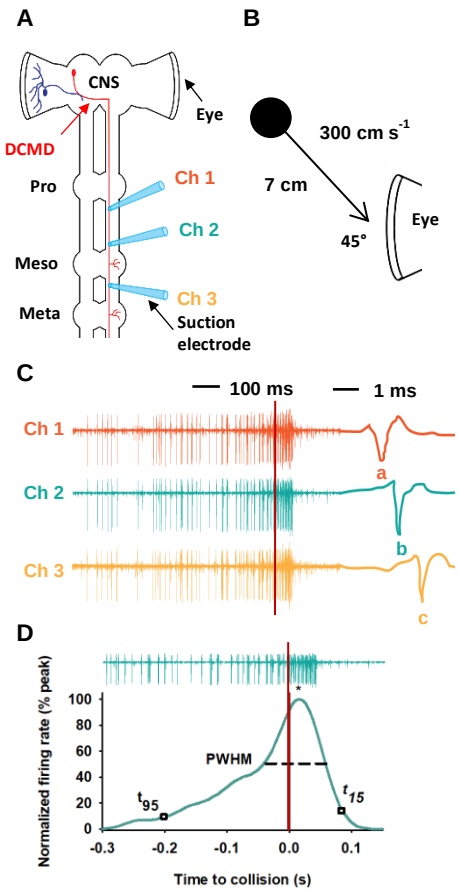

Figure 3.1: Electrophysiology, experimental procedures and data analysis. A) Suction electrodes recorded the activity of the DCMD axon at three points along the ventral nerve cord: posterior to the prothoracic ganglion, and anterior and posterior to the mesothoracic ganglion. B) I presented locusts with the image of a 7 cm diameter disk looming at 300 cm/s at 45° from the front of the animal. C) Raw extracellular recordings from the ventral nerve cord during presentation of a looming stimulus. Waveforms to the right of the traces show individual DCMD spikes in a shorter time window, with the relative timing of letters highlighting the peak of each spike used to calculate conduction velocity. D) Raw recording and corresponding peristimulus time histogram (PSTH) constructed as the firing rate versus time using a 1 ms bin width and smoothed with a 50 ms Gaussian filter. Firing parameters including peak time and peak firing rate (*), peak width at half maximum (PWHM), rise phase (t_{95}, the time when the histogram last increased above the 95% confidence interval with a positive slope, to *) and decay phase (* to t_{15}, the time the histogram when the firing rate decayed to 15% of the peak) were measured from the PSTHs to compare responses before and after treatment.

3.3.5. Data analysis

Spike sorting of the three channels of continuous neural data was performed using DataView. Raw continuous data were upsampled to 90 kHz. The large amplitude DCMD spike times were extracted with a threshold analysis (Figure 3.1C). Spike times were aligned to the

stimulus pulse and exported into Neuroexplorer analysis software (NEX Technologies, Littleton, MA) to construct peristimulus time histograms (PSTHs) with a 1 ms bin width and smoothed with a 50 ms Gaussian filter (Figure 3.1D). Matlab (The MathWorks, Natick, MA) was used to calculate DCMD firing parameters from the PSTHs. DCMD conduction velocity was calculated between the three channels as the reciprocal of the delay between spikes along the connective and across the mesothoracic ganglion and normalized as a proportion of the conduction velocity of the first spike of the first control recording for each animal (Cross and Robertson 2016).

3.3.6. Statistical analysis

Statistical analyses were performed using SigmaStat 3.5, and figures were created with SigmaPlot 12.5 (Systat Software Inc., Richmond, CA) and Illustrator CS2 (Adobe Systems, San Jose, CA). Normally distributed variables were compared using two-way Repeated Measures ANOVA (two-way RM ANOVA) with F statistic and subscripted degrees of freedom and residual, followed by a Holm-Sidak post-hoc analyses comparing across treatment and time to the control and pre-treatment, respectively. Variables that failed tests of normality or equal variance were compared using one-way ANOVA within time (pre-treatment, 30 minutes and 60 minutes), and treatments were compared post-hoc to the vehicle using Dunn's method. Parametric data were plotted as bar graphs including positive standard error of the mean bars (s.e.m.), and non-parametric data were plotted as boxplots showing the median value, 25th and 75th percentile as box boundaries and 10th and 90th percentiles as error bars. Significance was assessed at $P<0.05$.

3.4. Results

3.4.1. Behaviour

Locust flight and escape behaviours were tested in a wind tunnel, using the image of a looming stimulus to elicit escape manoeuvres. While all pre-treatment locusts (n=30) flew and responded to the looming stimulus with an escape manoeuvre (turn or glide), treatment with 10 ng/g IMD, OLE or 5OH reduced or abolished behavioural responses, resulting in locusts that either flew without responding to the looming stimulus or did not fly (Figure 3.2). The parent compound, IMD had the smallest effect, with 40% of animals flying and responding to the

stimulus, while 30% flew and did not respond and 30% could not fly 1 hour after treatment. OLE resulted in 50% of animals unable to fly, 40% of animals flying but not responding to the stimulus, and 10% flying and responding with an escape manoeuvre. 5OH had the largest effect on flight, with 80% of animals unable to fly 1 hour after injection, and the remaining 20% flew, but did not respond to the looming stimulus. These results show that, while all compounds affected flight behaviour at the concentration used, the effects varied across treatments.

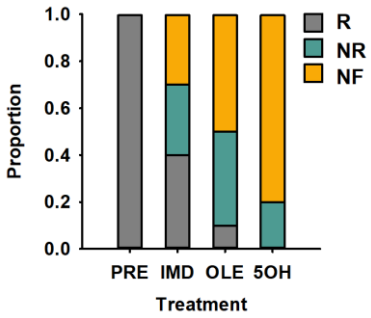

Figure 3.2: Flight and escape behaviours before (PRE) and after treatment with IMD, OLE or 5OH. Loosely tethered flight behaviour of locusts was recorded in a wind tunnel during presentation of a looming disk before (PRE) and after treatment with IMD, OLE and 5OH. Animals that responded to the stimulus with a turn or a glide were scored as responding (R), and those that did not respond to the stimulus were scored as not responding (NR). Animals that were not able to fly in a coordinated manner after treatment were scored as not flying (NF).

3.4.2. DCMD responses to looming stimuli

I examined the responses of the DCMD to a looming stimulus before treatment and over 1 hour after treatment with 10 ng/g of IMD, OLE, or 5OH. The response profile of the DCMD was altered after treatment with IMD, OLE or 5OH compared to the vehicle control group (Figure 3.3). The effect of IMD and metabolites is visible 30 minutes after treatment, with the peak of the PSTHs lowered to approximately 80% of pre-treatment levels. This effect was enhanced 60 minutes after treatment, with the peak firing rates reduced to 75% of the pre-treatment peak, and slight differences in the rising and falling slopes of the histograms between treatments.

Mean PSTH shape was compared between treatments to the vehicle and across time to pre-treatment values by examining individual response parameters (Figure 3.4). The total number of DCMD spikes per stimulus presentation was significantly affected across treatments (two-way RM ANOVA, $F_{3,47} = 3.675$, $p = 0.025$). Post-hoc multiple comparisons (Holm-Sidak)

showed that the number of spikes was significantly reduced at both 30 and 60 minutes after treatment with IMD and 5OH compared to the control (IMD: 30 min = 71.6%, 60 min = 71.3%; 5OH 30 min = 80.4%, 60 min = 68.6%). The peak firing rate was affected by treatment (two-way RM ANOVA, $F_{3,26}$ =5.006, p=0.007) and time after treatment (two-way RM ANOVA, $F_{1,26}$ =4.263, p=0.049). Post-hoc analysis showed the peak firing rate was reduced for OLE and 5OH at 30 minutes after treatment (OLE = 81.5%; 5OH = 83.6%), and for all treatments at 60 minutes after treatment (IMD = 79.2%; OLE = 75.6%; 5OH = 74.3%). The peak firing rate was significantly lower for 5OH at 60 minutes compared to 30 minutes after treatment.

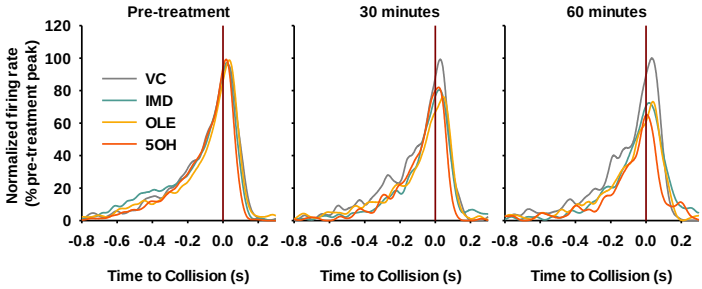

Figure 3.3: Mean peristimulus time histograms (PSTHs). Data are from all animals in each treatment group normalized as a percent of the pre-treatment peak firing rate before treatment (pre-treatment), 30 minutes, and 60 minutes after treatment with 10 ng/g of locust of IMD (n=9), OLE (n=6) or 5OH (n=8), or the vehicle control (n=7). Vertical red lines at 0s represent the projected time of collision of the looming stimulus.

Despite a reduction in total number of spikes and peak firing rate, there was no effect on PWHM or peak time for any treatment (p>0.05). Histogram shape was compared in higher resolution by examining the rise and decay phases. Rise phase was affected by treatment at 60 minutes after treatment (one-way ANOVA, $F_{3,25}$ =12.081, p<0.001), while there was no effect on rise phase at 30 minutes after treatment. Holm-Sidak multiple comparison versus the control group showed a significantly shortened rise phase with the IMD and 5OH treatments. Similarly, there was no effect of treatment on the decay phase of the histogram, while there were significant effects at 60 minutes (one-way ANOVA on Ranks, H_3=9.504, p=0.023). Dunn's post hoc analysis showed the IMD treatment resulted in an increased decay phase 60 minutes after treatment.

In summary, these results show that the treatments reduced the total number of spikes and peak firing rate of the DCMD in response to a looming stimulus, and that the effects were on

peak firing rate were present for the 5OH and OLE treatments already by 30 minutes after treatment. In addition, I see effects on the histogram shape, with a shortened rise phase and lengthened decay phase for the IMD treatment at 60 minutes, and a shortened rise phase for the 5OH treatment at 60 minutes after treatment.

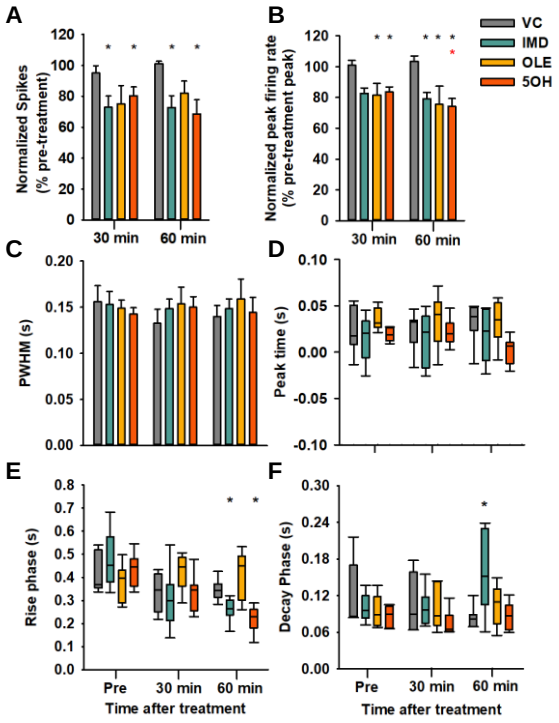

Figure 3.4: Comparison of DCMD response parameters. Measurements included: A) total number of spikes per stimulus presentation, B) normalized peak firing rate, C) peak width at half the maximum firing rate, D) peak time, E) rise and F) decay phases of the histograms. Bars display positive s.e.m. and boxplots display the median line and 25th and 75th percentiles, with whiskers at the 5th and 95th percentiles. Asterisks above bars represent significance from a Two-Way Repeated Measures ANOVA. Black asterisks compare treatments to the vehicle (VC) within time (pre-treatment, 30 minutes and 60 minutes after treatment), and coloured asterisks compare within treatment over time. Asterisks above box plots denote significance of treatment compared to VC within time after treatment from One Way ANOVA tests.

3.4.3. Conduction velocity

The relative conduction velocity along the DCMD axon was altered by treatment of IMD, OLE or 5OH, and these effects depended on firing rate and location (along the ventral connective versus across the mesothoracic ganglion). Figure 3.5 shows the relationship between conduction velocity, both along the ventral connective (CVC) and across the mesothoracic ganglion (CVM),

and the firing rate of the DCMD during the approach of the looming stimulus. The firing rate peaked close to TOC and was associated with reduced conduction velocity for all treatments, including the vehicle, which was reduced by approximately 20% at peak firing rates. IMD, OLE, and 5OH also displayed a reduced conduction velocity at peak firing rates, but these were also associated with firing rates that were reduced to approximately 70% of pre-treatment levels.

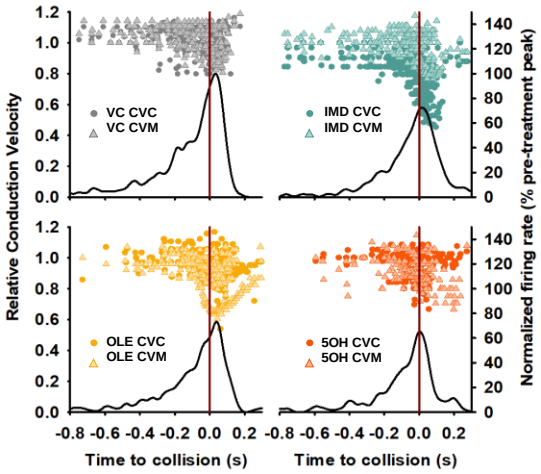

Figure 3.5: Effects of treatment on conduction velocity. Relative DCMD conduction velocity versus time to collision for all DCMD spikes recorded along the ventral connective (CVC) and across the mesothoracic ganglion (CVM) for all animals in each treatment group during the approach of a looming stimulus at 60 minutes after treatment, and the corresponding mean PSTHs (black lines). Projected time of collision is marked with a red vertical line. Darker colours and circles represent measurements along the ventral connective, while triangles and lighter colours represent measurements across the mesothoracic ganglion.

The relationship between conduction velocity and firing rate appears to have been affected by treatments differentially along the connective or across the mesothoracic ganglion (Figure 3.6A). Conduction velocity decreased with increasing firing rate for all treatments (including vehicle). I compared conduction velocity among treatments with the firing rate binned into three categories: <100 spikes/s, 100-200 spikes/s, and >200 spikes/s (Figure 3.6B). Conduction velocity was binned to isolate the effect of firing rate (Cross and Robertson 2016). All spike rates above 350 spikes/s were removed for this analysis since IMD, OLE, and 5OH reduced peak firing rates to below this level. There was a significant effect of treatment and frequency group on CVC (two-way RM ANOVA, treatment $F_{3,32}$=7.024, p=0.003; frequency $F_{2,32}$=28.620, p<0.001). Comparison of CVC within firing rate bin shows a significant effect of IMD and OLE at all firing rate bins. At firing rates >200 spikes/s, CVC was also significantly

reduced with 5OH. CVC was significantly reduced with 5OH in the 100-200 spikes/s bin compared to the <100 spikes/s bin, and in the >200 spikes/s bin the conduction velocity of all treatments was significantly lower than values in the <100 bin within each treatment.

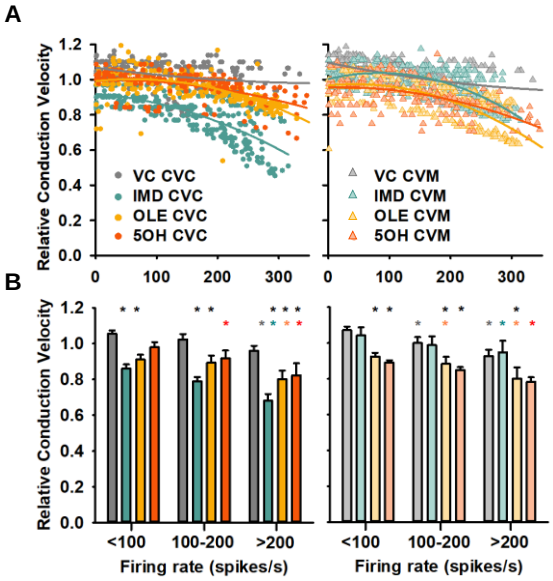

Figure 3.6: Relative conduction velocity as a function of instantaneous firing rate along the ventral connective (CVC) and across the mesothoracic ganglion (CVM). A) Conduction velocity of each DCMD spike recorded from all animals 60 minutes after treatment within each treatment group during the approach of a looming stimulus versus instantaneous firing rate along the connective (left) or across the mesothoracic ganglion (right). Nonlinear regressions were fit for data within each treatment using a polynomial quadratic equation. B) Bar graphs (with positive s.e.m.) illustrating the effects of treatment and firing rate on CVC (left) and CVM (right). Asterisks denote results of two-way Repeated Measures ANOVA with black asterisks comparing treatments to the vehicle (VC) within each firing rate group and coloured asterisks comparing within treatment to the <100 spikes/s firing rate group.

Conduction velocity was also affected by treatment (two-way RM ANOVA, $F_{3,30}$=4.773, p=0.014) and firing rate bin (two-way RM ANOVA, $F_{2,30}$=48.947, p<0.001) as the axon crossed the mesothoracic ganglion (CVM, Figure 3.6B, right panel). Holm-Sidak post hoc analysis showed that OLE had a significant effect on CVM, resulting in a lower velocity compared to the vehicle within each firing rate bin. Additionally, the decrease in CVM with OLE was significantly greater at the 100-200 and >200 spikes/s bins compared to the <100 bin 5OH significantly decreased CVM compared to the vehicle in the lowest bin only, but CVM was significantly reduced in the >200 bin compared to the <100 bin. In the >200 bin the vehicle and IMD CVM was significantly reduced compared to the <100 bin within each treatment.

Overall, while conduction velocity was reduced for all treatments (including vehicle) at the highest firing rates (>200 spikes/s), both along the ventral connective and across the mesothoracic ganglion, there was a significant decrease in conduction velocity compared to the vehicle within each frequency group that resulted from treatment with IMD, OLE and 5OH. OLE had a significant effect across all firing rates and locations whereas IMD produced the most dramatic effect along the ventral connective only.

3.5. Discussion

While a large body of research exists highlighting the toxicological effects of neonics, relatively few studies examine the contributions of the neurotoxic metabolites even though some metabolites persist longer *in vivo* and in the environment (Suchail et al. 2004; Codling et al. 2016). Identification of the specific contributions of neonic metabolites to toxicity enables a greater understanding of primary and secondary effects of these insecticides and highlight the significance of their presence in the environment.

Potential limitations of the current study included the method of administering the treatments differing between behavioural and electrophysiological assays, and the metabolism of IMD that would naturally occur within the time frames tested. For electrophysiological assays the locust was dissected dorsally and filled with saline, into which the chemicals were added, and during behavioural assays the chemicals were injected with a small volume of saline containing the treatment directly into the hemolymph. Despite these differences the total amount of each chemical used was the same between experiments (10 ng/g), thus comparison of electrophysiological and behavioural assays is valid. Future studies should consider the time required for IMD to be metabolized in vivo in the locust and determine relative concentrations of OLE and 5OH within 1 hour of treatment.

For behaviour and electrophysiology, I used a consistent dose of 10 ng/g of locust, which I showed previously to be sublethal at 0.04% of the LD50 (2500 ng/g) when injected into the hemolymph (Parkinson et al. 2017). In *Apis mellifera* imidacloprid has an acute toxicity (LD50) value of 570 ng/g for imidacloprid, 280 ng/g for imidacloprid-olefin, and 2580 ng/g for the 5-hydroxy metabolite (Suchail et al. 2001), roughly ranging across an order of magnitude. Our previous findings used a concentration of imidacloprid that was two orders below the LD50 for

locusts. Therefore, assuming a similar range of metabolite toxicity in bees and locusts, I suggest that the metabolite doses I used here were also sublethal.

Behaviour

I found that IMD, OLE and 5OH affected collision avoidance behaviour and flight 1 hour after treatment. The effects were greatest for the 5OH metabolite, and IMD had the smallest effect overall. Sublethal doses of IMD are known to decrease collision avoidance behaviours in locusts 2 and 24 hours after treatment (Parkinson et al. 2017) and here I confirm that this effect is already present 1 hour after treatment, although there is more variability between animals. Effects on forward flight versus flight steering suggest toxicity is occurring at different locations in the nervous system. Animals that were able to fly but did not respond (NR) suggest toxicity is targeted to visual interneurons, like the DCMD, that convey information about the looming stimulus, while motor control of flight, such as the thoracic central pattern generators, were unaffected. Toxic effects extended to the control of central pattern generators or directly to the innervation of flight muscles for animals unable to fly. Contrasting vertebrates, the synapses at neuromuscular junctions in insects are glutamatergic (Usherwood 1977), while acetylcholine is the primary neurotransmitter within the insect central nervous system, mediating excitatory and inhibitory synapses via nicotinic and muscarinic receptors, respectively (Trimmer 1995). However, insect motorneurons contain nAChRs as a primary excitatory synapse (Parker and Newland 1995), and inactivation of motorneurons by IMD or its metabolites would result in animals that are unable to fly.

It is plausible that the effects on flight behaviour are caused by the metabolites of imidacloprid rather than the parent compound, as there is a greater effect of the metabolites when administered at the same dose. Imidacloprid is rapidly metabolized to OLE, 5OH and other metabolites, with OLE and 5OH measurable in the head, thorax, abdomen and hemolymph within 20 minutes of treatment in honeybees (Suchail et al. 2004). Given the quick metabolism of IMD in vivo, it is likely that the behavioural effects observed here are due partially to the metabolites, which could explain the enhanced effects of the metabolite treatments.

Visual Motion Detection

Visual motion detection was affected by IMD, OLE and 5OH 30 and 60 minutes after treatment, measured primarily as a decreased peak firing rate and total number of spikes, with no effect on the time of the peak and PWHM. Reduction in the total number of spikes and peak firing rate are measures of decreased DCMD excitation in response to the looming stimulus. As there was little or no effect on PWHM or peak time, it is likely that inhibitory neurons upstream of the LGMD/DCMD are also affected by IMD and its metabolites, resulting in decreased activity of these neurons as well. Inhibitory synapses in the locust optic lobe are primarily muscarinic cholinergic (Rind and Leitinger 2000; Zhu et al. 2018), and IMD has not been shown to affect these synapses (Buckingham et al. 1997). However, dendritic receptors activating inhibitory neurons may be nicotinic cholinergic, so it is possible that IMD and its metabolites are affecting these neurons in the same way as the DCMD, resulting in an overall reduced firing rate with less effect on the slope of the response.

I propose two potential mechanisms for the inactivation of nAChRs by IMD and its metabolites. The first is via the direct desensitization of the receptors resulting from prolonged exposure to the agonists (Nauen et al. 2003; Oliveira et al. 2011). An alternative mechanism is that IMD-mediated increased intracellular calcium ($[Ca^{2+}]_i$) results in the inhibition of nAChRs via phosphorylation-dependent mechanisms, such as the cAMP-mediated pathway. Insect nAChRs are regulated via second messengers including cAMP, which is activated by adenylyl cyclase and may be regulated directly by $[Ca^{2+}]_i$ (Thany et al. 2007). Neonics have been shown to directly alter $[Ca^{2+}]_i$ via interactions of nAChRs with voltage-gated calcium channels that amplify IMD-induced increases in $[Ca^{2+}]_i$ (Jepson et al. 2006). Furthermore, desnitro-IMD, a form of IMD highly toxic to mammals, activates the extracellular signal-regulated kinase cascade, which may result in deficiencies in cell survival/cell death via alterations in $[Ca^{2+}]_i$ resulting from activation of the nAChR (Tomizawa and Casida 2003). Taken together, it is likely that the reduction in DCMD firing shown here results from decreased activity of nAChR caused both directly and indirectly by the binding of IMD and its metabolites to the receptors.

Waveform Propagation

I report that the conduction velocity along the DCMD axon is reduced by IMD, OLE and 5OH, and that these effects depended on firing rate and location along the axon, the latter likely

due to physical properties of the axon. The DCMD axon runs along the dorsomedial region of the connective and decreases in diameter as it crosses the mesothoracic ganglion, with collateral projections to the medial, lateral and ventral regions of the neuropil (Gray et al. 2010). At high firing rates, the ion concentrations within the ganglion may be altered due to the many active synapses between the DCMD and other neurons in the ganglion. High frequency firing can result in decreased conduction velocity in dorsal root ganglion cells and is associated with an increase in $[Ca^{2+}]_i$ (Luscher et al. 1994). The effect may be responsible for the observed decrease in conduction velocity at high firing rates across the ganglion, but not along the ventral connective. Given that IMD had no effect on conduction velocity across the ganglion, but a very large effect (mean reduction of 32%) at high frequencies along the connective, I suggest that the isolation provided by the neuropil may reduce the effects of IMD. The mechanism by which IMD, OLE and 5OH decrease conduction velocity in the unmyelinated DCMD axon has not been examined directly, but it is possible this effect is caused by alterations to $[Ca^{2+}]_i$.

Conclusions

In summary, I found that exposure to 10 ng/g (100 µg/kg) imidacloprid and two of its metabolites, imidacloprid-olefin and 5-hydroxy-imidacloprid, affected flight and collision avoidance behaviours, with greater effects for 5OH than OLE, and for OLE than IMD. Additionally, I found that IMD and its metabolites decreased visual motion detection, as measured from the activity of the DCMD neuron, and that effects on the peak DCMD firing rate occurred sooner following direct treatment with the metabolites. These results support our hypothesis and suggest that the main effects on behaviour and neural coding are due, primarily to exposure to metabolites. One hour after treatment, IMD would be metabolized partly to 5OH and OLE, but at lower concentrations given the breakdown of IMD to 5OH, OLE and other, non-neurotoxic metabolites (Nauen et al. 2001). Given that the metabolites have the same or greater effect than the parent compound on both behaviour and neural processing highlights the importance of considering the environmental longevity and concentrations of these metabolites as well as the parent compound.

I additionally found that conduction velocity was significantly reduced with IMD, OLE and 5OH, which corresponds with effects measured in humans exposed to agricultural neonics (Huang et al. 2016; Zhang et al. 2018). Additional research is needed to uncover the mechanism

affecting conduction velocity of neonics. Overall, I have described and compared the effects of two neonic metabolites on flight behaviour and visual processing and found that these metabolites display similar toxicity to the parent compound. This study should inform future studies examining ecological presence of neonics, as the presence of certain metabolites may be equally or more toxic to non-target organisms including important pollinators.

Chapter 4: Attenuation of excitation in optic lobes by imidacloprid, not sulfoxaflor, results in ineffective visual motion detection in a neural population[3]

4.1. Abstract

Insect nervous systems offer unique advantages for studying interactions between sensory systems and behaviour given that they are complex and yet highly tractable. By examining the neural coding of salient environmental stimuli and resulting behavioural output in the context of environmental stressors, we gain an understanding of the effects of these stressors on brain and behaviour and provide insight into normal function. Flight behaviours, including orientation, navigation and collision avoidance are essential to the survival of many animals and are guided primarily by the processing of visual information, which may be affected by insecticides like neonicotinoids. The locust (*Locusta migratoria*) possesses tractable descending visual interneurons, including the Descending Contralateral Movement Detector (DCMD) whose activity arises from the combined input of excitatory and inhibitory signals within the optic lobes to encode the approach of looming objects. Inhibitory neurons are involved with shaping the responses of visual motion sensitive neurons and facilitate habituation to repeated stimulus presentations. The target of neonicotinoids, the nicotinic acetylcholine receptor (nAChR) can be found at excitatory synapses throughout the locust CNS, including potentially on the dendrites of

[3] The content of this chapter come from the following manuscript in preparation. Formatting and layout changes have been made to provide consistency between chapters.

Parkinson RH, Zhang S, and Gray JR (in prep). Attenuation of excitation in optic lobes by imidacloprid, not sulfoxaflor, results in ineffective visual motion detection in a neural population

Author contributions & justification for use in this thesis: R.H.P. designed and carried out experimentation, analyzed the data, interpreted the results, prepared the figures, and wrote and revised the manuscript. S.Z. analyzed the data. J.R.G. conceived experiments, interpreted the results, revised the manuscript, and approved the final version.

inhibitory neurons. Here I measured the effects of imidacloprid (neonicotinoid) and sulfoxaflor on collision avoidance behaviour and population coding of descending visual interneurons. I showed that both excitatory and inhibitory neurons were affected by imidacloprid, with the greatest effects on excitation due to relatively more synapses in these circuits containing nAChRs, and I provided new insight into how a population of visual interneurons habituates, both with and without treatment. I solidified the use of these neuroethological assays for comparative neurotoxicology, as I showed reduced toxicity of sulfoxaflor under the same treatment concentrations.

4.2. Introduction

The use of agrochemicals has become increasingly important to sustain large-scale monocultures that are vulnerable to pests (Meehan et al. 2011). Many modern insecticides are applied as seed treatments to prophylactically address this threat, and these products are available as complex mixtures containing multiple insecticides and fungicides. Of the seed treatments, the most nefarious insecticidal group is the neonicotinoids (neonics), which are nicotinic acetylcholine receptor (nAChR) agonists with specificity for insect receptor subunits (Matsuda et al. 2001). Neonics have been implicated in contributing to declines of non-target insects, with wild bee populations displaying the greatest sensitivity to these compounds (Goulson 2013; Rundlöf et al. 2015; Woodcock et al. 2016). The sublethal effects of neonics, however, are very complex, and it is difficult to link effects observed across levels of biological organization and estimate risk of exposure in the field. For example, the presence of alternate food sources should reduce the threat posed by treated crops, but it has been shown that bees prefer food laced with neonicotinoids (Kessler et al. 2015; Arce et al. 2018).

The development of novel insecticides is necessary to contend with insecticidal resistance in target organisms that can arise from receptor polymorphisms and enhanced detoxification pathways (Ihara and Matsuda 2018). A novel group of insecticides, the sulfoximines, display a similar mode of action to the neonics, but do not display cross-resistance (Longhurst et al. 2013) related to differential detoxification pathways of these insecticidal groups (Sparks et al. 2012). While a sulfoximine insecticide, sulfoxaflor, is already marketed in seed treatment mixtures, the range of sublethal effects on non-target organisms is not fully understood. Sulfoxaflor has

recently been shown to negatively affect reproductive success in bumblebees (Siviter et al. 2018). The introduction of new agrochemicals to the ecosystem prior to a complete understanding of the negative effects results in a repeating pattern of ecological damage. To mitigate these effects, toxicological assays should be developed that simultaneously address effects at multiple levels of biological organization.

The neonic imidacloprid (IMD) has previously been shown to affect visual motion processing and collision avoidance behaviour in the locust (*Locusta migratoria*) (Parkinson et al. 2017; Parkinson and Gray 2019). The locust possesses a tractable and well-described descending interneuron, the descending contralateral movement detector (DCMD), which responds preferentially to objects approaching on a direct collision course (looming) (Simmons and Rind 1992; Gabbiani et al. 1999). This neuron displays bursting activity (McMillan and Gray 2015) and is important for the generation of escape behaviours (Parker and Newland 1995; Rind et al. 2008). In addition, this neuron habituates to repeated stimulus presentation (Gray 2005), a phenomenon that is related to the inhibitory pathways in the optic lobe that are activated in tandem with excitatory pathways (Rind and Bramwell 1996; Gabbiani et al. 1999; Wang et al. 2018a). There are other descending interneurons that can be recorded from the ventral nerve cord, with differing response profiles to the DCMD in response to a looming stimulus, however the population response of these neurons has been examined in only one study (Dick et al. 2017), and another neuron, the late DCMD (LDCMD) is known to habituate less than the DCMD (Gray et al. 2010)

Here, using a combination of multichannel extracellular recordings, I defined the effects of imidacloprid and the novel insecticide sulfoxaflor on the population responses of descending neurons during presentation of a looming stimulus. Effects on the population of descending interneurons were correlated with effects on collision avoidance behaviour. Overall, I found imidacloprid had a significant effect on the population response, while sulfoxaflor did not significantly affect the responses of these descending neurons to object motion. Correspondingly, there were dramatic effects on jumping behaviour, with no animals jumping to avoid the looming stimulus after treatment with imidacloprid, while most of the animals still responded after treatment with sulfoxaflor. These results are significant as they show the first evidence of the effects of a neonicotinoid on a population response and neural habituation, and additionally that sulfoxaflor has reduced toxicity in this context.

4.3. Methods

4.3.1. Animals

Locusta migratoria were reared in a crowded colony at the University of Saskatchewan at 25-28ºC with a 12h light:dark cycle and fed a diet of wheat grass and bran flakes. All experiments were performed on adult males aged two to four weeks past the last imaginal moult.

4.3.2. Treatments

Locusts were fed a small piece of organic lettuce with a 1µl droplet of testing solution containing 100 ng imidacloprid or sulfoxaflor + 0.2% (v/v) acetone in reverse osmosis water, or the vehicle (reverse osmosis water + 0.2% acetone). Locusts then were observed for a short time to ensure they consumed wheat grass and were housed individually for 24 hours with ad libitum access to wheat grass. Locusts that did not consume any food after treatment were discarded from the study. A 100 ng dose of imidacloprid was previously found to be sublethal when injected (Parkinson et al. 2017), while the LD50 value for SFX in locusts is unknown. Only animals that consumed wheat grass after oral treatment were used for subsequent experiments. In general, animals treated with IMD showed neurotoxic effects (trembling, sporadic movements, paralysis) within 30 minutes of treatment, as described previously (Parkinson et al. 2017), while those treated with SFX displayed no behavioural effects at this time point. Subsequent behavioural and electrophysiological assays were conducted 24 hours after the single oral treatment, with no mortality observed in any treatment group at that time.

4.3.3. Visual stimuli

To elicit behavioural and neural responses to visual motion, I used a looming 7 cm diameter black disc approaching at 300 cm/s at 90° perpendicular to the animal. The visual stimulus program was custom written in Python using Pyglet (Stott et al. 2018). An Arduino was programmed to output a single 5 V pulse at the projected time of collision (TOC) of the looming stimulus. The image was displayed on a 1080p Samsung LCD screen (P2570 HD) with an 85 Hz refresh rate. Animals were presented with 5 consecutive stimuli, spaced 3 minutes apart to avoid habituation for behavioural and electrophysiological assays. In addition, I examined the effects

of habituation on neural population coding within the treatment groups using a series of 10 looming stimuli presented at 8 second intervals.

4.3.4. Collision avoidance behaviour assay

All locusts were tested behaviourally prior to treatment, and again 24 hours after treatment. The behavioural assay involved placing untethered locusts in a 30 cm^3 fine mesh wire cage adjacent to a computer monitor displaying the looming stimulus at 3-minute inter-stimulus intervals. If locusts responded to the stimulus with a jump they were scored as responding (Parkinson et al. 2017). Locusts were presented with the looming stimulus 5 times. Those that responded to the stimulus responded every time they were facing the screen.

4.3.5. Electrophysiology

Locusts were dissected dorsally with wings and legs removed and pinned open ventral side down to a cork platform, with gut and muscles cut to expose the ventral nerve cords (Parkinson and Gray 2019). A silver wire hook electrode was used to lift and stabilize the right nerve cord anterior to the prothoracic ganglion. I constructed twisted wire tetrodes following the methods of Guo et al (Guo et al. 2014). For stability, I threaded tetrodes through a sharp glass electrode with the tip broken off at a diameter just wide enough for the tetrode wires to pass through, and these wires were exposed 2-3 mm past the tip of the glass. The protective sheath surrounding the right nerve cord was carefully cut, and the tetrode was lowered vertically into the nerve cord just anterior to the position of the hook electrode. Upon verification of a clean recording by observing neural responses to motion (waving hand) as continuous neural data, I applied petroleum jelly to the nerve cords and surrounding the recording electrodes to prevent desiccation and insulate the recordings.

Of the 15 animals per treatment group tested behaviourally, I obtained recordings that were sufficiently clear for analysis from 12 animals in each group. All five channels (4 channels of the multichannel tetrode, 1 channel for the hook electrode) were amplified with a differential amplifier (A-M Systems 1700, 300 Hz high pass, 5 kHz low pass filters, 100x gain), digitized (DT9818-OEM, TechnaTron Instruments Inc., Laval, QC) and recorded at 25 kHz with DataView version 11.3 (W.J. Heitler, University of St. Andrews, Scotland). Animals were

oriented parallel to the computer monitor, with the centre of the left eye directed toward the screen.

4.3.6. Spike sorting

The activity of individual neurons (units) was discriminated with Offline Sorter v 4.4 (Plexon Inc., Dallas, TX). The four channels associated with the tetrode recording were imported into the program and arranged into a tetrode configuration [Same electrode tip = same channel number across recordings]. Individual data files from all stimulus presentations (5 stimuli spaced 3 minutes apart, 10 stimuli spaced 8 seconds apart) were combined in a single file per animal. The threshold for spike detection was set to three standard deviations from the mean voltage on each continuous data channel. A semi-automatic sorting method was used, based on the K-means algorithm. Cluster centroids were manually selected based on visually determined clusters in 3D feature space. Following an initial sort, units were discriminated manually based on waveform shape and amplitude (Figure 4.1B). MANOVA analysis was used to determine that sorted units from each locust were statistically well-separated in 3D space (Figure 4.1B). In total, I discriminated 246 units across 36 animals (Table 4.1). Raw spike times for individual units were used to construct peristimulus time histograms (PSTHs), smoothed with a 50 ms Gaussian filter and aligned to the projected time of collision of the stimulus (TOC).

4.3.7. Spike train analysis

Using these PSTHs, I determined which units were responding to the stimulus by plotting the cumulative sum of spike counts over an ellipse that represented the 99% confidence level. The cumulative sum was calculated in Neuroexplorer with the following algorithm: for bin 1, cs(1) = bc(1)A; for bin 2, cs(2) = bc(1) + bc(2)-A X 2l for bin 3: cs(3) = bc(1) + bc(2) + bc(3)-A X 3, etc. Thus, the cumulative sum (cs) at each bin count (bc) includes the counts from previous bins plus the current bin, minus the average (A) of the entire histogram. A cumulative sum that did not pass outside or touch the edge of the 99% confidence level ellipse represented a firing rate that showed no significant change as a result from the stimulus, while those that touched or expanded past the edge of the ellipse were considered to have a significant, stimulus evoked, firing rate change (Dick et al. 2017). Units that were not responding were removed from

subsequent analysis. Figure 4.1C shows an example of the PSTHs and cumulative sum from a unit that is responding (left) and one that is not responding (right) to the visual stimulus.

For stimuli spaced at 8 second intervals, I calculated a habituation index (*H*) of all responding units, using the proportions of the total number of spikes and mean frequency of every stimulus presentation normalized to the first stimulus of the sequence such that:

$$H = \frac{\left(\frac{sp_{i+1}}{sp_i}\right) + \left(\frac{mf_{i+1}}{mf_i}\right)}{2} - 1$$

Where *sp* = number of spikes between -1.5 to 0.5 seconds, *i* = approach number > 1, and *mf* = mean frequency.

4.3.8. Statistical analysis

Parameters measured from neural data were compared between treatment groups using One-way analysis of variance (ANOVA) for normally distributed data or one-way ANOVA on Ranks for non-parametric data, with Dunn's Method post-hoc analyses. Results from behavioural assays were compared using Chi-squared. Rise phase data was compared between treatments and unit group using two-way ANOVA with Holm-Sidak multiple comparison post-hoc analysis.

4.4. Results

4.4.1. Collision avoidance behaviour

All animals (n=45) responded to the looming stimulus with a jumping escape behaviour prior to treatment (data not shown). However, oral treatment with 100ng IMD (n=15) resulted in all animals unresponsive to the looming stimulus 24 hours after treatment (Figure 4.1A). Treatment with SFX (n=15) at the same dose had a greatly reduced effect on behaviour, with 12/15 animals still responding to the looming stimulus. All vehicle control animals (n=15) responded to the stimulus with an escape behaviour.

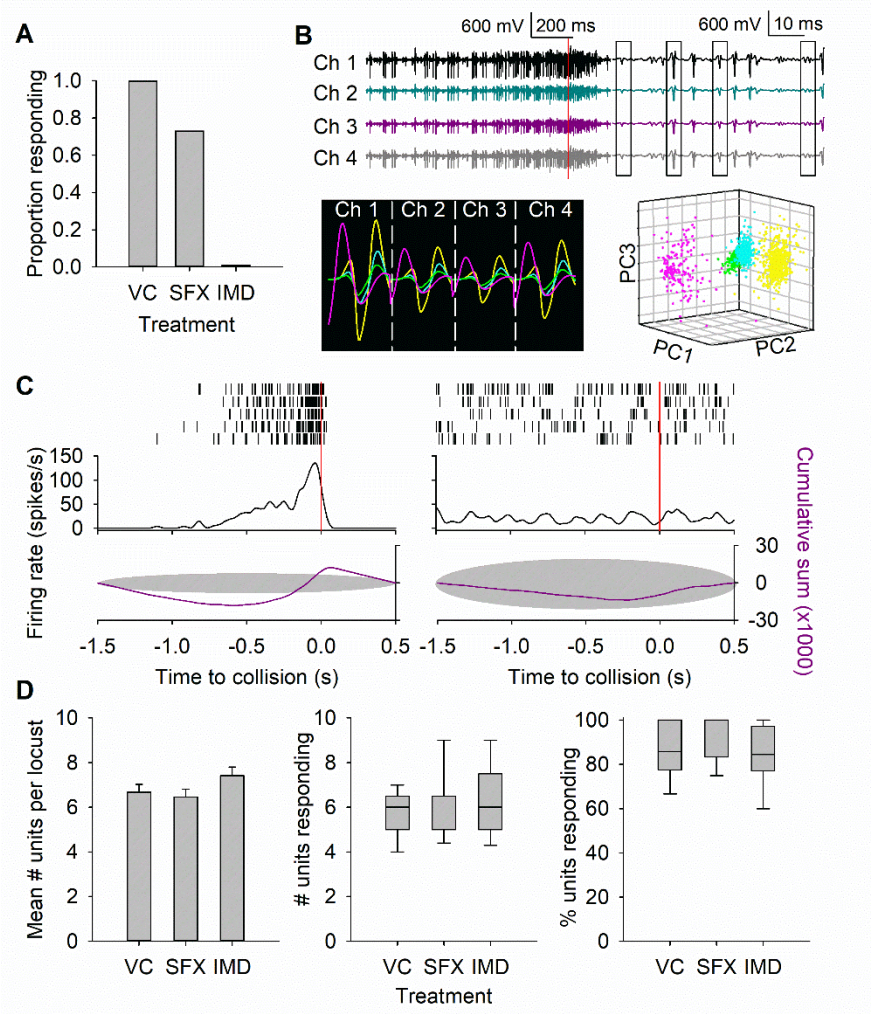

Figure 4.1: Collision avoidance behaviour and classification of spikes belonging to units that respond to a looming stimulus based on treatment with vehicle, sulfoxaflor, or imidacloprid. A) Proportion of locusts jumping in response to looming stimulus 24 hours after a single oral treatment with the vehicle (VC), sulfoxaflor (SFX) or imidacloprid (IMD). B) Raw tetrode recording from the ventral nerve cord during visual stimulation with a looming stimulus (top left, red vertical line marks the time of collision), individual spikes are marked by black boxes (top right) and displayed as the mean of the sorted units across the entire recording for each channel (bottom left). Clusters representing all spikes within each unit are distinct in 3-dimensional feature space (bottom right). C) Raster plots (top) and mean peristimulus time histogram (PSTH, middle) constructed from a single unit over five stimulus presentations, with the time of collision marked by a vertical red line. The cumulative sum of the histogram is displayed over an ellipse representing the 99% confidence level (bottom). A unit is said to be responding if the cumulative sum exits the ellipse (left), or not responding if it does not (right). D) Comparison of the total mean number of units per locust per treatment (left), the number of responding units per locust per treatment (middle), and the percent of responding units per locust per treatment (right). Columns show mean and SEM while boxes show median, 25th and 75th percentile with 10th and 90th percentile shown with whiskers.

Table 4.1 Summary statistics for sorted spikes for each animal by treatment group and animal ID number. Treatments included: vehicle control (VC), imidacloprid (IMD), and sulfoxaflor (SFX).

Vehicle Control				Imidacloprid				Sulfoxaflor			
ID	Spikes	Units	MANOVA	ID	Spikes	Units	MANOVA	ID	Spikes	Units	MANOVA
VC_{03}	8192	6	$P << 0.001$ $F_{15,22593} = 3.8$	IMD_{01}	4869	7	$P << 0.001$ $F_{18,15288} = 10.4$	SFX_{01}	9369	6	$P << 0.001$ $F_{15,25825} = 22.1$
VC_{04}	7933	8	$P << 0.001$ $F_{21,22751} = 9.8$	IMD_{02}	5861	8	$P << 0.001$ $F_{21,16781} = 3.8$	SFX_{02}	5831	6	$P << 0.001$ $F_{15,16075} = 15.6$
VC_{05}	5632	5	$P << 0.001$ $F_{12,14883} = 11.1$	IMD_{03}	8193	9	$P << 0.001$ $F_{24,23719} = 14.0$	SFX_{03}	8705	6	$P << 0.001$ $F_{15,24006} = 10.3$
VC_{06}	8332	6	$P << 0.001$ $F_{15,22516} = 7.4$	IMD_{04}	9387	6	$P << 0.001$ $F_{15,25883} = 6.5$	SFX_{04}	11761	7	$P << 0.001$ $F_{18,33240} = 3.2$
VC_{07}	8432	9	$P << 0.001$ $F_{24,24421} = 5.4$	IMD_{05}	5043	6	$P << 0.001$ $F_{15,13889} = 8.8$	SFX_{05}	10088	7	$P << 0.001$ $F_{18,28508} = 5.2$
VC_{08}	5595	7	$P << 0.001$ $F_{18,15800} = 12.5$	IMD_{07}	6134	9	$P << 0.001$ $F_{24,17759} = 10.6$	SFX_{06}	8841	6	$P < 0.001$ $F_{15,12981} = 3.0$
VC_{09}	5350	7	$P << 0.001$ $F_{18,15107} = 9.3$	IMD_{09}	8879	9	$P << 0.001$ $F_{24,25715} = 34.3$	SFX_{07}	4723	6	$P < 0.001$ $F_{15,19716} = 2.9$
VC_{10}	6925	6	$P << 0.001$ $F_{15,19095} = 8.3$	IMD_{11}	9646	6	$P << 0.001$ $F_{15,26596} = 18.1$	SFX_{08}	8912	7	$P << 0.001$ $F_{18,25165} = 3.6$
VC_{11}	8992	7	$P << 0.001$ $F_{18,25400} = 3.5$	IMD_{12}	8681	7	$P << 0.001$ $F_{15,26596} = 21.7$	SFX_{09}	7959	9	$P << 0.001$ $F_{24,23052} = 11.4$
VC_{12}	11819	8	$P << 0.001$ $F_{21,33907} = 12.2$	IMD_{13}	8547	7	$P << 0.001$ $F_{18,24135} = 8.4$	SFX_{10}	7459	5	$P << 0.001$ $F_{12,19716} = 5.3$
VC_{13}	7536	5	$P << 0.001$ $F_{12,19899} = 12.5$	IMD_{14}	10447	9	$P << 0.001$ $F_{15,25118} = 14.2$	SFX_{14}	7065	6	$P << 0.001$ $F_{15,19454} = 5.1$
VC_{14}	6899	6	$P << 0.001$ $F_{15,18999} = 11.1$	IMD_{15}	9136	6	$P << 0.001$ $F_{15,25883} = 6.5$	SFX_{15}	7416	6	$P << 0.001$ $F_{15,20451} = 5.1$
Total	91637	80		**Total**	94823	89		**Total**	98129	77	
Mean	7636	7		**Mean**	792	7		**Mean**	8177	6	
S.D.	1792	1.2		**S.D.**	1906	1.3		**S.D.**	1732	1.1	
Min	5350	5		**Min**	4869	6		**Min**	4723	5	
Max	11819	9		**Max**	10447	9		**Max**	11761	9	

4.4.2. Electrophysiology

The spikes from individual neurons (units) were sorted for each animal from the tetrode recordings (Figure 4.1B). In total I discriminated 80 units in the vehicle control group across 12

animals, 89 units across 12 animals in the IMD group, and 77 units across 12 animals in the SFX group, or a mean of 7 units per animal for the vehicle and IMD groups, and 6 units/animal in the SFX group. I show that the clusters of sorted spikes within the units for each animal are statistically distinct in three-dimensional space (Table 4.1). Using the constructed PSTHs and cumulative sum plots for each unit, I removed all units that did not have a significant change in firing rate in relation to the stimulus (Figure 4.1C). There was no significant difference in the mean number of units per animal per group, the number of units responding per animal per group, or the percent of units responding per animal per group (Figure 4.1D).

An initial population response analysis involved constructing mean PSTHs that contained all units from all animals for each treatment (Figure 4.2A). These histograms were strikingly similar for the control and sulfoxaflor treatments, while the population response of the imidacloprid group was generally attenuated in comparison. I measured the mean frequency of all units within 0.5 second blocks from -1.5 seconds (before TOC) to 0.5 seconds after (Figure 4.1A) and confirmed that for all blocks leading to TOC the mean frequency was lower for units in the imidacloprid group, while after TOC there was no significant difference between treatments (results from one way ANOVA on Ranks: -1.5 to -1 s H_2=16.455, p<0.001; -1 to -0.5 s H_2=20.855, p<0.001; -0.5 to 0 s H_2=16.358, p<0.001).

To further assess the general attenuation of neural firing across units in the IMD treatment, I divided the responses of different units into distinct unit response groups based on several histogram parameters (Figure 4.2A). For units that displayed a clear peak in firing rate around TOC, I divided into groups based on peak firing rate, whether it was greater than 100 spikes/s (A), between 50 and 100 spikes/s (B), 25 and 50 spikes/s (C), or less than 25 spikes/s (D). The remainder of units displayed baseline tonic firing, that either decreased around TOC (E) or increased during the approach of the stimulus with no distinct peak (F). Despite there being no significant difference in the number of responding units per treatment group, I did find a significant difference in the distribution of the units amongst these unit response groups (Figure 4.2B, X^2_{10}=20.252, p<0.05). While the distribution of units in the response groups were similar for the control and sulfoxaflor treatments, the imidacloprid treatment had a large disparity in units contained in the low and moderate frequency peak groups (B-D), and very few units that displayed tonic spontaneous firing with increases or decreases around TOC (E-F).

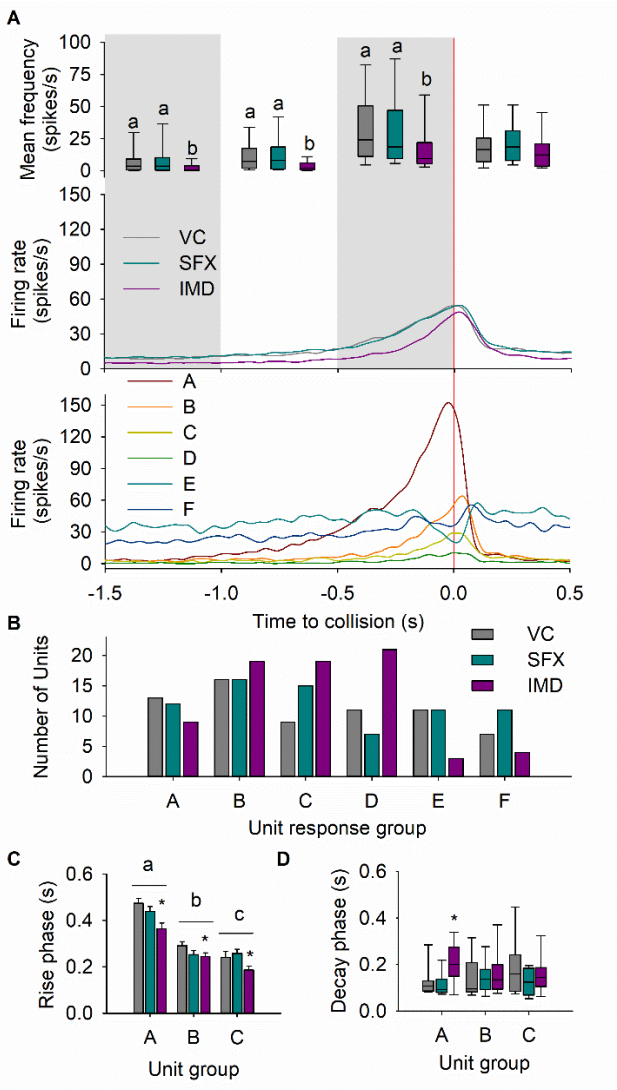

Figure 4.2: Response properties of descending visual interneurons are affected by imidacloprid, not sulfoxaflor. A) Pooled mean frequency and corresponding PSTHs for all units within each treatment group, divided into 0.5 s sections to show how these measurements change during the approach of the looming stimulus (top and middle), with TOC marked by a vertical red line. Boxes are median, 25th and 75th percentile, with 10th and 90th percentile whiskers. Units were classified into six groups based on peak firing rate (groups A-D), a decreased firing rate at TOC (E) or a steadily increasing firing rate with no distinct peak (F, bottom). B) The total number of units allocated to each unit response group for each treatment. C) The rise phase of the PSTHs for units from groups A-C across all treatments (mean + SEM). Rise phase is measured from the PSTH from the last time the histogram crosses the 95% confidence interval until the peak. Letters above unit groups denote significant differences between groups, and asterisks denote significant effect of treatment within unit group. D) The decay phase of the PSTHs for units from groups A-C across all treatments (median, 25th and 75th percentiles, with 10th and 90th percentile whiskers). Decay phase was measured from the peak of the histogram until the time the histogram has decreased to 15%. Asterisk denotes significant effect of treatment within unit group.

I measured the rise phase of the histograms of units with a distinctive peak, i.e. from unit response groups A-C (Figure 4.2C). While the rise phase was significantly shorter with lower peak firing rates, this was enhanced with the imidacloprid treatment and these units displayed the shortest rising phases (two-way ANOVA by treatment: F_2=9.733, p<0.001, by unit group: F_2<71.690, p<0.001). Measurements of the decay phases of the PSTHs of units from groups A-C (Figure 4.2D) showed a significantly lengthened decay phase for units of the imidacloprid treatment in group A only (one-way ANOVA on Ranks H_2=8.497, p<0.05).

4.4.3. Dynamic factor analysis

I performed a dynamic factor analysis (DFA), which is a method for identifying common trends among time series data (Zuur et al. 2003), to reduce the dimensionality of the data. DFA was conducted on PSTHs that used 50 ms bins with all units pooled within each treatment group (VC=69 units, SFX=72 units, IMD=75 units) using Brodgar 2.7.9 (Highland Statistics Inc., Newburgh, UK). When selecting the number of common trends to include in the model, criteria included AIC, distribution of the residuals, and biological interpretation (Zuur et al. 2003). I tested DFA models that included 4, 6, and 8 trends, and although the AIC value was lowest for the model with 8 trends (Table 4.2), I determined the 6 trend model to be most biologically relevant given our initial analysis of the PSTHs that facilitated grouping neural responses into 6 unit response groups (Figure 4.3).

Table 4.2. Results from the dynamic factor analysis including three measures of model fit used for model selection, Akaike information criterion (AIC), Bayesian information criterion (BIC), and the 'consistent' AIC (CAIC).

Treatment	# Common trends	AIC	BIC	CAIC
VC	4	18440.396	20856.974	21264.974
	6	18140.641	21321.284	21858.284
	8	18029.803	21950.82	22612.82
SFX	4	19685.737	22227.059	22653.059
	6	19412.349	22759.02	23320.02
	8	19173.62	23301.777	23993.777
IMD	4	17855.695	20522.522	20966.522
	6	17447.359	20961.084	21546.084
	8	17193.722	21530.32	22252.32

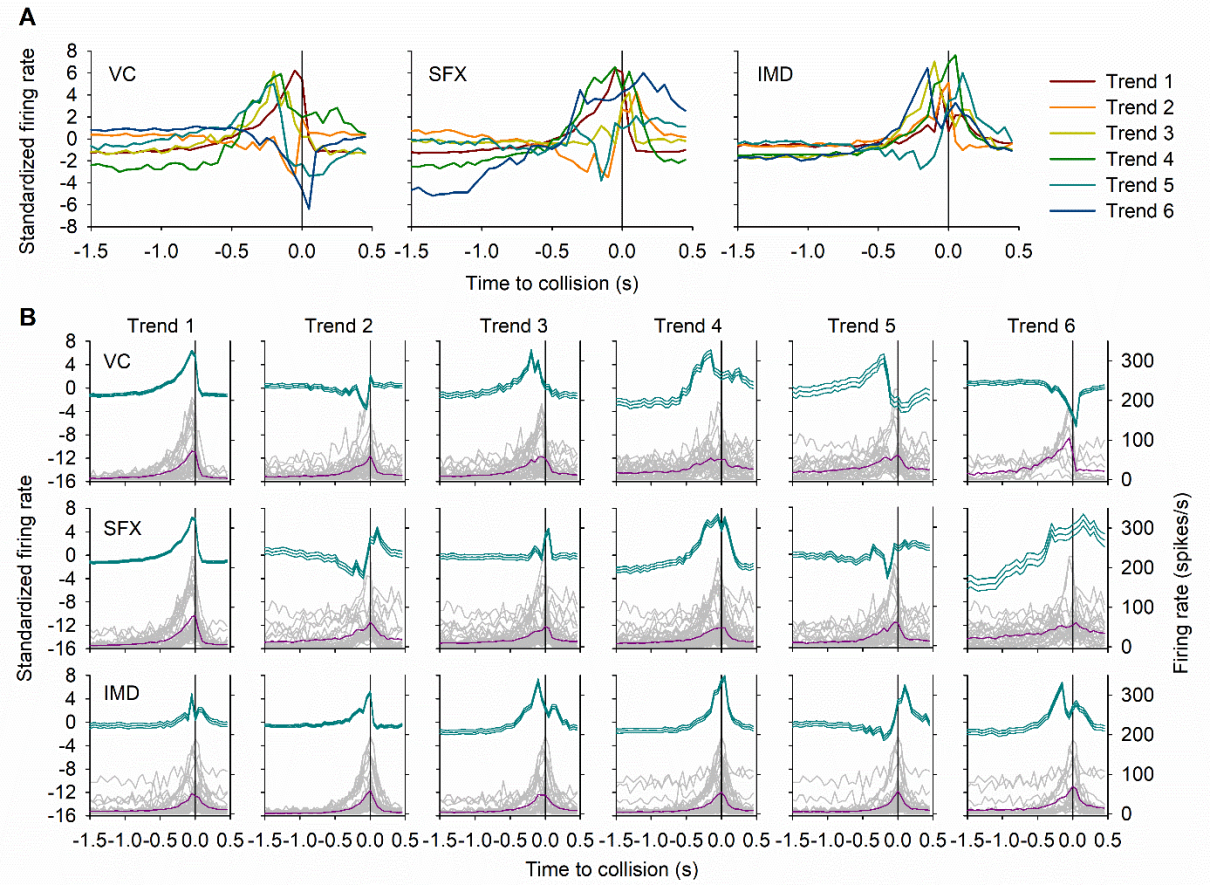

Figure 4.3: Dimensionality reduction of population response shows reduced variation in common trends when treated with imidacloprid. A) Common trends resulting from dynamic factor analysis on the neural population within each treatment. B) Individual common trends for each treatment with upper and lower 95% confidence limits (dark cyan), as well as the mean PSTHs for all units that contributed significantly to the trend and the mean of those units (purple).

4.4.4. Habituation

I used a series of 10 stimuli presented consecutively at 8 second intervals to observe how the populations of visual interneurons habituate. Visual interneurons, such as the DCMD, are known to habituate, primarily with a reduction in peak firing rate and total number of spikes (Gray 2005). I found that units with a medium or high frequency peak (from groups A and B) display a sharp decrease in firing, while those with more tonic firing patterns do not habituate (Figure 4.4A). I omitted units from group D (lower than 25 spikes/s peak) from these analyses as these units displayed high variability between stimulus presentations.

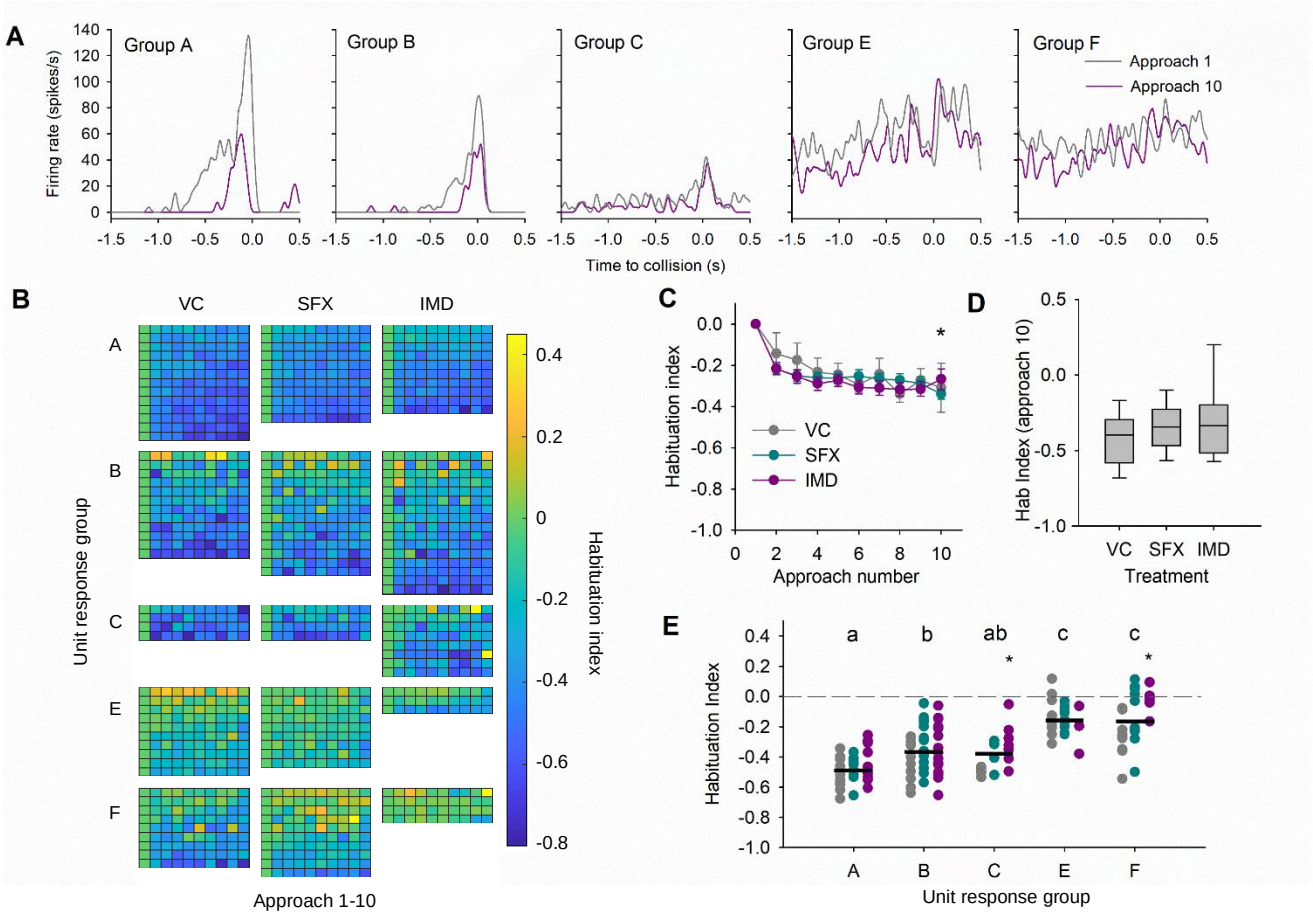

Figure 4.4: Habituation of populations of visual interneurons shows that some units habituate, while others do not. A) Responses of a single unit from each unit group from stimulus presentation 1 (Approach 1) versus stimulus presentation 10 (Approach 10) in a sequence of 10 stimuli spaced at 8 second intervals. B) Heatmaps of the habituation index for all units from each treatment group for stimuli 1 through 10, with a habituation index of 0 representing no change from approach 1. C) Habituation index (mean plus SEM) for all units from each treatment group across stimulus approaches 1-10, asterisk denotes significant difference between approach 10 and 1. D) Comparison of the habituation index for approach 10 for all units across treatment groups. Boxes represent the medians with 25th and 75th quartiles, whiskers are the 10th and 90th quartiles. E) The habituation index for individual units within each unit response group across treatments. Each data point shows the mean habituation index for a single unit across approaches 6-10, and asterisk denotes significant effect of treatment within unit response group.

To find a measure of habituation that would apply to all units, including those that do not display a pronounced peak, I calculated a habituation index that uses the total number of spikes and mean frequency, both normalized to the responses to the first (i.e. unhabituated) stimulus. Thus, a habituation index of 0 or higher represents a response that has not habituated, while

increasingly negative numbers are associated with units that habituate to a greater degree (Figure 4.4B). Across treatment groups, I find that the habituation index decreases sharply from the first to the second stimulus, but plateaus by the 4th or 5th stimulus presentation (Figure 4.4C). There is a significant difference in habituation index between the 1st and 10th stimulus presentations for all units (Wilcoxon Signed Rank Test Z=-5.794, p<0.001). The habituation index does not differ between treatment groups at approach 10 (Figure 4.4D). When examining the habituation index divided by unit group, I find that units from groups A-C (with a defined peak) are habituating to a greater degree than those from groups E-F (one-way ANOVA on Ranks, H_4=66.210, p<0.001). In addition, within unit group, I found a lesser degree of habituation of units from the imidacloprid group, with significantly higher habituation index values (compared to the control) for units from groups C (one-way ANOVA F_2=4.372, p<0.05) and F (one-way ANOVA F_2=4.622, p<0.05).

4.5. Discussion

Collision avoidance behaviour is affected 24 hours after oral exposure to imidacloprid

The effects of 100 ng/g IMD on jumping behaviour at 24 hours after treatment with an oral dose were similar to those found with an equal injected dose (Parkinson et al 2017). While this dose is sublethal (Parkinson et al 2017), their behaviour was negatively affected. Contrasting this, SFX had little effect on jumping, suggesting reduced toxicity of this insecticide in comparison with IMD in the context of this important collision avoidance behaviour.

Tetrode recordings of visual interneurons show population-level effects of imidacloprid.

The tetrode recordings showed that while there were no differences in the numbers of responding units per animal across treatments, the distribution of response types varied after treatment with imidacloprid. The definition of unit response type and histogram shape showed several important features of the population response of visual interneurons that are affected by imidacloprid. The overall attenuation of firing rate and spontaneous firing suggests that excitatory synapses in the CNS are being affected similarly across various visual pathways, resulting in a bulk decrease in neural firing that can be seen across the population of visual interneurons recorded here. The decreased excitation in the optic lobes results in decreased

sensitivity for object motion: objects must be larger (i.e. closer) before these descending neurons begin encoding object approach. This was measured as a shortened rising phase of the neural responses that display a peak aligned with the time of collision of the stimulus. Inhibitory neurons may also be attenuated after treatment with imidacloprid, but to a lesser degree, as suggested with the measurements of the decay phase, in which a longer decay phase is found for units with high frequency peaks (group A) only. Inhibitory neurons may contain nAChRs on the dendrites, so their activation could be affected by IMD, whereas the inhibitory synapses themselves would be unaffected as these synapses are muscarinic (Rind and Simmons 1998; Zhu et al. 2018). Previous studies have shown that excitation is mediated by acetylcholine in the optic lobes (Rind and Leitinger 2000), so although this was not tested directly with the neurons recorded in this study, I am confident that these synapses are cholinergic given the results described here.

Imidacloprid reduces the variation of common trends with dimensionality reduction

Qualitative visual examination of the 6 common trends within each treatment shows properties that support our conclusions from the classification of individual units. With the imidacloprid treatment group, there is no common trend that represents a sharp decrease of standardized firing rate near TOC, while VC and SFX have trends that decrease around TOC, similar to unit group E. The common trends that represent the population response from the IMD treatment all share the feature of a peak firing rate either before or after TOC. Additionally, I see little variation in the standardized firing rate before -0.5 seconds (before collision) in the imidacloprid treatment, while SFX and VC show broad variation between trends. This analysis further highlights the effect of IMD on spontaneous firing and attenuation of the neural population and serves as an illustration of the variation in trends of the population response of descending neurons to looming stimuli.

Some visual interneurons habituate, while others do not.

The effect of habituation on a population of visual interneurons had not previously been examined in the locust. Habituation of the DCMD visual interneuron is thought to be caused by the activity of inhibitory neurons in the optic lobes (Gray 2005). I found a decreased effect of habituation on units in the imidacloprid treatment, which further supports my hypothesis that the

activity of both inhibitory neurons that contain dendritic nAChRs and excitatory neurons are attenuated, but this effect is less pronounced for the inhibitory neurons as inhibitory synapses are not under nicotinic cholinergic control.

Comparative toxicity of imidacloprid and sulfoxaflor

Contrary to my predictions, treatment with sulfoxaflor did not result in effects on the population responses of descending visual interneurons and collision avoidance behaviours compared to the control. This is a significant finding as sulfoxaflor and imidacloprid act on the same target, the nAChR, although they are metabolized through different pathways (Sparks et al. 2012). In Chapter 3, I found that metabolites of IMD, including imidacloprid-olefin and 5-hydroxy imidacloprid display toxic effects on this collision avoidance pathway that are equal to or greater than the parent compound (Parkinson and Gray 2019). The detoxification pathway of sulfoxaflor may result in metabolites that do not bind to the nAChR or are more hydrophilic and can be readily excreted, so SFX would cause toxicity initiating from binding to the nAChR prior to metabolism only. Evidence shows, however, that SFX is not metabolized by the same cytochrome p450 enzymes, like the CYP6G1 monooxygenase, that mediate neonic metabolism and resistance in insects (Sparks et al. 2012), and it is not currently known how this insecticide is metabolized, or what effects its metabolites may display. Another explanation for the reduced toxicity of SFX compared to IMD observed here is that SFX may display low affinity for the nAChR subunits expressed in the locust. SFX and IMD display differential binding at the agonist binding site, with SFX having lower affinity than a variety of neonics (Wang et al. 2016). It is possible, however that the benefit of metabolic stability outweighs the cost of reduced receptor affinity for use against insects resistant to neonics (Sparks et al. 2013). Additional research is needed to determine whether the reduced toxicity of SFX compared to IMD seen here is due to reduced receptor affinity of SFX, or if these differences result from reduced metabolism of SFX or metabolites that do not display toxicity to this collision avoidance pathway.

Conclusions

Overall, these results offer evidence that a neonicotinoid insecticide causes reduced firing of neurons innervated through nicotinic cholinergic synapses located in the central nervous system. I show a widespread alteration of the neural responses transmitted by a population of

visual interneurons which is associated with reduced escape behaviour. This effect is present 24 hours after an acute oral treatment at a dose that is sublethal (Parkinson et al. 2017). Interestingly, I find no significant effect on either behaviour or neural firing resulting from an equal dose of sulfoxaflor. I propose that neuroethological methods, such as those employed in this study, may be used in comparative toxicological analyses to provide accurate sublethal effects linking changes in neural coding to animal behaviour.

Chapter 5: General discussion

5.1. Effects of imidacloprid on object motion detection

Throughout Chapters 2, 3 and 4, I show that imidacloprid has significant effects on neurons that encode object motion, and that these effects are present 1 to 24 hours after an acute, sublethal exposure. Given the specific firing parameters that are affected, including reduced peak firing rates, disrupted bursting, reduced mean firing rates and shortened rising phases, along with reduced habituation and lengthened decay phases, I conclude that the insecticide affects excitation globally within the optic lobes, with excitatory pathways affected to a greater degree than inhibitory pathways due to containing larger proportion of nAChR activated synapses (Figure 5.1).

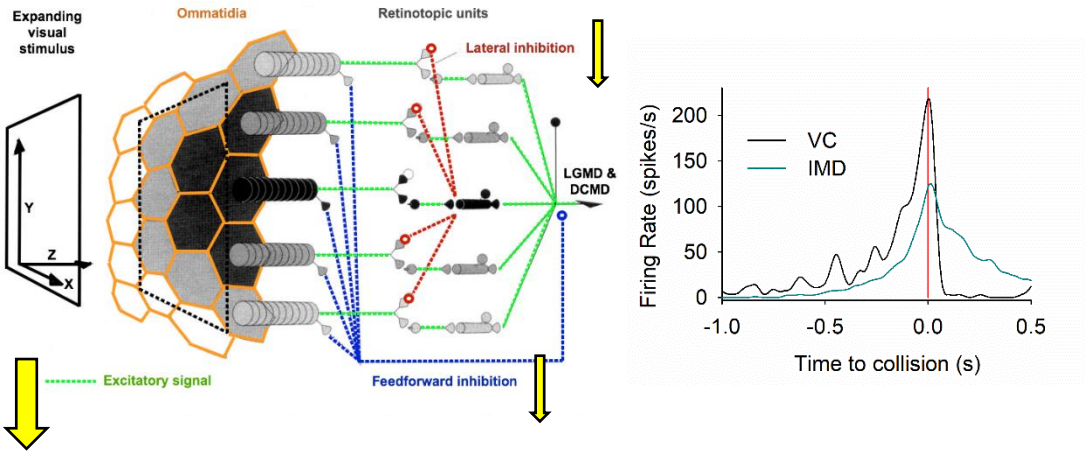

Figure 5.1: Diagram showing the relative degree of attenuation by imidacloprid of the excitatory and inhibitory pathways in the optic lobes that are activated during the approach of a looming stimulus (left) and the effects on the DCMD PSTH compared to the vehicle control (right). PSTHs show the mean response across 20 animals before (VC) and 24 hours after treatment with 100 ng/g imidacloprid (IMD). Adapted from Rind and Bramwell (1996) and Parkinson et al (2017).

Exposure to neonics causes receptor desensitization, which can lead to neural inactivation, increased oxidative stress, and cell death (Oliveira et al. 2011; Palmer et al. 2013; Wu et al. 2015; Wang et al. 2018b). I propose that the observed effects result from imidacloprid binding and inactivating these receptors, which are located throughout the optic lobes. A major result of this neural inactivation is time-dependent effects on neural coding: descending neurons are responding later to object motion, which would affect the ability of the insect to perform an escape behaviour before an imminent collision. This, in combination with the reduced axonal conduction velocity caused by imidacloprid and its metabolites, would affect gating of these action potentials onto motorneurons downstream (Santer et al. 2006). The ability to see motion hinges on accurate measurements of the displacement between two images with a known time delay (Borst and Egelhaaf 1989). A disruption of signalling within the optic lobes caused by the neonic would affect these temporal cues resulting in the inaccurate perception of motion.

5.2. Effects on escape behaviours

I have shown that sublethal exposure to imidacloprid reduces escape behaviours in flight, which would have an impact on predation as these insects represent an easier target. For insects that fly in swarms, including locusts, they would additionally be ill-equipped to avoid collisions with conspecifics. Jumping escape behaviours were also affected by low concentrations of neonics: this is evidence that these effects are due to sensory processing rather than effects on flight circuitry. It can thus be inferred that other visually-elicited escape behaviours, such as those employed by aquatic invertebrates, could similarly be affected. There are secondary effects of these deficits that pass through the food chain to insect predators, like insectivorous birds. Populations of insectivorous birds are declining, and these declines are associated with high environmental presence of neonics (Hallmann et al. 2014; Gibbons et al. 2015). Insects with reduced motion detection would be easier to catch, both on the wing and on land, and thus may be consumed more frequently than insects with lower concentrations of neonics, further exacerbating the trophic accumulation of neonics.

5.3. Implications for visually-guided flight

In Chapter 2, I found that DCMD responses to looming stimuli were further attenuated when the stimulus was presented over a flow field. In that paradigm, locust DCMDs were encoding object motion in tandem with processing the visual cues associated with optic flow. It is not known if the processing of other forms of visual motion, like self-motion, is affected by imidacloprid, but I predict that there would be similar effects to those described in this thesis. Insects use the visual cues provided by optic flow during flight to maintain their body orientation, in a process termed the optomotor response (Srinivasan et al. 1999). Furthermore, by maintaining optic flow constant, insects can control their flight speed, altitude, and calculate distance (Srinivasan and Zhang 2004). Thus, the detection of movement is critical for visually-guided flight. Aspects of flight have been shown to be affected by neonics in bees, although these effects are typically associated with deficits in memory or motor impairment (Fischer et al. 2014; Samuelson et al. 2016; Tosi et al. 2017). Given the effects described in this thesis, I suggest that there may be additional issues with sensory processing that result in bees and other insects that are unable to properly assess visual cues provided by optic flow.

5.4. Adverse Outcome Pathway of imidacloprid toxicity

I have constructed an AOP using results from the experiments performed throughout this thesis (Figure 5.2). The final adverse outcome of decreased locust survival due to predation is inferred from the other results, although this has not been tested directly. I propose that both IMD and IMD metabolites result in receptor desensitization, which begins the cascade leading to reduced escape behaviours. Using the neuroethological assays described in Chapters 2, 3 and 4, I have been able to directly or indirectly assess the key events and form the key event relationships for this AOP.

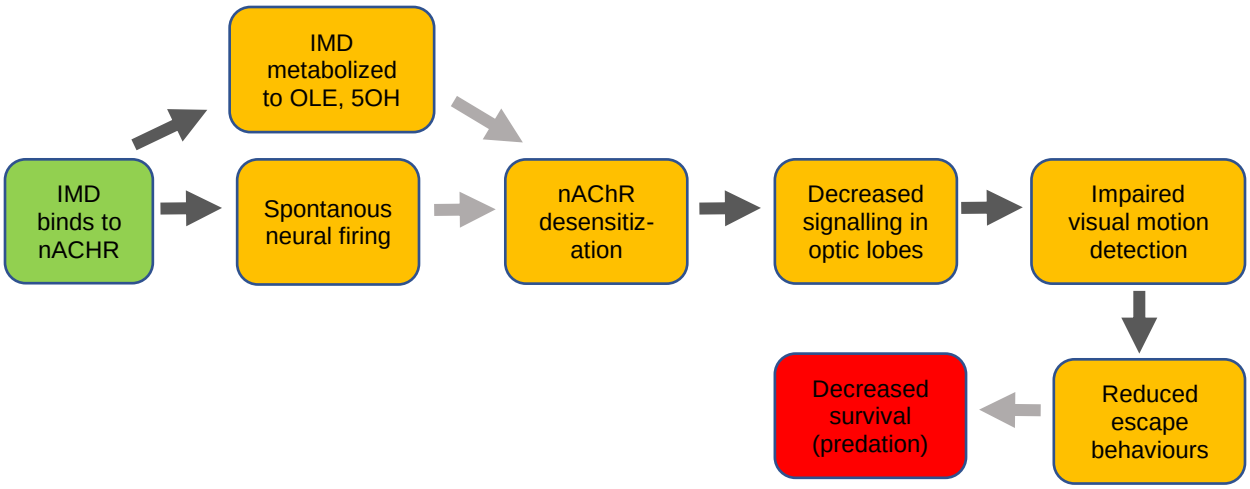

Figure 5.2: Adverse Outcome Pathway linking the molecular initiating event (green) of imidacloprid binding to the nAChR to the adverse outcome (red) of decreased survival. Key events (orange) with key event relationships in dark grey have been directly tested, while those in light grey are inferred.

5.5. Comparative effects of sulfoxaflor

The experiments performed in Chapter 4 are the first to examine whether sulfoxaflor affects any form of sensory processing, and additionally are an important look into the comparative effects of this new class of insecticides with the neonics. Given that both sulfoxaflor and imidacloprid act on the same target, the nAChR, I predicted that these insecticides would be similar both in potency and effect. The results show, however, that at comparable doses sulfoxaflor does not affect visual motion processing, and 24 hours after treatment locusts are still able to respond to a looming stimulus with appropriate escape behaviours. These results, which are discussed in Chapter 4, are potentially due to differences in receptor affinity of SFX versus IMD (Wang et al. 2016), differential metabolism of SFX versus IMD (Sparks et al. 2012), and additionally may result from the neurotoxicity of IMD metabolites which perpetuates the toxic effect of IMD over time (Parkinson and Gray 2019). It is not known whether the reduced toxicity of SFX compared to IMD described in Chapter 4 also occurs in other insects, and additional research is required to determine if non-target insects may benefit from a shift in agricultural use from neonics to sulfoximines.

5.6. Toxicology through the lens of Neuroethology

An important theme throughout this thesis is the use of neuroethological assays to answer questions in toxicology to link toxic effects on the brain with behaviour. I argue that by using these multi-level assays, that have been developed by neuroethologists to explain how the nervous system senses the environment and processes these sensory cues to respond with appropriate behaviours, we can formulate a holistic and causative description of toxicological pathways. Results from these experiments provide multiple key events that can be used to construct AOPs for which the key event relationships are intuitive and tested, rather than inferred and uncertain.

In the context of neonicotinoid toxicity, purely behavioural experiments may be described in different ways if the underlying effects on neural coding and physiology are not understood. One example is whether bees can detect (taste) neonics in food sources, as bees tend to develop a preference for neonic-laced food sources. A purely behavioural assay determined that they could, as their preference for treated food sources remained even when the feeders were moved (Arce et al. 2018). However, using a combination of electrophysiological and behavioural assays, another study showed that bumblebees are unable to detect neonics in sucrose, even at the level of the sensory neuron (Kessler et al. 2015). This example highlights the importance of combining behaviour with electrophysiology, and in fact using the results from behavioural assays to direct the use of electrophysiology so that a complete and accurate picture may be formed.

Chapter 4 showed the utility of using neuroethological assays for comparative toxicology, as I was able to show that when two compounds that display the same molecular initiating event can result in very different effects. Although it is not possible to infer whether other levels of biological organization would be affected differentially, that study showed a very marked and clear difference between the toxicological profiles of IMD compared to SFX. These assays are highly adaptable and can easily be scaled for various exposure methods (oral versus injected, for example), time periods (acute versus chronic), and compounds, including other novel insecticides or insecticide mixtures for which there is a paucity of data detailing their sublethal effects.

5.7. Future directions

The research avenues opened by the studies I have conducted throughout this thesis are numerous, and there are many unanswered questions. The most pertinent way to direct future studies, however, is to determine whether bees experience similar effects on visual motion detection that might explain some of the behavioural deficits linked to neonicotinoid exposure. Although bees do not display robust collision avoidance behaviours compared to the locust, optic flow detection is imperative for flight and navigation (Dacke and Srinivasan 2007), and similar neural pathways are shown to detect widefield visual motion and object expansion in bees (Ibbotson et al. 2017). If low, sublethal amounts of neonics disrupt visual motion detection in bees as they do in locusts, there would be an explanation for observed effects on foraging behaviour. Additional studies could examine the effects of novel insecticides and pesticide mixtures, such as those found in commercially available seed treatments, and on visual motion detection using assays detailed throughout this thesis.

Ultimately, the methods I employed to complete these projects have myriad potential applications for testing and comparing agrochemicals and other neurotoxicants. It is my hope that toxicity testing can shift towards a more holistic approach to reveal the underlying mechanisms of sublethal toxicity and link these to behavioural effects that may be difficult to understand. It is paramount, now perhaps more than ever, to apply the collective scientific mind, honed through basic research, to understanding how human actions are affecting the inhabitants and ecosystems of this planet. Through interdisciplinary and collaborative actions, we can develop and employ effective mitigation strategies to avoid repeating history and end the cycle of releasing chemicals into the environment prior to fully considering their impact.

Literature cited

Andrione M, Vallortigara G, Antolini R, Haase A (2016) Neonicotinoid-induced impairment of odour coding in the honeybee. Sci Rep 6:38110.

Ankley GT, Bennett RS, Erickson RJ, et al (2010) Adverse outcome pathways: A conceptual framework to support ecotoxicology research and risk assessment. Environ Toxicol Chem 29:730–741.

Arce AN, Ramos Rodrigues A, Yu J, et al (2018) Foraging bumblebees acquire a preference for neonicotinoid-treated food with prolonged exposure. Proc R Soc London B Biol Sci 285:8–11.

Baader A, Schafer M, Rowell CHF (1992) The perception of the visual flow field by flying locusts: a behavioural and neuronal analysis. J Exp Biol 165:137–160.

Baines D, Wilton E, Pawluk A, et al (2017) Neonicotinoids act like endocrine disrupting chemicals in newly-emerged bees and winter bees. Sci Rep 7:1–18.

Baird E, Boeddeker N, Ibbotson M, Srinivasan M (2013) A universal strategy for visually guided landing. Proc Natl Acad Sci 110:1–15.

Baker PS, Gewecke M, Cooter RJ (1981) The natural flight of the migratory locust, Locusta migratoria L. J Comp Physiol A 141:233–237

Banks JE, Stark JD (1998) What is ecotoxicology? An ad-hoc grab bag or an interdisciplinary science? Integr Biol 1:195–202.

Bao H, Liu Y, Zhang Y, Liu Z (2017) Two distinctive β subunits are separately involved in two binding sites of imidacloprid with different affinities in Locusta migratoria manilensis. Pestic Biochem Physiol 140:36–41.

Bao H, Sun H, Xiao Y, et al (2015) Functional interaction of nicotinic acetylcholine receptors and Na+/K+ ATPase from Locusta migratoria manilensis (Meyen). Sci Rep 5:8849.

Benaragama I, Gray JR (2014) Responses of a pair of flying locusts to lateral looming visual stimuli. J Comp Physiol A Neuroethol Sensory, Neural, Behav Physiol 200:723–738.

Benson JA (1992) Electrophysiological pharmacology of the nicotinic and muscarinic cholinergic responses of isolated neuronal somata from locust thoracic ganglia. J Exp Biol 170:203–233.

Benzidane Y, Goven D, Abd-Ella AA, et al (2017) Subchronic exposure to sublethal dose of imidacloprid changes electrophysiological properties and expression pattern of nicotinic acetylcholine receptor subtypes in insect neurosecretory cells. Neurotoxicology 62:239–247.

Berry RP, Warrant EJ, Stange G (2007) Form vision in the insect dorsal ocelli: an anatomical and optical analysis of the Locust Ocelli. Vision Res 47:1382–93.

Blacquière T, van der Steen JJM (2017) Three years of banning neonicotinoid insecticides based on sub-lethal effects: can we expect to see effects on bees? Pest Manag Sci 73:1299–1304.

Bonmatin JM, Giorio C, Girolami V, et al (2015) Environmental fate and exposure; neonicotinoids and fipronil. Environ Sci Pollut Res 22:35–67.

Borst A, Egelhaaf M (1989) Principles of visual motion detection. Trends Neurosci 12:297–306.

Botías C, David A, Hill EM, Goulson D (2017) Quantifying exposure of wild bumblebees to mixtures of agrochemicals in agricultural and urban landscapes. Environ Pollut 222:73–82.

Botías C, David A, Horwood J, et al (2015) Neonicotinoid Residues in Wildflowers, a Potential Route of Chronic Exposure for Bees. Environ Sci Technol 49:12731–12740. doi:

Bradbury SP, Feijtel TCJ, Van Leeuwen CJ (2004) Meeting the scientific needs of ecological risk assessment in a regulatory context. Environ Sci Technol 38:463-470.

Brown RH (1967) Mechanism of locust jumping. Nature 214:939–941.

Brunet JL, Badiou A, Belzunces LP (2005) In vivo metabolic fate of [14C]-acetamiprid in six biological compartments of the honeybee, Apis mellifera L. Pest Manag Sci 61:742–748.

Buckingham SD, Lapied B, Corronc HLE, et al (1997) Imidacloprid actions on insect neuronal acetylcholine receptors. J Exp Biol 200:2685–2692.

Buhl E, Schildberger K, Stevenson P a (2008) A muscarinic cholinergic mechanism underlies activation of the central pattern generator for locust flight. J Exp Biol 211:2346–2357.

Burrows M (1996) The neurobiology of an insect brain. Oxford University Press Inc., New York, NY.

Burrows M, Rowell CHF (1973) Connections between descending visual interneurons and metathoracic motoneurons in the locust. J Comp Physiol A 85:221-234.

Burtt ET, Catton WT (1956) Electrical responses to visual stimulation in the optic lobes of the locust and certain other insects. J Physiol 133:68–88.

Byrne FJ, Visscher PK, Leimkuehler B, Fischer D (2013) Determination of exposure levels of honey bees foraging on flowers of mature citrus trees previously treated with imidacloprid. Pest Manag Sci 70:470-482.

Card G, Dickinson MH (2008) Visually mediated motor planning in the escape response of drosophila. Curr Biol 18:1300–1307.

Carson R (1962) Silent spring. Houghton Mifflin, Boston, MA

Casida JE (2018) Neonicotinoids and Other Insect Nicotinic Receptor Competitive Modulators: Progress and Prospects. Annu Rev Entomol 63:125–144.

Casida JE (2011) Neonicotinoid metabolism: Compounds, substituents, pathways, enzymes, organisms, and relevance. J Agric Food Chem 59:2923–2931.

Casida JE, Durkin K a (2013) Neuroactive insecticides: targets, selectivity, resistance, and secondary effects. Annu Rev Entomol 58:99–117.

Cavallaro MC, Morrissey CA, Headley J V., et al (2016) Comparative chronic toxicity of imidacloprid, clothianidin, and thiamethoxam to Chironomus dilutus and estimation of toxic equivalency factors. Environ Toxicol Chem 9999:1–11.

Centner TJ, Brewer B, Leal I (2018) Reducing damages from sulfoxaflor use through mitigation measures to increase the protection of pollinator species. Land use policy 75:70–76.

Chan RWM, Gabbiani F (2013) Collision-avoidance behaviors of minimally restrained flying locusts to looming stimuli. J Exp Biol 216:641–655.

Chapman RF (1998) The insects: structure and function, 4th edn. Cambridge University Press, Cambridge, UK.

Charpentier G, Louat F (2014) Lethal and Sublethal Effects of Imidacloprid, After Chronic Exposure, On the Insect Model Drosophila melanogaster. Environ Sci Technol 48:4096–4102.

Christen V, Mittner F, Fent K (2016) Molecular effects of neonicotinoids in honey bees (Apis mellifera). Environ Sci Technol acs.est.6b00678.

Codling G, Al Naggar Y, Giesy JP, Robertson AJ (2016) Concentrations of neonicotinoid insecticides in honey, pollen and honey bees (Apis mellifera L.) in central Saskatchewan, Canada. Chemosphere 144:2321–2328.

Cross KP, Robertson RM (2016) Ionic mechanisms maintaining action potential conduction velocity at high firing frequencies in an unmyelinated axon. Physiol Rep 4:e12814.

Dacke M, Srinivasan M V. (2007) Honeybee navigation: distance estimation in the third dimension. J Exp Biol 210:845–853.

De Almeida Rossi C, Roat TC, Tavares DA, et al (2013) Brain morphophysiology of Africanized bee Apis mellifera exposed to sublethal doses of imidacloprid. Arch Environ Contam Toxicol 65:234–243.

Déglise P, Grünewald B, Gauthier M (2002) The insecticide imidacloprid is a partial agonist of the nicotinic receptor of honeybee Kenyon cells. Neurosci Lett 321:13–6.

Dick PC, Gray JR (2014) Spatiotemporal stimulus properties modulate responses to trajectory changes in a locust looming-sensitive pathway. J Neurophysiol 111:1736–45.

Dick PC, Michel NL, Gray JR (2017) Complex object motion represented by context-dependent correlated activity of visual interneurones. Physiol Rep 5:1–21.

Domenici P, Booth D, Blagburn JM, Bacon JP (2008) Cockroaches keep predators guessing by using preferred escape trajectories. Curr Biol 18:1792–1796.

Douglas MR, Tooker JF (2015) Large-scale deployment of seed treatments has driven rapid increase in use of neonicotinoid insecticides and preemptive pest management in U.S. field crops. Environ Sci Technol 49:5088–5097.

Dupuis J, Louis T, Gauthier M, Raymond V (2012) Insights from honeybee (Apis mellifera) and fly (Drosophila melanogaster) nicotinic acetylcholine receptors: From genes to behavioral functions. Neurosci Biobehav Rev 36:1553–1564.

Elias MS, Evans PD (1983) Histamine in the insect nervous system: distribution, synthesis and metabolism. J Neurochem 41:562–8.

Ermak G, Davies KJA (2002) Calcium and oxidative stress: From cell signaling to cell death. Mol Immunol 38:713–721.

Fischer J, Müller T, Spatz A-K, et al (2014) Neonicotinoids interfere with specific components of navigation in honeybees. PLoS One 9:e91364.

Fotowat H, Fayyazuddin A, Bellen HJ, Gabbiani F (2009) A Novel Neuronal Pathway for Visually Guided Escape in Drosophila melanogaster. J Neurophysiol 102:875–885.

Gabbiani F, Cohen I, Laurent G (2005) Time-dependent activation of feed-forward inhibition in a looming-sensitive neuron. J Neurophysiol 94:2150–2161.

Gabbiani F, Krapp H, Laurent G (1999) Computation of object approach by a wide-field, motion-sensitive neuron. J Neurosci 19:1122–1141.

Gabbiani F, Krapp HG, Koch C, Laurent G (2002) Multiplicative computation in a visual neuron sensitive to looming. Nature 420:320–324.

Gabbiani F, Mo C, Laurent G (2001) Invariance of angular threshold computation in a wide-field looming-sensitive neuron. J Neurosci 21:314–329.

Gergalova G, Lykhmus O, Kalashnyk O, et al (2012) Mitochondria express α7 nicotinic acetylcholine receptors to regulate CA 2+ accumulation and cytochrome c release: Study on isolated mitochondria. PLoS One 7:2–9.

Gibbons D, Morrissey C, Mineau P (2015) A review of the direct and indirect effects of neonicotinoids and fipronil on vertebrate wildlife. Environ Sci Pollut Res 22:103–118.

Giraud-Guille MM (1984) Fine structure of the chitin-protein system in the crab cuticle. Tissue Cell 16:75–92.

Godfray HCJ, Blacquière T, Field LM, et al (2014) A restatement of the natural science evidence base concerning neonicotinoid insecticides and insect pollinators. Proc R Soc B Biol Sci 281:20140558.

Goulson D (2013) An overview of the environmental risks posed by neonicotinoid insecticides. J Appl Ecol 50:977–987.

Gray JR (2005) Habituated visual neurons in locusts remain sensitive to novel looming objects. J Exp Biol 208:2515–2532.

Gray JR, Blincow E, Robertson RM (2010) A pair of motion-sensitive neurons in the locust encode approaches of a looming object. J Comp Physiol A 196:927–938.

Gray JR, Robertson RM, Lee JK (2001) Activity of descending contralateral movement detector neurons and collision avoidance behaviour in response to head-on visual stimuli in locusts. J Comp Physiol A 187:115–129.

Guest BB, Gray JR (2006) Responses of a looming-sensitive neuron to compound and paired object approaches. J Neurophysiol 95:1428–1441.

Guo P, Pollack AJ, Varga AG, et al (2014) Extracellular Wire Tetrode Recording in Brain of Freely Walking Insects. J Vis Exp 1–8.

Guo W, Wang X, Ma Z, et al (2011) CSP and takeout genes modulate the switch between attraction and repulsion during behavioral phase change in the migratory locust. PLoS Genet 7:e1001291.

Guo Y, Zhang J, Yu R, et al (2012) Identification of two new cytochrome P450 genes and RNA interference to evaluate their roles in detoxification of commonly used insecticides in Locusta migratoria. Chemosphere 87:709–17.

Hallmann CA, Foppen RPB, Van Turnhout CAM, et al (2014) Declines in insectivorous birds are associated with high neonicotinoid concentrations. Nature 511:341–343.

Heitler WJ, Burrows M (1977) The locust jump I. The motor programme. J Exp Biol 66:203–219.

Hemmi JM, Tomsic D (2012) The neuroethology of escape in crabs: From sensory ecology to neurons and back. Curr Opin Neurobiol 22:194–200.

Henry M, Béguin M, Requier F, et al (2012) A common pesticide decreases foraging success and survival in honey bees. Science (80-) 336:3–5.

Hermann A, Sitdikova GF, Weiger TM (2015) Oxidative stress and maxi calcium-activated potassium (BK) channels. Biomolecules 5:1870–1911.

Hill MM, Adrain C, Martin SJ (2003) Portrait of a killer: the mitochondrial apoptosome emerges from the shadows. Mol Interv 3:19–26.

Hilton MJ, Jarvis TD, Ricketts DC (2016) The degradation rate of thiamethoxam in European field studies. Pest Manag Sci 72:388–397.

Hodgekin AL, Huxley AF (1952) Currents carried by sodium and potassium ions through the membrane of the giant axon of Loligo. J Physiol 116:449–472.

Hodgkin AL, Huxley AF (1952a) Propagation of electrical signals along giant nerve fibres. R Soc 899:177–183.

Hodgkin AL, Huxley AF (1952b) The dual effect of membrane potential on sodium conductance in the giant axon of Loligo. J Physiol 116:497–506.

Hsiao C-J, Lin C-L, Lin T-Y, et al (2016) Imidacloprid toxicity impairs spatial memory of echolocation bats through neural apoptosis in hippocampal CA1 and medial entorhinal cortex areas. Neuroreport 27:462–468.

Huang X, Zhang C, Hu R, et al (2016) Association between occupational exposures to pesticides with heterogeneous chemical structures and farmer health in China. Sci Rep 6:1–7.

Ibbotson MR, Hung YS, Meffin H, et al (2017) Neural basis of forward flight control and landing in honeybees. Sci Rep 7:1–15.

Id BZB, Huseth AS, Id RLG (2018) Widespread detections of neonicotinoid contaminants in central Wisconsin groundwater. PLoS One 13:1–17.

Ihara M, Matsuda K (2018) Neonicotinoids: molecular mechanisms of action, insights into resistance and impact on pollinators. Curr Opin Insect Sci 1–7.

Ihara M, Sattelle DB, Matsuda K (2015) Probing new components (loop G and the α – α interface) of neonicotinoid binding sites on nicotinic acetylcholine receptors. Pestic Biochem Physiol 121:47–52.

Jepson JEC, Brown LA, Sattelle DB (2006) The actions of the neonicotinoid imidacloprid on cholinergic neurons of Drosophila melanogaster. Invertebr Neurosci 6:33–40.

Jeschke P, Nauen R (2008) Pesticide residues in beeswax samples collected from honey bee colonies (Apis mellifera L.) in France. Pest Manag Sci 64:1084–1098.

Jeschke P, Nauen R, Schindler M, Elbert A (2011) Overview of the Status and Global Strategy for Neonicotinoids. J Agric Food Chem 59:2897–2908.

Jin N, Klein S, Leimig F, et al (2015) The neonicotinoid clothianidin interferes with navigation of the solitary bee Osmia cornuta in a laboratory test. J Exp Biol 218:2821–2825.

Jones AK, Sattelle DB (2010) Diversity of insect nicotinic acetylcholine receptor subunits. Adv Exp Med Biol 683:25–43.

Judge S, Rind F (1997) The locust DCMD, a movement-detecting neurone tightly tuned to collision trajectories. J Exp Biol 200:2209–2216.

Kazemi M, Tahmasbi A, Valizadeh R, et al (2012) Organophosphate pesticides: A general review. Agric Sci Res Journals 2:512–522.

Kessler SC, Tiedeken EJ, Simcock KL, et al (2015) Bees prefer foods containing neonicotinoid pesticides. Nature 521:74–76.

Kien J (1974a) Sensory integration in the locust optomotor system-I: Behavioural analysis. Vision Res 14:1245–1254.

Kien J (1974b) Sensory integration in the locust optomotor system-II: Direction selective neurons in the circumoesophageal connectives and the optic lobe. Vision Res 14:1255–1268.

Kouvatsos N, Giastas P, Chroni-Tzartou D, et al (2016) Crystal structure of a human neuronal nAChR extracellular domain in pentameric assembly: Ligand-bound α2 homopentamer. Proc Natl Acad Sci U S A 113:9635–40.

Krewski D, Acosta D, Andersen M, et al (2010) Toxicity testing in the 21st century: A vision and a strategy. J Toxicol Environ Heal - Part B Crit Rev 13:51–138.

Krupke CH, Hunt GJ, Eitzer BD, et al (2012) Multiple routes of pesticide exposure for honey bees living near agricultural fields. PLoS One 7:e29268.

LaLone CA, Villeneuve DL, Wu-Smart J, et al (2017) Weight of evidence evaluation of a network of adverse outcome pathways linking activation of the nicotinic acetylcholine receptor in honey bees to colony death. Sci Total Environ 584–585:751–775.

Longhurst C, Babcock JM, Denholm I, et al (2013) Cross-resistance relationships of the sulfoximine insecticide sulfoxaflor with neonicotinoids and other insecticides in the whiteflies Bemisia tabaci and Trialeurodes vaporariorum. Pest Manag Sci 69:809–813.

Luscher C, Streit J, Lipp P, Luscher HR (1994) Action potential propagation through embryonic dorsal root ganglion cells in culture. II. Decrease of conduction reliability during repetitive stimulation. J Neurophysiol 72:634–643.

MacCuaig RD (1957) the Cumulative Toxicity of y-BHC and Diazinon Applied in Small Doses To Locusts. Ann Appl Biol 45:114–121.

Main AR, Headley J V, Peru KM, et al (2014) Widespread use and frequent detection of neonicotinoid insecticides in wetlands of Canada's Prairie Pothole Region. PLoS One 9:e92821.

Main AR, Michel NL, Cavallaro MC, et al (2016) Snowmelt transport of neonicotinoid insecticides to Canadian Prairie wetlands. Agric Ecosyst Environ 215:76–84.

Maloney EM, Liber K, Headley J V., et al (2018) Neonicotinoid insecticide mixtures: validation of laboratory-based toxicity predictions under semi-controlled field conditions. Sci Total Environ. 243:1727-1739.

Markussen MDK, Kristensen M (2010) Low expression of nicotinic acetylcholine receptor subunit Mdα2 in neonicotinoid-resistant strains of Musca domestica L. Pest Manag Sci 66:1257–62.

Matheson T, Rogers SM, Krapp HG (2004) Plasticity in the visual system is correlated with a change in lifestyle of solitarious and gregarious locusts. J Neurophysiol 91:1–12.

Matsuda K, Buckingham SD, Kleier D, et al (2001) Neonicotinoids: Insecticides acting on insect nicotinic acetylcholine receptors. Trends Pharmacol Sci 22:573–580.

Matsuda K, Kanaoka S, Akamatsu M, Sattelle DB (2009) Diverse actions and target-site selectivity of neonicotinoids: structural insights. Mol Pharmacol 76:1–10.

McMillan G a, Loessin V, Gray JR (2013) Bilateral flight muscle activity predicts wing kinematics and 3-dimensional body orientation of locusts responding to looming objects. J Exp Biol 216:3369–3380.

McMillan GA, Gray JR (2012) A looming-sensitive pathway responds to changes in the trajectory of object motion. J Neurophysiol 108:1052–1068.

McMillan GA, Gray JR (2015) Burst Firing in a Motion-Sensitive Neural Pathway Correlates with Expansion Properties of Looming Objects that Evoke Avoidance Behaviors. Front Integr Neurosci 9:60.

Medan V, Oliva D, Tomsic D (2007) Characterization of Lobula Giant Neurons Responsive to Visual Stimuli That Elicit Escape Behaviors in the Crab Chasmagnathus. J Neurophysiol 98:2414–2428.

Meehan TD, Werling BP, Landis DA, Gratton C (2011) Agricultural landscape simplification and insecticide use in the Midwestern United States. Proc Natl Acad Sci 108:11500–11505.

Mehlhorn H, Mencke N, Hansen O (1999) Effects of imidacloprid on adult and larval stages of the flea Ctenocephalides felis after in vivo and in vitro application: A light- and electron-microscopy study. Parasitol Res 85:625–637.

Millar NS, Denholm I (2007) Nicotinic acetylcholine receptors: Targets for commercially important insecticides. Invertebr Neurosci 7:53–66.

Moffat C, Buckland ST, Samson AJ, et al (2016) Neonicotinoids target distinct nicotinic acetylcholine receptors and neurons, leading to differential risks to bumblebees. Sci Rep 6:24764.

Moffat C, Pacheco JG, Sharp S, et al (2015) Chronic exposure to neonicotinoids increases neuronal vulnerability to mitochondrial dysfunction in the bumblebee (Bombus terrestris). FASEB J 29:2112–2119.

Muth F, Leonard AS (2019) A neonicotinoid pesticide impairs foraging, but not learning, in free-flying bumblebees. Sci Rep 1–13.

Nareshkumar B, Akbar SM, Sharma HC, et al (2018) Imidacloprid impedes mitochondrial function and induces oxidative stress in cotton bollworm, Helicoverpa armigera larvae (Hubner: Noctuidae). J Bioenerg Biomembr 50:21–32.

Nauen R, Ebbinghaus-Kintscher U, Salgado VL, Kaussmann M (2003) Thiamethoxam is a neonicotinoid precursor converted to clothianidin in insects and plants. Pestic Biochem Physiol 76:55–69.

Nauen R, Ebbinghaus-Kintscher U, Schmuck R (2001) Toxicity and nicotinic acetylcholine receptor interaction of imidacloprid and its metabolites in Apis mellifera (Hymenoptera: Apidae). Pest Manag Sci 57:577–86.

Nauen R, Tietjen K, Wagner K, Elbert A (1998) Efficacy of plant metabolites of imidacloprid against Myzus persicae and Aphis gossypii (Homoptera: Aphididae). Pestic Sci 52:53–57.

Nguyen DTT, Blacker MJ, Goodchild JA (2012) Spontaneous electrical activity recorded from the aphid central nervous system. Invertebr Neurosci 12:139–146.

Nicholls DG, Budd SL (2000) Mitochondria and neuronal survival. Physiol Rev 80:315–60.

Nicodemo D, Maioli MA, Medeiros HCD, et al (2014) Fipronil and imidacloprid reduce honeybee mitochondrial activity. Environ Toxicol Chem 33:2070–2075.

Nishimura K, Kanda Y, Okazawa A, Ueno T (1994) Relationship between insecticidal and neurophysiological activities of imidacloprid and related compounds. Pestic Biochem Physiol 50:51–59.

O'Carroll DC, Bidwell NJ, Laughlin SB, Warrant EJ (1996) Insect motion detectors matched to visual ecology. Nature 382:63–66.

Ochoa ELM, Chattopadhyay A, McNamee MG (1989) Desensitization of the nicotinic acetylcholine receptor: Molecular mechanisms and effect of modulators. Cell Mol Neurobiol 9:141-178.

Oliveira EE, Schleicher S, Büschges A, et al (2011) Desensitization of nicotinic acetylcholine receptors in central nervous system neurons of the stick insect (Carausius morosus) by imidacloprid and sulfoximine insecticides. Insect Biochem Mol Biol 41:872–880.

Onyeocha FA, Fuzeau-Braesch S (1991) Circadian rhythm changes in toxicity of the insecticide dieldrin on larvae of the migratory locust Locusta migratoria migratorioides. Chronobiol Int 8:103–9.

Osorio D (1987) Temporal and spectral properties of sustaining cells in the medulla of the locust. J Comp Physiol A 161:441–448.

Palmer CR, Kristan WB (2011) Contextual modulation of behavioral choice. Curr Opin Neurobiol 21:520–526.

Palmer MJ, Moffat C, Saranzewa N, et al (2013) Cholinergic pesticides cause mushroom body neuronal inactivation in honeybees. Nat Commun 4:1634.

Parker D, Newland PL (1995) Cholinergic synaptic transmission between proprioceptive afferents and a hind leg motor neuron in the locust. J Neurophysiol 73:586–594.

Parkinson R, Gray J (2019) Neural conduction, visual motion detection, and flight behaviour of insects are disrupted by low doses of imidacloprid and its metabolites. Neurotoxicology 72:107–113.

Parkinson RH, Little JM, Gray JR (2017) A sublethal dose of a neonicotinoid insecticide disrupts visual processing and collision avoidance behaviour in Locusta migratoria. Sci Rep 7:936.

Peng TI, Jou MJ (2010) Oxidative stress caused by mitochondrial calcium overload. Ann N Y Acad Sci 1201:183–188.

Phelps JD, Strang CG, Gbylik-Sikorska M, et al (2018) Imidacloprid slows the development of preference for rewarding food sources in bumblebees (Bombus impatiens). Ecotoxicology 27:175–187.

Pinton P, Giorgi C, Siviero R, et al (2008) Calcium and apoptosis: ER-mitochondria Ca2+ transfer in the control of apoptosis. Oncogene 27:6407–6418.

Pinton P, Rizzuto R (2006) Bcl-2 and Ca2+ homeostasis in the endoplasmic reticulum. Cell Death Differ 13:1409–1418.

Portelli G, Ruffier F, Franceschini N (2010) Honeybees change their height to restore their optic flow. J Comp Physiol A 196:307–313.

Portelli G, Ruffier F, Roubieu FL, Franceschini N (2011) Honeybees' speed depends on dorsal as well as lateral, ventral and frontal optic flows. PLoS One 6:1–10.

Qin G, Jia M, Liu T, et al (2013) Characterization and Functional Analysis of Four Glutathione S-Transferases from the Migratory Locust, Locusta migratoria. PLoS One 8:1–11.

Quick MW, Lester RAJ (2002) Desensitization of neuronal nicotinic receptors. J Neurobiol 53:457–478.

Ramirez J, Pearson K (1993) Alteration of bursting properties in interneurons during locust flight. J Neurophysiol 70:2148–2160.

Rind F, Simmons P (1992) Orthopteran DCMD neuron: a reevaluation of responses to moving objects. I. Selective responses to approaching objects. J Neurophysiol 68:1654–1666.

Rind FC (1984) A chemical synapse between two motion detecting neurones in the locust brain. J Exp Biol 110:143–167.

Rind FC (1996) Intracellular characterization impending collision of neurons in the locust brain signaling. J Neurophysiol 75:986-995.

Rind FC, Bramwell DI (1996) Neural network based on the input organization of an identified neuron signaling impending collision. J Neurophysiol 75:967–985.

Rind FC, Leitinger G (2000) Immunocytochemical evidence that collision sensing neurons in the locust visual system contain acetylcholine. J Comp Neurol 423:389–401.

Rind FC, Santer RD, Wright G a (2008) Arousal facilitates collision avoidance mediated by a looming sensitive visual neuron in a flying locust. J Neurophysiol 100:670–80.

Rind FC, Simmons PJ (1998) Local circuit for the computation of object approach by an identified visual neuron in the locust. J Comp Neurol 395:405–415.

Robertson RM, Johnson AG (1993) Collision avoidance of flying locusts: steering torques and behaviour. J Exp Biol 183:35–60.

Robertson RM, Pearson K, Reichert H (1982) Flight interneurons in the locust and the origin of insect wings. Science 217:177-179.

Rogers SM, Krapp HG, Burrows M, Matheson T (2007) Compensatory plasticity at an identified synapse tunes a visuomotor pathway. J Neurosci 27:4621–4633.

Rogers SM, Matheson T, Sasaki K, et al (2004) Substantial changes in central nervous system neurotransmitters and neuromodulators accompany phase change in the locust. J Exp Biol 207:3603–3617.

Roveri A, Coassin M, Maiorino M, et al (1992) Effect of hydrogen peroxide on calcium homeostasis in smooth muscle cells. Arch Biochem Biophys 297:265–270.

Rundlöf M, Andersson GKS, Bommarco R, et al (2015) Seed coating with a neonicotinoid insecticide negatively affects wild bees. Nature 521:77–80.

Saha D (2016) Biochemical Insecticide Resistance in Tea Pests. In: Insecticides Resistance. InTech, pp 347–390.

Samuelson EEW, Chen-Wishart ZP, Gill RJ, Leadbeater E (2016) Effect of acute pesticide exposure on bee spatial working memory using an analogue of the radial-arm maze. Sci Rep 1–11.

Santer RD, Rind FC, Stafford R, et al (2006) Role of an Identified Looming-Sensitive Neuron in Triggering a Flying Locust's Escape. J Neurophysiol 95:3391–3400.

Santer RD, Simmons PJ, Rind FC (2005a) Gliding behaviour elicited by lateral looming stimuli in flying locusts. J Comp Physiol A 191:61–73.

Santer RD, Yamawaki Y, Rind FC, Simmons PJ (2005b) Motor activity and trajectory control during escape jumping in the locust Locusta migratoria. J Comp Physiol A 191:965–975.

Sattelle DB, Breert H (1990) Cholinergic nerve terminals in the central nervous system of insects. J Neuroendocrinol 2:241–256.

Sattelle DB, Jones AK, Sattelle BM, et al (2005) Edit, cut and paste in the nicotinic acetylcholine receptor gene family of Drosophila melanogaster. BioEssays 27:366–376.

Schaafsma A, Limay-Rios V, Xue Y, et al (2016) Field-scale examination of neonicotinoid insecticide persistence in soil as a result of seed treatment use in commercial maize (corn) fields in southwestern Ontario. Environ Toxicol Chem 35:295–302.

Si A (2003) Honeybee navigation: properties of the visually driven 'odometer'. J Exp Biol 206:1265–1273.

Silva AC, McMillan GA, Santos CP, Gray JR (2015) Background complexity affects response of a looming-sensitive neuron to object motion. J Neurophysiol 113:218–231.

Simmons PJ (1982) The function of insect ocelli. Trends Neurosci 5:182–183.

Simmons PJ (1980) Connexions between a movement-detecting visual interneurone and flight motoneurones of a locust. J Exp Biol 86:87–97.

Simmons PJ, Rind FC (1992) Orthopteran DCMD neuron: a reevaluation of responses to moving objects. II. Critical cues for detecting approaching objects. J Neurophysiol 68:1667–1682.

Simmons PJ, Rind FC, Santer RD (2010) Escapes with and without preparation: the neuroethology of visual startle in locusts. J Insect Physiol 56:876–883.

Simpson SJ, Caffery ARM, Ha BF, et al (1999) A behavioural analysis of phase change in the desert locust. Biol Rev 74:461–480.

Simpson SJ, Despland E, Hägele BF, Dodgson T (2001) Gregarious behavior in desert locusts is evoked by touching their back legs. Proc Natl Acad Sci U S A 98:3895–3897.

Siviter H, Brown MJF, Leadbeater E (2018) Sulfoxaflor exposure reduces bumblebee reproductive success. Nature 561:109-112.

Sparks TC, DeBoer GJ, Wang NX, et al (2012) Differential metabolism of sulfoximine and neonicotinoid insecticides by Drosophila melanogaster monooxygenase CYP6G1. Pestic Biochem Physiol 103:159–165.

Sparks TC, Watson GB, Loso MR, et al (2013) Sulfoxaflor and the sulfoximine insecticides: Chemistry, mode of action and basis for efficacy on resistant insects. Pestic Biochem Physiol 107:1–7.

Srinivasan M V., Poteser M, Kral K (1999) Motion detection in insect orientation and navigation. Vision Res 39:2749–2766.

Srinivasan M V., Zhang S (2004) Visual motor computations in insects. Annu Rev Neurosci 27:679–696.

Stanley DA, Russell AL, Morrison SJ, et al (2016) Investigating the impacts of field-realistic exposure to a neonicotinoid pesticide on bumblebee foraging, homing ability and colony growth. J Appl Ecol 53:1440–1449.

Stanley J, Sah K, Jain SK, et al (2015) Evaluation of pesticide toxicity at their field recommended doses to honeybees, Apis cerana and A. mellifera through laboratory, semi-field and field studies. Chemosphere 119:668–674.

Stewart SD, Lorenz GM, Catchot AL, et al (2014) Potential exposure of pollinators to neonicotinoid insecticides from the use of insecticide seed treatments in the mid-southern United States. Environ Sci Technol 48:9762–9769.

Stott TP, Olson EGN, Parkinson RH, Gray JR (2018) Three-dimensional shape and velocity changes affect responses of a locust visual interneuron to approaching objects. J Exp Biol 221:jeb191320.

Straw AD (2008) Vision Egg: an open-source library for realtime visual stimulus generation. Front Neuroinform 2:4.

Suchail S, De Sousa G, Rahmani R, Belzunces LP (2004) In vivo distribution and metabolization of 14C-imidacloprid in different compartments of Apis mellifera L. Pest Manag Sci 60:1056–1062.

Suchail S, Guez D, Belzunces L (2000) Characteristics of imidacloprid toxicity in two Apis mellifera subspecies. Environ Toxicol Chem 19:1901–1905.

Suchail S, Guez D, Belzunces L (2001) Discrepancy between acute and chronic toxicity induced by imidacloprid and its metabolites in Apis mellifera. Environ Toxicol Chem 20:2482–2486.

Sutton GP, Burrows M (2008) The mechanics of elevation control in locust jumping. J Comp Physiol A 194:557–563.

Taly A, Corringer P-J, Guedin D, et al (2009) Nicotinic receptors: allosteric transitions and therapeutic targets in the nervous system. Nat Rev Drug Discov 8:733–750.

Tan K, Chen W, Dong S, et al (2014) Imidacloprid alters foraging and decreases bee avoidance of predators. PLoS One 9:3–10.

Taylor GK, Krapp HG (2007) Sensory systems and flight stability: What do insects measure and why? Adv In Insect Phys 34:231–316.

Thany SH, Gauthier M (2005) Nicotine injected into the antennal lobes induces a rapid modulation of sucrose threshold and improves short-term memory in the honeybee Apis mellifera. Brain Res 1039:216–219.

Thany SH, Lenaers G, Raymond-Delpech V, et al (2007) Exploring the pharmacological properties of insect nicotinic acetylcholine receptors. Trends Pharmacol Sci 28:14–22.

Tharp CI, Johnson GD, Onsager JA (2000) Laboratory and field evaluations of imidacloprid against Melanoplus sanguinipes (Orthoptera : Acrididae) on small grains. J Econ Entomol 93:293–299.

Tomizawa M (2002) Desnitro-imidacloprid Activates the Extracellular Signal-Regulated Kinase Cascade via the Nicotinic Receptor and Intracellular Calcium Mobilization in N1E-115 Cells. Toxicol Appl Pharmacol 184:180–186.

Tomizawa M (2004) Neonicotinoids and Derivatives: Effects in Mammalian Cells and Mice. J Pestic Sci 29:177–183.

Tomizawa M, Casida JE (2001) Structure and diversity of insect nicotinic acetylcholine receptors. Pest Manag Sci 57:914–22.

Tomizawa M, Casida JE (2005) Neonicotinoid insecticide toxicology: mechanisms of selective action. Annu Rev Pharmacol Toxicol 45:247-68.

Tomizawa M, Casida JE (2003) Selective toxicity of neonicotinoids attributable to specificity of insect and mammalian nicotinic receptors. Annu Rev Entomol 48:339–64.

Tosi S, Burgio G, Nieh JC (2017) A common neonicotinoid pesticide, thiamethoxam, impairs honey bee flight ability. Sci Rep 7:1–8.

Trimmer BA (1995) Current excitement from insect muscarinic receptors. Trends Neurosci 18:104–111.

Tsuneki H, Klink R, Léna C, et al (2000) Calcium mobilization elicited by two types of nicotinic acetylcholine receptors in mouse substantia nigra pars compacta. Eur J Neurosci 12:2475–2485.

Usherwood PNR (1977) Neuromuscular Transmission in Insects. In: Hoyle G (ed) Identified Neurons and Behavior of Arthropods. Springer US, Boston, MA, pp 31–48.

Uteshev V V (2012) α7 nicotinic ACh receptors as a ligand-gated source of Ca2+ ions: the search for a Ca2+ optimum. Adv Exp Med Biol 740:603–638.

van der Sluijs JP, Amaral-Rogers V, Belzunces LP, et al (2015) Conclusions of the Worldwide Integrated Assessment on the risks of neonicotinoids and fipronil to biodiversity and ecosystem functioning. Environ Sci Pollut Res Int 22:148–154.

Vehovszky, Farkas A, Acs A, et al (2015) Neonicotinoid insecticides inhibit cholinergic neurotransmission in a molluscan (Lymnaea stagnalis) nervous system. Aquat Toxicol 167:172–179.

Walters K (2013) Data, data everywhere but we don't know what to think? Neonicotinoid insecticides and pollinators. Outlooks Pest Manag 24:151–155.

Wang H, Dewell RB, Wang H, et al (2018a) Feedforward Inhibition Conveys Time-Varying Stimulus Information in a Collision Detection Circuit. Curr Biol 28:1509-1521.e3.

Wang NX, Watson GB, Loso MR, Sparks TC (2016) Molecular Modeling of Sulfoxaflor and Neonicotinoid Binding in Insect Nicotinic Acetylcholine Receptors: Impact of the Myzus β1 R81T Mutation. Pest Manag Sci.

Wang X, Ana on A, Wu Q, et al (2018b) Mechanism of Neonicotinoid Toxicity: Impact on Oxidative Stress and Metabolism. Annu Rev Pharmacol Toxicol Annu Rev Pharmacol Toxicol 58:471–507.

Wang X, Anadón A, Qinghua W, et al (2018c) Mechanism of Neonicotinoid Toxicity: Impact on Oxidative Stress and Metabolism. Annu Rev Pharmacol Toxicol 58:annurev-pharmtox-010617-052429.

Wang X, Fang X, Yang P, et al (2014) The locust genome provides insight into swarm formation and long-distance flight. Nat Commun 5:2957.

Wang X, Kang L (2014) Molecular Mechanisms of Phase Change in Locusts. Annu Rev Entomol 59:225–244.

Wang X, Meng X, Liu C, et al (2015a) Cys-loop ligand-gated ion channel gene discovery in the Locusta migratoria manilensis through the neuron transcriptome. Gene 561:276–282.

Wang X, Sun H, Zhang Y, et al (2015b) Transcriptional Changes in nAChRs , Interactive Proteins and P450s in Locusta migratoria manilensis (Orthoptera : Acrididae) CNS in Response to High and Low Oral Doses of Imidacloprid. J Insect Sci 15:102–107.

Watson AHD, Schürmann FW (2002) Synaptic structure, distribution, and circuitry in the central nervous system of the locust and related insects. Microsc Res Tech 56:210–226.

Weeks JC, Jacobs GA (1987) A reflex behavior mediated by monosynaptic connections between hair afferents and motoneurons in the larval tobacco hornworm, Manduca sexta. J Comp Physiol A 160:315–329.

Wiersma CAG (1947) Giant nerve fiber system of the crayfish. A contribution to comparative physiology of synapse. J Neurophysiol 10:23–38.

Williamson SM, Baker DD, Wright GA (2013) Acute exposure to a sublethal dose of imidacloprid and coumaphos enhances olfactory learning and memory in the honeybee Apis mellifera. Invertebr Neurosci 13:63–70.

Williamson SM, Willis SJ, Wright GA (2014) Exposure to neonicotinoids influences the motor function of adult worker honeybees. Ecotoxicology 23:1409–1418.

Wilson M (1978) The functional organization of locust ocelli. J Comp Physiol 124:297–316.

Wine JJ, Krasne FB (1972) The organization of escape behaviour in the crayfish. J Exp Biol 56:1–18.

Wolf H, Pearson K (1988) Proprioceptive input patterns elevator activity in the locust flight system. J Neurophysiol 59:1831–1853.

Woodcock BA, Isaac NJB, Bullock JM, et al (2016) Impacts of neonicotinoid use on long-term population changes in wild bees in England. Nat Commun 7:1–8.

Wu YY, Zhou T, Wang Q, et al (2015) Programmed cell death in the honey bee (Apis mellifera) (Hymenoptera: Apidae) worker brain induced by imidacloprid. J Econ Entomol 108:1486–1494.

Yakubowski JM, McMillan GA, Gray JR (2016) Background visual motion affects responses of an insect motion-sensitive neuron to objects deviating from a collision course. Physiol Rep 4:e12801.

Yamawaki Y, Toh Y (2009a) A descending contralateral directionally selective movement detector in the praying mantis Tenodera aridifolia. J Comp Physiol A 195:1131–1139.

Yamawaki Y, Toh Y (2009b) Responses of descending neurons to looming stimuli in the praying mantis Tenodera aridifolia. J Comp Physiol A 195:253–264.

Zafeiridou G, Theophilidis G (2004) The action of the insecticide imidacloprid on the respiratory rhythm of an insect: the beetle Tenebrio molitor. Neurosci Lett 365:205–9

Zaworra M, Koehler H, Schneider J, et al (2019) Pharmacokinetics of three neonicotinoid insecticides upon contact exposure in the western honey bee, Apis mellifera. Chem Res Toxicol 32:35–37.

Zhang C, Sun Y, Hu R, et al (2018) A comparison of the effects of agricultural pesticide uses on peripheral nerve conduction in China. Sci Rep 8:4–11

Zhang E, Nieh JC (2015) The neonicotinoid imidacloprid impairs honey bee aversive learning of simulated predation. J Exp Biol 218:3199–3205.

Zhang Y, Liu Y, Bao H, et al (2017) Alternative splicing in nicotinic acetylcholine receptor subunits from Locusta migratoria and its influence on acetylcholine potencies. Neurosci Lett 638:151–155.

Zhu Y, Dewell RB, Wang H, Gabbiani F (2018) Pre-synaptic muscarinic excitation enhances the discrimination of looming stimuli in a collision-detection neuron. Cell Rep 23:2365–2378

Zhu Y, Loso MR, Watson GB, et al (2011) Discovery and characterization of sulfoxaflor, a novel insecticide targeting sap-feeding pests. J Agric Food Chem 59:2950–2957.

Zupanc GKH (2010) Behavioral Neurobiology An Integrative Approach, 2nd edn. Oxford University Press Inc., New York

Zuur AF, Tuck ID, Bailey N (2003) Dynamic factor analysis to estimate common trends in fisheries time series. Can J Fish Aquat Sci 60:542–552.

Zwart R, Oortgiesen M, Vijverberg H (1994) Nitromethylene heterocycles: Selective agonists of nicotinic receptors in locust neurons compared to mouse N1E-115 and BC3H1 cells. Pestic Biochem Physiol 48:202–213